Detection of Explosives via Photolytic Cleavage of Nitroesters and Nitramines

Citation: Andrew, Trisha L., and Timothy M. Swager. "Detection of Explosives via Photolytic Cleavage of Nitroesters and Nitramines." The Journal of Organic Chemistry 76.9 (2011): 2976–2993.

As Published: http://dx.doi.org/ 10.1021/jo200280c

Publisher: American Chemical Society (ACS)

Persistent URL: http://hdl.handle.net/1721.1/74230

Version: Author's final manuscript: final author's manuscript post peer review, without publisher's formatting or copy editing

Detection of Explosives via Photolytic Cleavage of Nitroesters and Nitramines

Journal:	*The Journal of Organic Chemistry*
Manuscript ID:	jo-2011-00280c.R1
Manuscript Type:	Featured Article
Date Submitted by the Author:	n/a

Complete List of Authors:	Andrew, Trisha; Massachusetts Institute of Technology Swager, Timothy; Mass. Inst. of Tech., Chemistry; Massachusetts Institute of Technology, Department of Chemistry 18-597

Detection of Explosives via Photolytic Cleavage of Nitroesters and Nitramines

*Trisha L. Andrew, Timothy M. Swager**

Department of Chemistry, Massachusetts Institute of Technology, 77 Massachusetts Avenue, Cambridge, MA 02139

tswager@mit.edu

RECEIVED DATE (to be automatically inserted)

ABSTRACT. The nitramine-containing explosive RDX and the nitroester-containing explosive PETN are shown to be susceptible to photofragmentation upon exposure to sunlight. Model compounds containing nitroester and nitramine moieties are also shown to fragment upon exposure to UV irradiation. The products of this photofragmentation are reactive, electrophilic NO_x species, such as nitrous and nitric acid, nitric oxide, and nitrogen dioxide. *N*,*N*-Dimethylaniline is capable of being nitrated by the reactive, electrophilic NO_x photofragmentation products of RDX and PETN. A series of 9,9-disubstituted 9,10-dihydroacridines (DHAs) are synthesized from either *N*-phenylanthranilic acid methyl ester or a diphenylamine derivative and are similarly shown to be rapidly nitrated by the photofragmentation products of RDX and PETN. A new (turn-on) emission signal at 550 nm is observed upon nitration of DHAs due to the generation of fluorescent donor-acceptor chromophores. Using fluorescence spectroscopy, the presence of ca. 1.2 ng of RDX and 320 pg of PETN can be detected by DHA indicators in the solid state upon exposure to sunlight. The nitration of aromatic amines by the photofragmentation products of RDX and PETN is presented as a unique, highly selective detection mechanism for nitroester- and nitramine-containing explosives and DHAs are presented as inexpensive

and impermanent fluorogenic indicators for the selective, standoff/remote identification of RDX and PETN.

Introduction

Detecting hidden explosive devices in war zones and transportation hubs is an important pursuit. The three most commonly used highly energetic compounds in explosive formulations are: 2,4,6-trinitrotoluene (TNT), 1,3,5-trinitrotriazinane (RDX), and pentaerythritol tetranitrate (PETN) (Figure 1). Numerous technologies are currently capable of detecting the energetic chemical components of explosive devices, including: analytical spot tests;[1] fluorescent sensors using either small-molecule fluorophores[2] or fluorescent conjugated polymers;[3] chemiresistive sensors;[4] portable mass spectrometers;[5] and X-ray systems.[6] Each example listed has unique advantages and limitations. For instance, while X-ray systems are capable of detecting bulk hidden explosive devices and portable mass spectrometers are capable of identifying the exact chemical structures of suspect chemicals, the practical deployment and/or longevity of these hardware-intensive technologies in complex environments is non-trivial.[5] Fluorescent sensors are comparatively technology-unintensive, have desirably low detection limits, and are also capable of identifying (responding to) entire *classes* of molecules (such as nitroaromatics) or particular functional groups (vide infra).[3] Chemical spot tests can be more specific than fluorescent sensors but are not as sensitive and do not have the analytical advantages of an emissive signal, such as remote line-of-sight (stand-off) detection or prospects for complex signal processing (i.e., fluorescence lifetimes, depolarization).

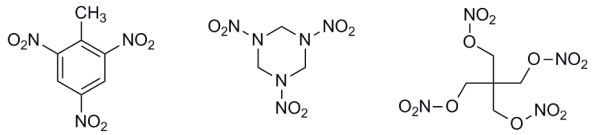

Figure 1. Structures of common high explosives.

We previously reported a turn-on fluorescence chemosensing scheme based on the photoreaction between a hydride donor and either RDX or PETN, wherein the nitramine or nitroester component was

photoreduced by 9,10-dihydroacridine (**AcrH$_2$**, Figure 2) or its metalated analogues.[7] The acridinium products (**AcrH$^+$**) of this photoreaction had a high fluorescence quantum yield and resulted in a significant fluorescence turn-on signal in the presence of RDX and PETN.

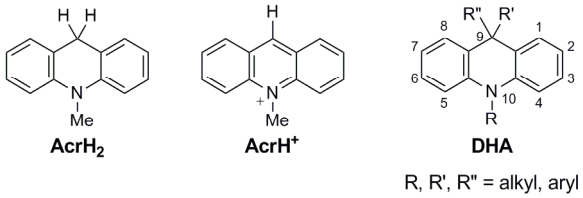

Figure 2. Structures of the hydride donor **AcrH$_2$**, its oxidation product **AcrH$^+$**, and the 9,9-disubstituted 9,10-dihydroacridines, **DHA**s, studied herein.

While studying this photoreaction, we became interested in the photochemical stability of nitramine and nitroester compounds under ultraviolet (UV) irradiation. Nitroesters and nitramines have been known to degrade under highly acidic or basic conditions and established spot tests for PETN and RDX detect these chemical degradation products as opposed to directly detecting intact PETN or RDX.[1] The base-promoted digestion of nitroglycerin (NG) has also been studied and is thought to evolve a mixture of nitrate and nitrite anions, among other degradation products (Scheme 1A).[8] Similarly, RDX is also known to decompose in basic media and produce nitrite ions (Scheme 1A).[9] The Greiss test[10] for nitrite ions can, therefore, be employed to confirm the evolution of nitrite upon base-promoted degradation of RDX and PETN. The chemistry behind the commercially-available Greiss test (Scheme 1B) involves the reaction of sulfanilamide (**4**) with nitrite to form diazonium salt **6**, which then reacts with an arylamine (**5**) to form a brightly-colored azo dye (**7**).[11] As seen in Scheme 1C, when nitrite test strips impregnated with the modified Greiss reagent were dipped into solutions of either RDX or PETN in 2:1 acetonitrile:1 M NaOH, a bright pink color evolved, indicating the presence of nitrite anions.

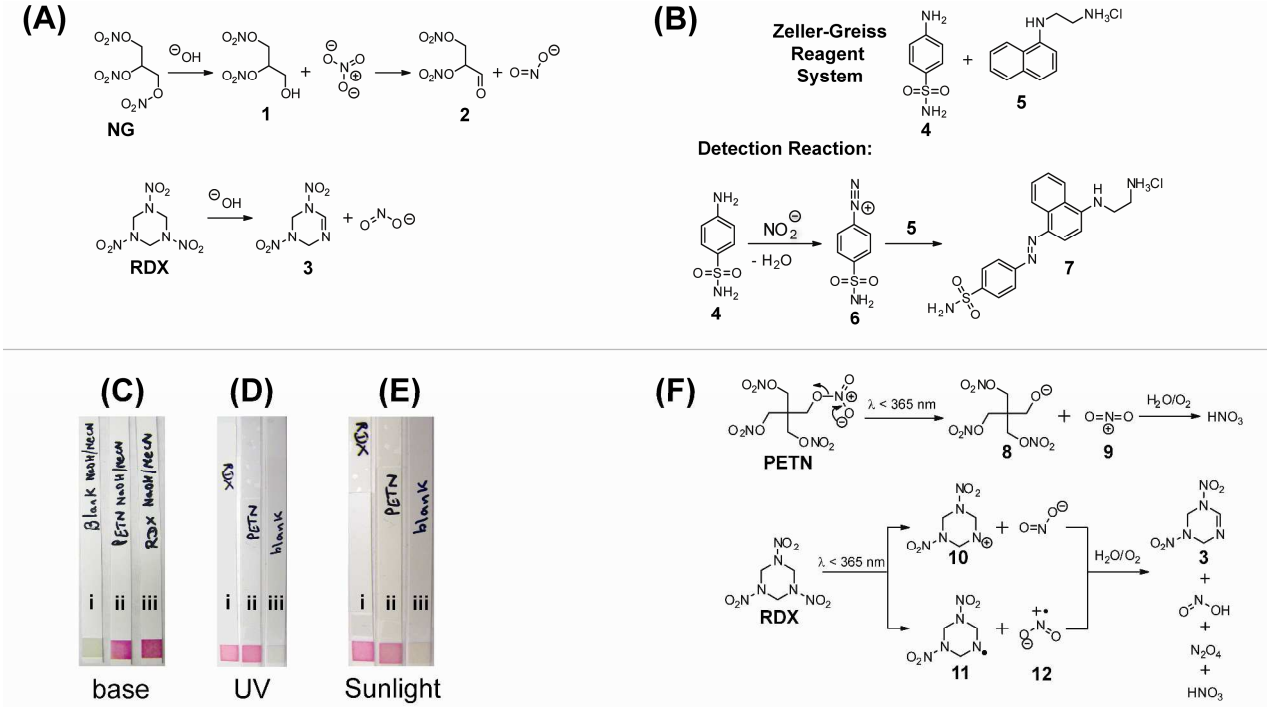

Scheme 1. (A) Degradation mechanisms of nitroesters and nitramines in basic media. (B) Active components and detection mechanism of the Zeller-Greiss test for nitrite ions. (C) Nitrite ion test on base-degraded RDX and PETN. Test strips were dipped into blank 2:1 MeCN: 1M NaOH (i), or 17 mg PETN (ii) or 10 mg RDX (iii) in 3 mL 2:1 MeCN: 1M NaOH. (D) Nitrite ion test on photolyzed RDX and PETN. Test strips were dipped into (i) 10 mg RDX or (ii) 15 mg PETN in 3 mL MeCN, or (iii) neat MeCN and irradiated at 254 nm for one minute. (E) Nitrite ion test on RDX and PETN exposed to sunlight. Test strips were dipped into (i) 10 mg RDX or (ii) 15 mg PETN in 3 mL MeCN, or (iii) neat MeCN and irradiated with polychromatic light from a solar simulator for 30 minutes. (F) Proposed photolytic cleavage pathway of nitroesters and nitramines and select photofragmentation products.

Interestingly, when the same nitrite test strips were dipped into base-free acetonitrile solutions of RDX or PETN, dried and irradiated (λ = 254 nm), formation of the pink azo dye was also observed (Scheme 1D), suggesting the evolution of nitrite ions upon the photolysis of RDX and PETN. Photolysis at 313 nm, 334 nm and 365 nm similarly resulted in a positive Greiss test; however, non-UV controls did not

yield a pink color. Moreover, extended exposure (30 minutes) to polychromatic light from a solar simulator was also observed to photolyze RDX and PETN and yield a positive Greiss test (Scheme 1E).

The photolysis of nitroester and nitramine-based energetic compounds under various conditions has been studied and found to produce a number of small-molecule degradation products, including nitrous and nitric acid, nitric oxide, nitrogen dioxide, formaldehyde and ammonia.[12] The proposed photolytic degradation mechanisms for PETN and RDX are shown in Scheme 1F. In the case of PETN, it is hypothesized that heterolytic cleavage of the O-NO_2 bond initially produces an alkoxide (**8**) and a highly reactive nitronium ion (**9**) that rapidly forms nitric acid under ambient conditions.[13] For RDX, evidence of both the homolytic and heterolytic scission of the N-NO_2 bond of RDX (to produce nitrogen dioxide (**12**) or nitrite, respectively) exists and the exact nature of the initial photoreaction is ambiguous.[14,12d] Nevertheless, it can be agreed that the proposed initial products of RDX and PETN photolysis are highly reactive, electrophilic NO_x species, which can conceivably convert sulfanilamide **4** to the diazonium cation **6** necessary to produce a positive result in the Zeller-Greiss test.

Unfortunately, the Greiss test or variations thereof cannot meet the detection requirements for RDX and PETN. First, simple standoff detection (detection at a distance) with colorimetric spot tests is not a viable possibility because of the difficulty in getting a clear optical signal returned from a purely absorptive process. Moreover, even with optimized reagent systems, the detection limit of the Greiss test is in the microgram regime,[15] which is not competitive with existing methods to detect RDX and PETN.

Herein, we propose instead a sensing scheme that is uniquely selective to the photolytic cleavage of nitroester and nitramine compounds through the formation of nitroaromatic products that provide a new fluorescence signal. The pro-fluorescent, or fluorogenic, indicators described herein are capable of efficiently reacting with the photofragments of RDX and PETN and constitute a new, highly selective and sensitive detection scheme for these explosives.

Results and Discussion

Indicator Design. Considering the electrophilic nature of the NO_x species generated by the photofragmentation of RDX and PETN and their resemblance to the active electrophiles in aromatic nitration reactions, we targeted reactions between electron-rich tertiary aromatic amines and the photofragments of RDX and PETN. It was found that photolysis (λ = 313 nm) of a mixture of *N*,*N*-dimethylaniline (DMA) and 2 equivalents of either RDX or PETN for 10 minutes in acetonitrile under anaerobic conditions afforded the formation of *N*,*N*-dimethyl-4-nitroaniline (DMNA) in 14% yield (GC yield). Higher yields of DMNA were obtained with longer photolysis times and DMNA was formed in ca. 80% yield after 1 hour. The photoreaction between DMA and either RDX or PETN under anaerobic conditions was observed to produce only a *single*, yellow-colored product (DMNA) and other side products were not evident by TLC or GC-MS analyses. The ^{1}H-NMR, IR and high-resolution mass spectra of the isolated yellow product exactly matched those obtained for an authentic commercial sample of DMNA. Conducting the photolysis under aerobic conditions resulted in partial demethylation of DMA[16] and yielded a mixture of DMNA and its demethylated analog, *N*-methyl-4-nitroaniline (**13**) (see Scheme 2). Photolysis of DMA with ammonium nitrate was also found to produce DMNA, although longer photolysis times (>30 minutes) were required and greater amounts of demethylated side products were observed (most likely due to the presence of water or other nucleophiles in the solutions).

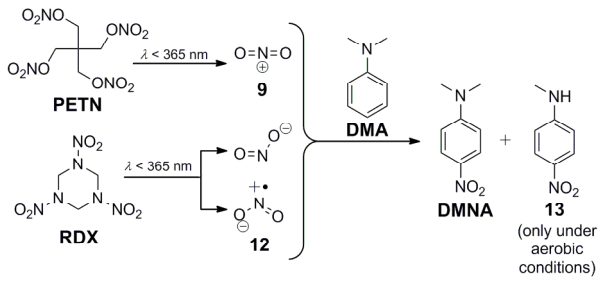

Scheme 2. Nitration of *N*,*N*-dimethylaniline with the photofragmentation products of RDX and PETN.

A distinct absorbance band centered at 400 nm was found to accompany the formation of the nitrated products under both aerobic and anaerobic conditions, which also matched the low-energy charge-transfer band displayed by commercial DMNA. However, DMNA has a very low fluorescence quantum yield[17] and, therefore, a significant turn-on fluorescence signal is not generated upon reaction of DMA with the photofragmentation products of RDX and PETN.

To probe the scope of the photonitration reaction, we investigated whether 9,9-dioctylfluorene, anisole and 1,2-dimethoxybenzene could be nitrated by RDX and PETN. Extended photolysis (5 h) of a mixture of 9,9-dioctylfluorene and either RDX or PETN in 1:1 acetonitrile:THF at either 254, 313, 334, or 356 nm failed to generate any observable products and 9,9-dioctylfluorene was recovered in ca. 90% yield. Photolysis of anisole with RDX or PETN yielded only trace amounts of 4-nitroanisole (<1% GC yield) after 4 hours. Photolysis of 1,2-dimethoxybenzene with either RDX or PETN yielded 1,2-dimethoxy-4-nitrobenzene in only ca. 8% yield after 2 hours; moreover this reaction did not proceed cleanly and numerous polar photoproducts were observed. Therefore, we concluded that anilines were the best candidates for a potential indicator.

To create fluorogenic indicators based on the facile nitration reaction between aromatic amines and the photofragmentation products of RDX and PETN, 9,9-disubstituted 9,10-dihydroacridines (DHAs, Figure 2) were targeted as chemosensors. We hypothesized that, upon nitration, the comparatively rigid DHAs would generate donor-acceptor chromophores possessing high fluorescence quantum yields.[18]

Synthesis. As shown in Schemes 3-5, a series of 9,9-disubstituted DHAs were synthesized, starting from either *N*-phenylanthranilic acid methyl ester (Routes A and C) or a diphenylamine derivative[19] (Route B). DHAs were accessed by an acid-catalyzed cyclization of a tertiary alcohol intermediate (for example, structure **16**). In Route A (Scheme 3), intermediate **16** is accessed by a double 1,2-addition of an alkyl or aryl Grignard reagent to either *N*-phenylanthranilic acid methyl ester (**14**) or its *N*-methyl derivative (**15**); this strategy to synthesize DHAs has previously been reported.[20] In Route B (Scheme 4), tertiary alcohol intermediates **19**-**21** are accessed from 1,2-addition of the aryl lithium species derived from **18** to an appropriate ketone. This strategy was adopted to synthesize unsymmetric DHAs (**DHA10**-

13) that have two different substituents at the 9-position, a spiro-DHA (**DHA14**), and a CF_3-containing DHA (**DHA15**).

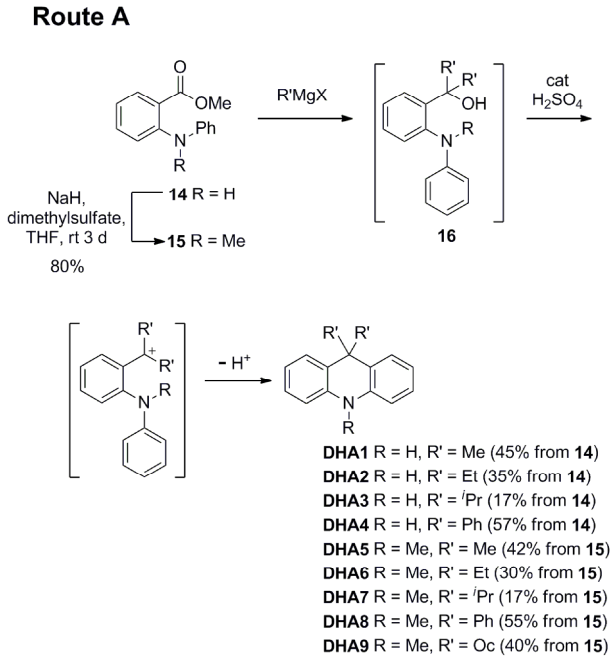

Scheme 3. Route A for the synthesis of 9,9-disubstituted 9,10-dihydroacridines.

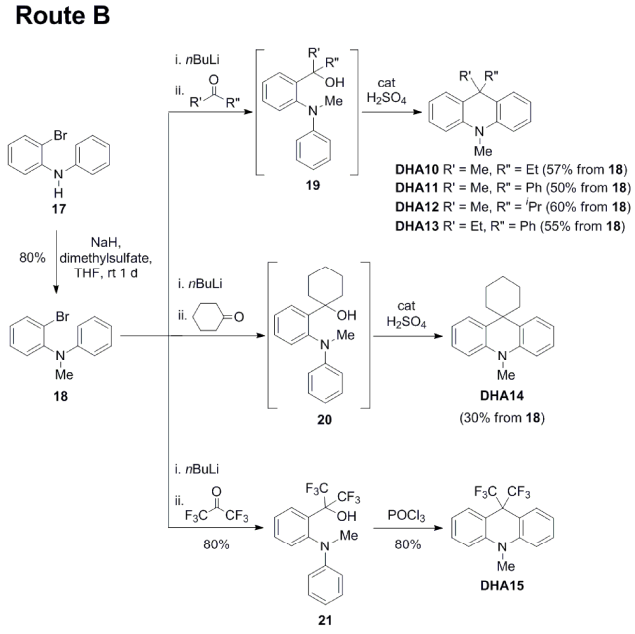

Scheme 4. Route B for the synthesis of 9,9-disubstituted DHAs.

In all cases except one, adding a catalytic amount of concentrated sulfuric acid resulted in Friedel-Crafts reaction/cyclization of the respective tertiary alcohol intermediates to yield 9,9-disubstituted

DHAs. As shown in Scheme 3, we posit that this transformation proceeds via formation of a carbocation. The X-ray crystal structure of **DHA8** thus obtained is shown in Figure 3. The cyclization of compound **21** was uniquely challenging, as neither the use of strong acids, Lewis acids, nor thionyl chloride yielded **DHA15**.[21] However, it was found that refluxing a solution of **21** in $POCl_3$ produced **DHA15** in high yield.

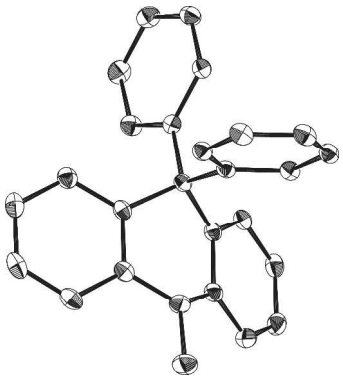

Figure 3. X-ray crystal structure of **DHA8**.

Lastly, Route C was followed to synthesize *N*-aryl DHAs (Scheme 5). Copper-catalyzed *N*-arylation of **14** with 4-bromotoulene initially furnished **22**, which was then reacted with 2.5 equivalents of methylmagnesium bromide and catalytic concentrated sulfuric acid. Unfortunately, the Friedel-Crafts cyclization of intermediate **23** yielded a nearly-statistical mixture of **DHA16** and **DHA17** (1:1.3 **DHA16**:**DHA17**), which could not be acceptably separated by either column chromatography or recrystallization. Therefore, compound **24** was synthesized by copper-catalyzed *N*-arylation of **14** with 2-bromomesitylene and subsequently reacted with methylmagnesium bromide and sulfuric acid to access **DHA18**.

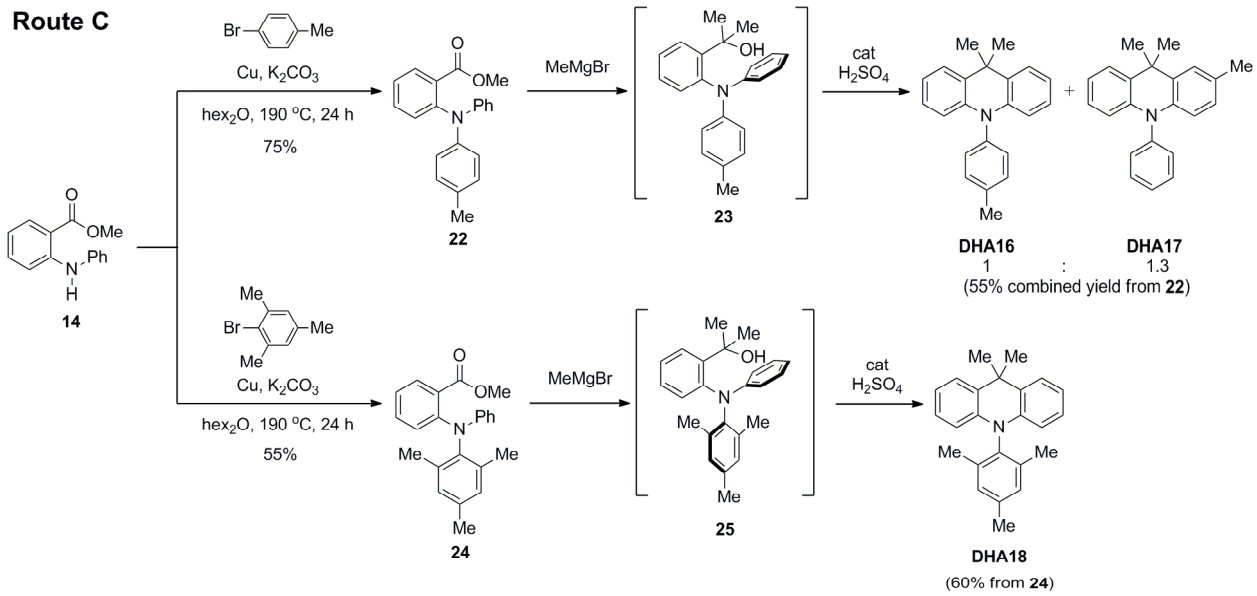

Scheme 5. Route C for the synthesis of *N*-aryl DHAs.

Photophysics. The optical properties of **DHA1**-**18** are summarized in the supporting information (Table S1). The DHAs reported herein displayed similar UV-vis absorption spectra, with absorption maxima around 290 nm. Additionally, **DHA1**-**18** generally displayed a single emission band centered at ca. 350 nm and were found to have similar fluorescence quantum yields and excited-state lifetimes.

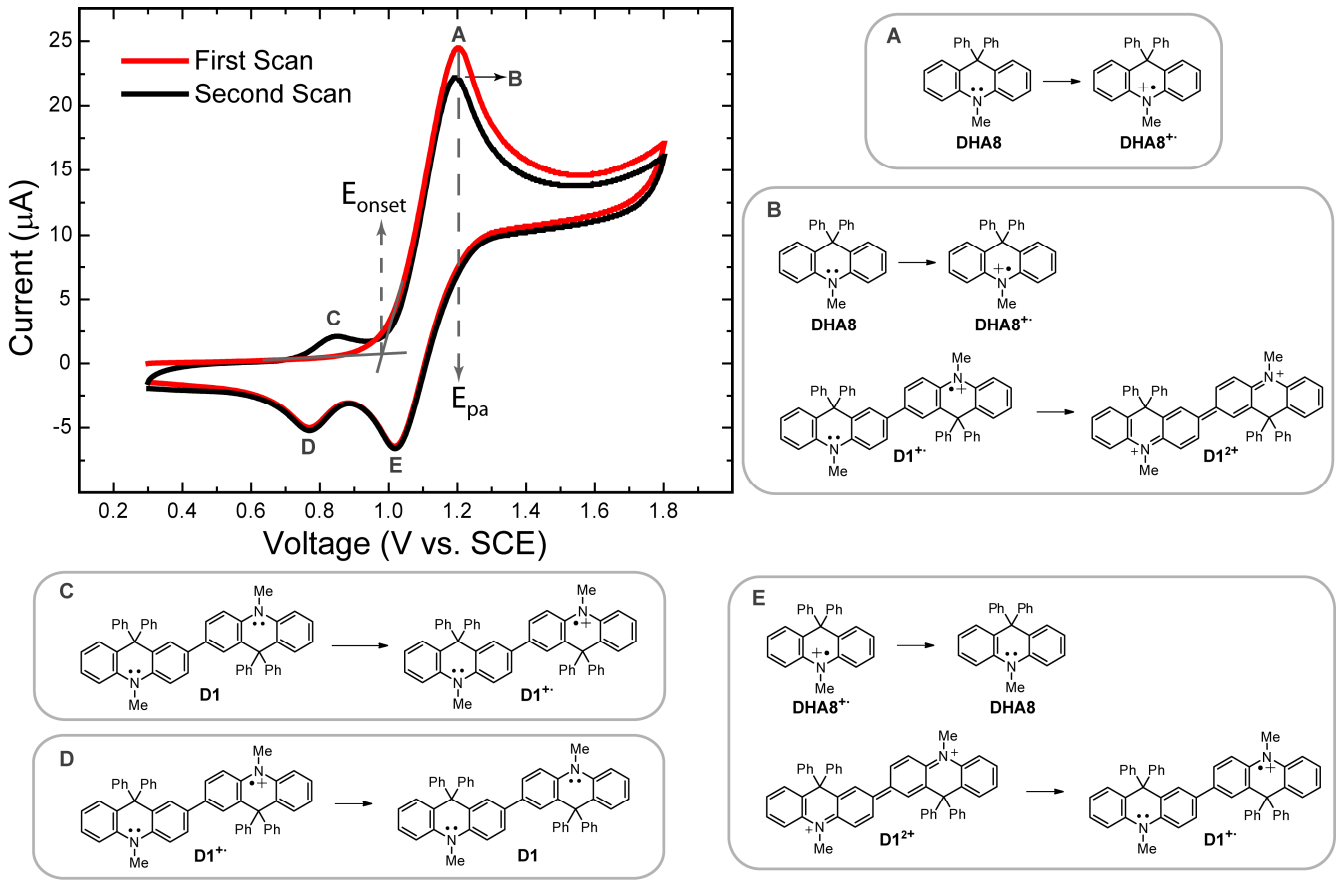

Figure 4. Cyclic voltammogram of **DHA8** (Pt button electrode, 0.1 M $TBAPF_6$ in CH_2Cl_2, 100 mV/s). The redox reactions giving rise to each anodic (A, B and C) and cathodic (D and E) peak are shown, and the first anodic peak potential (E_{pa}) and onset potential (E_{onset}) for the first scan are labeled.

Electrochemistry. Cyclic voltammograms (CVs) of select DHAs were recorded in CH_2Cl_2 with tetrabutylammonium hexafluorophosphate ($TBAPF_6$) as a supporting electrolyte and were found to reveal behavior suggestive of irreversible chemical transformations. The CV of **DHA8** is shown in Figure 4 as a representative example. The first anodic sweep resulted in a single oxidation peak at ca. 1.20 V vs SCE, which can be ascribed to the formation of the radical cation of **DHA8**. However, the corresponding cathodic sweep revealed two cathodic peaks, arising from the reduction of two different species in solution. Furthermore, a subsequent anodic sweep displayed two oxidation peaks. Such behavior has been previously observed for triphenylamine (TPA),[22] and is attributed to the rapid dimerization of TPA radical cations following oxidation; the electroactive TPA dimer thus formed leads

to the growth of an additional anodic and cathodic peak after an initial anodic sweep. Based upon assignments made for the CV of TPA,[22] the redox reactions responsible for the individual anodic and cathodic peaks observed in the CV of **DHA8** were identified and are shown in Figure 3.

The dimerization of radical cations of **DHA8** in the electrochemical cell to form **D1** was confirmed by independently synthesizing **D1**. Oxidation of **DHA8** with $FeCl_3$ or $[Et_3O^+SbCl_6^-]$[23] afforded **D1** in 30-40% yield (Scheme 6). This oxidation reaction was found to selectively yield the dimeric product (by TLC and crude ^{1}H NMR analyses); moreover, we were able to recover the remaining, unreacted **DHA8** upon reaction workup. The use of hydrogen peroxide and *tert*-butyl-hydrogen peroxide was also investigated; however, surprisingly, **D1** was only formed in less than 5% yield with these reagents and **DHA8** was recovered in ca. 90% yield after reaction workup. Attempts to affect an oxidative polymerization of **DHA8** were not successful and only **D1** was isolated. This observation can be explained by the fact that **D1**, once formed, can be oxidized to a stable, closed-shell dication (**D1**$^{2+}$, see Figure 4) that cannot participate in subsequent radical coupling reactions to form polymers. Dimer **D1** is a faint-yellow compound that displays an absorption band centered at 457 nm and an emission band centered at 478 nm (Φ 0.20). The CV of **D1** (see Supporting Information, Figure S1) was found to match the second scan of the CV of **DHA8** (see Figure 4), thus confirming the aforementioned assignments for the anodic and cathodic peaks observed in the CV of **DHA8**.

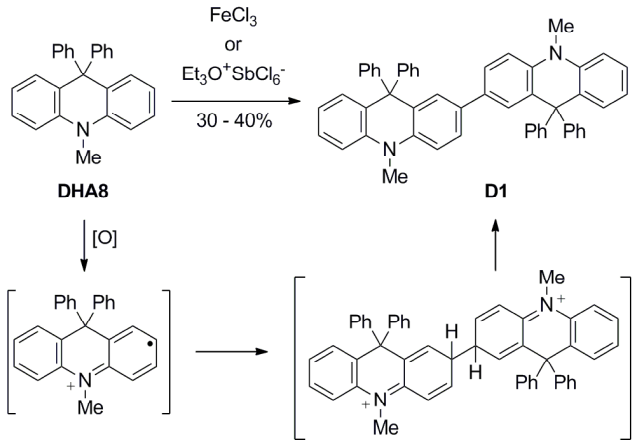

Scheme 6. Oxidative dimerization of **DHA8** to form **D1**.

The electrochemical behavior of **DHA8** was similar to that of the rest of the reported DHAs and also similar to the electrochemical behavior of DMA–i.e., the respective radical cations dimerized in the electrochemical cell after the first anodic sweep. The values for the first anodic peak potential (E_{pa}) and onset potential (E_{onset}) for the first scan of the CVs of select DHAs, DMA and TPA are summarized in the supporting information (Table S2). In general, similar values of E_{pa} and E_{onset} were observed for most DHAs; however, the electron-deficient, CF_3-containing **DHA15** was an outlier and displayed significantly higher E_{pa} and E_{onset} values.

Reaction with RDX/PETN Photofragmentation Products. The photoreactions between **DHA1**-**18** and either RDX or PETN were initially investigated in acetonitrile solutions. In general, irradiating solutions containing **DHA1**-**18** and either RDX or PETN (which were initially colorless) at 313 nm under aerobic conditions lead to the evolution of a bright yellow/orange color after approximately 30 seconds to 5 minutes. Irradiating solutions of **DHA1**-**18** in the absence of either RDX or PETN did not result in the same bright yellow/orange color, although faint yellowing of the DHA solutions was noticed after greatly extended exposure (> 60 minutes) to UV light under aerobic conditions.

The photolyses (λ = 313 nm) of select DHAs with a stoichiometric amount of either RDX or PETN were conducted on a *preparative* scale in order to isolate and characterize the reaction products formed. In these studies, long irradiation times (generally 60 minutes) were employed to ensure complete reactant conversion. TLC and GC-MS analyses of crude reaction mixtures indicated that only a single, highly-colored product was formed in all cases. The yellow-orange products from the reactions of **DHA1**, **DHA4**, and **DHA18** with either RDX or PETN were isolated by flash column chromatography and identified to be the mono-nitrated structures (**26**, **28**, and **30**, respectively) shown in Scheme 7 by their ^{1}H NMR, FT-IR and high resolution mass spectra (see Supporting Information). Compounds **26**, **28** and **30** were isolated in 70-80% yield after column chromatography, along with ca. 10-15% of unreacted **DHA1**, **DHA4**, or **DHA18**. Similarly, **DHA5** and **DHA8** were confirmed to produce **27** and **29**,

respectively, in approximately 70% yield (GC yield) upon photolysis with RDX or PETN (30 minutes). Additionally, **DHA1** and **DHA4** were independently nitrated under mild conditions using SiO_2:HNO_3[24] and the products thus obtained were found to match those isolated from the photoreactions of **DHA1** and **DHA4** with RDX/PETN.

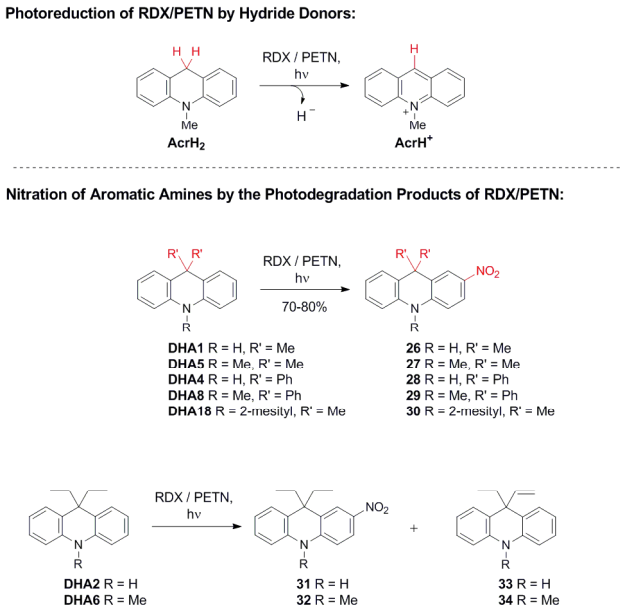

Scheme 7. Photoreactions of various 9,10-dihydroacridines with RDX and PETN. The photoreduction of RDX/PETN by **$AcrH_2$** has been previously reported.[7]

The photoreaction of **DHA2** with either RDX or PETN yielded the nitrated product **31**; however, compound **33** was also isolated from the reaction mixture (Scheme 7). The yield of **33** was found to be somewhat dependent on the concentration of **DHA2**, with a higher amount of **33** over **31** observed in dilute solutions. The yield of **33** was also higher relative to that of **31** when the photolysis of **DHA2** and RDX/PETN was conducted in slightly wet acetonitrile. Compounds **31** and **33** were generally isolated in 80% combined yield after flash column chromatography of the photoreactions between **DHA2** and either RDX or PETN. Furthermore, **DHA6** was confirmed to produce **32** and **34** (by GC-MS analysis) upon photolysis in the presence of RDX/PETN. We hypothesize that **33** and **34** are formed as a result of either H· or hydride abstraction reactions between **DHA2** or **DHA6** and the photodegradation products

of RDX and PETN. However, we are currently unsure as to the origins of the concentration dependence of the yield of **33**.

GC-MS analyses of the photoreactions between the remaining DHAs (**DHA3**, **DHA7**, **DHA9**, **DHA10-17**) and either RDX or PETN similarly revealed the formation of mono-nitrated derivatives of the respective DHAs.

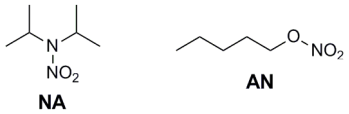

Figure 5. Structures of a model nitramine, *N*,*N*-diisopropylnitramine (**NA**), and a model nitroester, amylnitrate (**AN**).

Other Nitroesters and Nitramines. The photoreactions between **DHA1**-**18** and either a model nitramine or nitroester compound—*N*,*N*-diisopropylnitramine (**NA**) and amyl nitrate (**AN**), respectively (Figure 5)—were also investigated. The reaction products observed upon photolysis (λ = 313 nm) of mixtures of **DHA1**-**18** and either **NA** or **AN** were identical (as established by TLC and GC-MS analyses) to the aforementioned nitrated products observed with RDX and PETN. However, the observed yields (GC yields) of nitrated DHAs were significantly lower with **NA/AN**, as compared to RDX/PETN. For example, whereas **26** was formed in 75% yield upon photolysis with either RDX or PETN for 30 minutes, the photolysis of **DHA1** with **NA** or **AN** afforded **26** in only 30% yield under identical reaction conditions. Therefore, it can be tentatively inferred that RDX and PETN are more susceptible to photolytic cleavage than their respective model compounds.

Differences in DHA Reaction Mechanisms. As shown in Scheme 7, it is interesting to note the difference in photochemical reaction mechanisms between various 9,10-dihydroacridines. As previously reported,[7] *N*-methyl-9,10-dihydroacridine (**AcrH$_2$**) participates in a hydride transfer reaction with either

RDX, PETN, **NA** or **AN**. Dialkylation or diarylation of the 9-position of **$AcrH_2$** effectively nullifies its ability to donate a hydride ion and promotes the photonitration reaction detailed herein.

Light Sources. Importantly, precise timing and sophisticated, high-intensity light sources were not found to be necessary to effect the reaction between **DHA1**-**18** and the degradation products of either RDX or PETN. Simply exposing a mixture of **DHA1**-**18** and RDX/PETN to polychromatic light from a solar simulator effected the photolytic cleavage of RDX/PETN and subsequent formation of mono-nitrated DHAs. For example, compounds **26** and **28** could both be isolated in 75% yield (after flash column chromatography) after a mixture of RDX or PETN and **DHA1** or **DHA4**, respectively, in acetonitrile were exposed to simulated sunlight for 45 minutes. The yields of compounds **26** and **28** thus obtained are similar to those reported earlier for photolysis at 313 nm.

Other NO_x Sources. The (photo)reactions of **DHA1**-**18** with sodium nitrite, potassium nitrate, and NO were also investigated to judge the limitations of using **DHA1**-**18** as stand-off indicators for RDX/PETN. Exposing a mixture of either **DHA1**, **DHA5**, **DHA4** or **DHA8** and excess sodium nitrite in 2:1 acetonitrile:water to simulated sunlight for 2 hours did not result in significant nitration of these DHAs (<1% GC yields of **26**-**29** were generally observed). However, upon addition of 100 μL acetic acid to the same reaction mixtures, compounds **26**-**29** were formed in approximately 8% yield in the *absence* of light. Protonating nitrite salts generates nitrous acid, which is known to decompose and form HNO_3 (among other species), which most likely nitrated the DHAs in this case.

The addition of a large excess of monomeric NO gas to dry, oxygen-free solutions of the aforementioned DHAs failed to generate the characteristic yellow-orange color of **26**-**29**; however, upon introduction of oxygen to these solutions, the nitrated DHAs were observed to be formed by eye (in the absence of light). Subsequent GC-MS analyses confirmed that **26**-**29** were formed in ca. 20% yield. Once again, NO is known to form nitrogen dioxide upon exposure to oxygen, which most likely resulted in nitration of the DHAs.

Mixtures of **DHA1**, **DHA5**, **DHA4** or **DHA8** and a large excess of potassium nitrate in 2:1 acetonitrile:water did not immediately result in nitration. If left standing for 24 h, **26**-**29**, along with multiply-nitrated derivatives of the aforementioned DHAs, were formed in less than 5% combined yield (GC yield). Adding acetic acid to DHA/KNO_3 mixtures resulted in the formation of multiply nitrated DHAs, with 2,7-dinitro DHAs being the major products. Exposing mixtures of either **DHA1**, **DHA5**, **DHA4** or **DHA8** and a large excess of potassium nitrate in 2:1 acetonitrile:water to simulated sunlight for 60 minutes similarly yielded multiply-nitrated derivatives of these DHAs in approximately 20% combined yield. Stoichiometric or sub-stoichiometric amounts of potassium nitrate, or shorter irradiation times failed to generate observable quantities of nitrated DHAs.

Optical Properties of Nitrated DHAs. The photophysical properties of select nitrated DHAs, which were either isolated from the photolysis reactions between DHAs and RDX/PETN or synthesized by nitrating an appropriate DHA, are listed in Table 1. In general, the nitrated DHAs displayed similar absorbance bands as DMNA, with the lowest energy bands centered at ca. 400 nm. Additionally, emission bands centered at ca. 540 nm were observed for all isolated mono-nitrated DHAs. The fluorescence quantum yields of the compounds listed in Table 1 were found to be solvent dependent, with the lowest quantum yields observed in acetonitrile.[25] Moreover, compounds **26**, **28**, **30** and **31** were found to display significant emission in the solid state (in cellulose acetate films containing 10 wt% of the appropriate compound).

Table 1. Optical properties of select mono-nitrated DHAs.

cmpd	λ_{max}[a]	λ_{em}[a]	Φ

	(log ε)		
DMNA	395 (3.9)	530	<0.01 (MeCN)[b] 0.09 ($CHCl_3$)[b] 0.17 (film)[c,d]
26	408 (4.1)	535	0.09 (MeCN)[b] 0.27 ($CHCl_3$)[b] 0.35 (film)[c,d]
28	410 (4.1)	540	0.10 (MeCN)[b] 0.30 ($CHCl_3$)[b] 0.42 (film)[c,d]
30	413 (4.2)	548	0.14 (MeCN)[b] 0.37 ($CHCl_3$)[b] 0.45 (film)[c,d]
31	409 (4.1)	539	0.05 (MeCN)[b] 0.22 ($CHCl_3$)[b] 0.33 (film)[c,d]

[a] in MeCN [b] Measured against perylene in EtOH (Φ 0.94) [c] 10 wt% in cellulose acetate [d] Measured against 10 wt% perylene in PMMA (Φ 0.78)

Optical Characterization of Indicator Response. The absorption and emission profiles for the reaction between **DHA5** and RDX under aerobic conditions are shown in Figure 6. An absorption band centered at ca. 408 nm was observed to evolve when **DHA5** is photolyzed (λ 313 nm) with RDX, which corresponds to the formation of **27**. An emission band at approximately 540 nm concomitantly evolved, which can be assigned to emission from **27** based on the emission profile recorded for its *N*-H analog **26**. A ca. 27-fold increase in the emission intensity at 540 nm was generated after 2 minutes of UV irradiation. Exactly similar absorption and emission profiles were obtained for the photoreaction between **DHA5** and PETN. Moreover, the presence or absence of oxygen did not noticeably change the observed optical response.

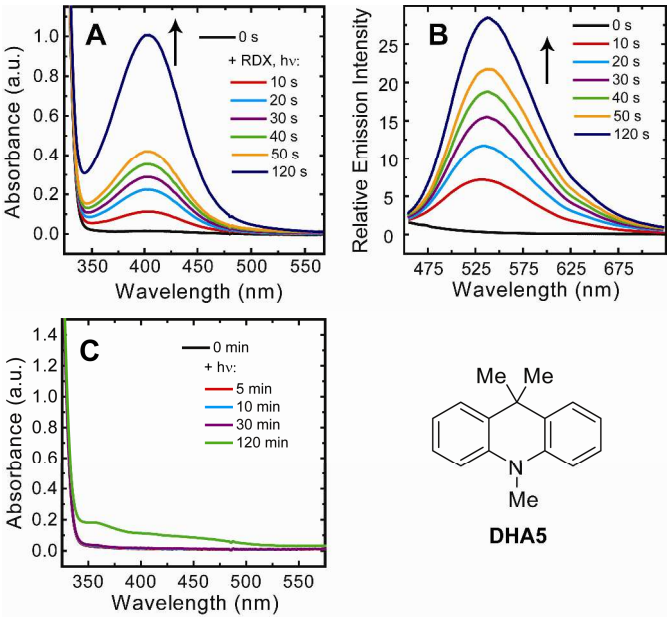

Figure 6. Absorption (A) and emission (B, λ_{ex} = 415 nm) profiles of the photoreaction of **DHA5** with RDX in acetonitrile upon irradiation at 313 nm. [**DHA5**] = 1.3×10^{-4} M. [RDX] = 5.4×10^{-5} M. Identical profiles are observed for the photoreactions of **DHA5** with PETN. The presence or absence of oxygen similarly does not affect the observed absorption and emission profiles. The absorption profile for the extended irradiation of a blank, aerated solution of **DHA5** is also shown (C).

Photolysis of **DHA5** under aerobic conditions in the absence of RDX/PETN failed to generate a distinct absorbance band at 408 nm. Surprisingly, electron-rich **DHA5** was found to be relatively photostable: 30 minutes of continuous UV irradiation did not result in a noticeable change in the absorption spectrum of **DHA5** (Figure 6C), and its emission peak at 355 nm was found to be bleached by only 10%. Further UV irradiation eventually lead to slight yellowing of **DHA5** solutions, and poorly-defined absorbance peaks at 356 nm and ca 440 nm appeared in the absorption spectrum after 2 hours of continuous UV irradiation under air (Figure 6C). These new absorption peaks most likely correspond to the formation of radical cations, *N*-demethylated species, and/or *N*-oxide derivatives of **DHA5**. Notably, though, a significant portion of this photolyzed **DHA5** solution remained unoxidized after 2 hours, and, therefore, the subsequent addition of RDX or PETN nonetheless lead to evolution of a 408 absorbance peak and 540 nm emission peak (5-fold emission turn-on) after a 20 second exposure to 313 nm light.

As seen in Figure 7, exposing a mixture of **DHA5** and RDX to broad-band light from a solar simulator lead to the evolution of the same 408 nm peak observed with irradiation at 313 nm. The rate of formation of the 408 nm peak upon exposure to simulated sunlight also matched that observed upon exposure to monochromatic 313 nm light from a xenon arc lamp (Figure 7B). Therefore, simulated sunlight was preferentially used as the light source in subsequent studies to prove that the DHAs can function as technology-unintensive, fluorogenic indicators for RDX/PETN under ambient sunlight.

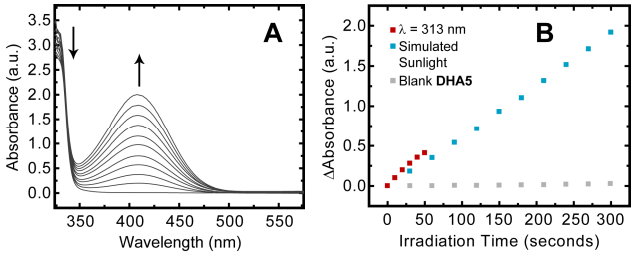

Figure 7. (A) Absorption profile of the photoreaction of **DHA5** and RDX in acetonitrile upon exposure to broad-band light from a solar simulator. [**DHA5**] = 1.3×10^{-4} M. [RDX] = 5.4×10^{-5} M. (B) The rate of formation of the 408 nm absorbance peak in the presence of RDX upon exposure to either simulated sunlight (120 mW/cm^2) or monochromatic 313 nm light (10 mW/cm^2).

DHA6 behaved similar to **DHA5** in terms of its optical response (the absorption and emission profiles for the reaction between **DHA6** and PETN upon exposure to simulated sunlight are shown in the supporting information, Figure S2). Specifically, an absorbance peak at 409 nm evolved in the presence of either RDX or PETN, accompanied with evolution of an emission band at 540 nm. The presence or absence of oxygen did not affect the observed optical response to RDX/PETN. **DHA6** was also found to be relatively photostable, with no change in its absorption spectrum and a 5% bleaching of its emission band at 382 nm observed after 30 minutes of continuous exposure to sunlight. The only significant difference between **DHA5** and **DHA6** was the rate of formation of the 409 nm /540 nm absorption/emission peaks. **DHA5** was found to yield a turn-on signal approximately three times faster than **DHA6**. We hypothesize that this comparatively slow response is because **DHA6** forms a mixture of **32** and **34** upon reacting with RDX/PETN (see Scheme 7).

The optical response of **DHA18** to either RDX or PETN was also similar to that of **DHA5** (see supporting information, Figure S3). An absorbance band at 413 nm and an emission peak at 550 nm evolved upon exposure to simulated sunlight in the presence of either RDX or PETN. **DHA18** was also relatively photostable, with no change in its absorption spectrum and a 5% bleach of its emission band at 371 nm observed after continuous exposure to simulated sunlight for 30 minutes. The rate of photoreaction of **DHA18** with RDX/PETN was slower than that of **DHA5** but faster than that of **DHA6**.

9,9-Diphenyl-substituted **DHA8** differed slightly from the other DHAs explored in this work, as an absorbance band centered at 470 nm, as opposed to ca. 410 nm, evolved during its photoreaction with either RDX or PETN (Figure 8). Based on accompanying GC-MS analyses, this absorbance band could be assigned to the formation of **29**. An emission band at 550 nm was also observed to evolve concomitantly. An approximately 25-fold increase in the emission intensity at 550 nm was generated in the presence of either RDX or PETN upon exposure to simulated sunlight for 40 seconds. The rates of reaction of **DHA5** and **DHA8** with RDX/PETN were approximately similar.

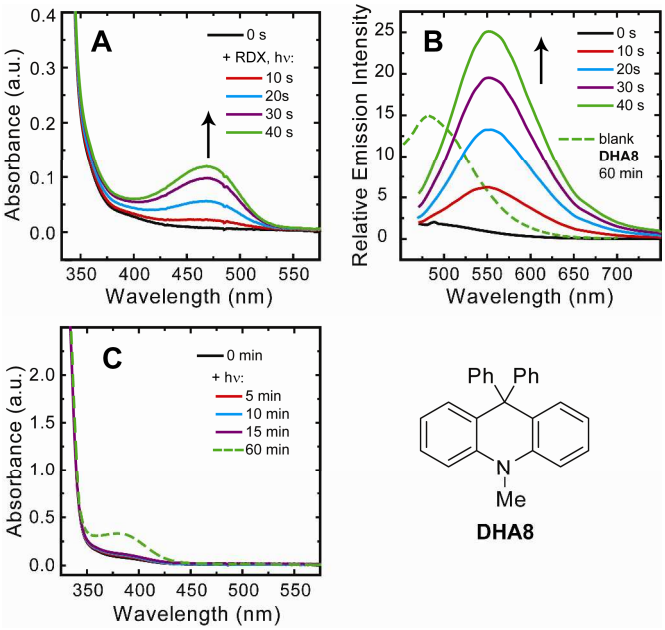

Figure 8. Absorption (A) and emission (B, λ_{ex} = 470 nm) profiles of the photoreaction of **DHA8** with RDX in acetonitrile upon exposure to simulated sunlight. [**DHA8**] = 1.3×10^{-4} M. [RDX] = 5.4×10^{-5} M. The dashed green line depicts the emission spectrum obtained for a blank solution of **DHA8** after irradiation under either aerobic or anaerobic conditions for 60 minutes. The absorption profile for the irradiation of a blank, aerated solution of **DHA8** is also shown (C); the same profile is also obtained for oxygen-free solutions of **DHA8**.

Unlike **DHA5**, **DHA6** and **DHA18**, exposing solutions of **DHA8** to sunlight (or monochromatic UV light) in either the presence or absence of oxygen lead to the formation of a distinct absorbance band at 380 nm, with an accompanying emission band centered at 478 nm. The same photoreactivity was also observed for other DHAs that contained at least one phenyl substituent in the 9-position (**DHA4**, **DHA11** and **DHA13**). Since these absorption/emission bands were observed to evolve even in the absence of oxygen, they are most likely not generated by simple photooxidation products of **DHA8**. Moreover, the evolution of the absorbance band at 380 nm cannot be ascribed to a photodimerization event, as the product of such a reaction, **D1** (Scheme 6), has an absorption maximum of 457 nm. We are currently unsure as to the origin of the photoproduct responsible for the 380 nm/478 nm absorption/emission peak but suspect that a photocyclization reaction occurs in DHAs with at least one phenyl substituent in the 9-position. Nevertheless, for the purposes of this work, it can be seen in Figure 8 that the competing photoreaction in blank solutions of **DHA8** (dashed green line) is slower than the photonitration of **DHA8** in the presence of RDX/PETN and an emission peak at 550 nm is cleanly generated by these explosives in under 10 seconds.

Reaction Kinetics. The most significant difference between the DHAs reported in this work involved the rate of formation of the nitrated photoproducts upon reaction with RDX or PETN. By following the evolution of the characteristic low-energy charge transfer band (centered at ca. 400 nm) of the nitrated

DHAs with irradiation time, we were able to identify differences in the reactivities of **DHA1**-**18** (Figures 9 and 10). As can be seen in Figure 9, the substituents at the 9-position of DHAs significantly affected their reactivities. DHAs with at least one methyl or phenyl substituent at the 9-position were rapidly nitrated in the presence of RDX or PETN. DHAs with alkyl (other than methyl) substituents at the 9-position displayed relatively slower rates of nitration, with isopropyl substituents leading to the slowest reaction rates. Replacing the 9-methyl substituents with trifluoromethyl moieties also retarded the reaction rate. Nominally faster reaction rates were generally observed with PETN over RDX for all DHAs. 9,9-Dioctylfluorene was used as a negative control for these studies and, in all cases, the DHAs reported in this work yielded a significant absorption signal at 400 nm over background.

The nature of the *N*-substituent was also found to affect the rate of photonitration in the presence of RDX/PETN. As seen in Figure 10, for DHAs with ethyl or isopropyl substituents at the 9-position, the *N*-H analogues reacted faster the *N*-Me analogues. For DHAs with phenyl or methyl substituents in the 9-position, this trend was reversed and *N*-Me analogues displayed the fastest reaction rates. Moreover, *N*-arylation was found to significantly retard the rate of photonitration.

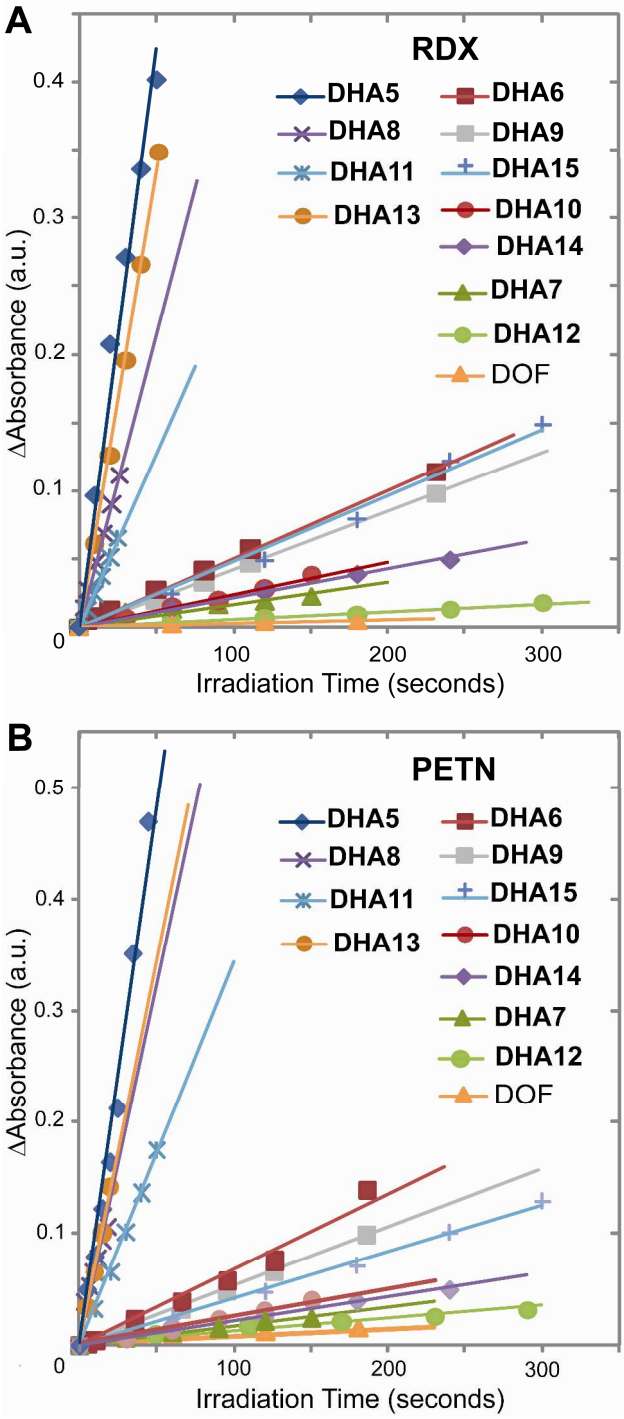

Figure 9. The effect of the substituents at the 9-position of DHAs on their photoreactions with RDX and PETN. Shown are the rates of evolution of the absorbance peak at 410 nm (470 nm for **DHA8**) for the photoreactions between **DHA5-15** and (A) RDX or (B) PETN. DOF is 9,9-dioctylfluorene, which was used as a negative control.

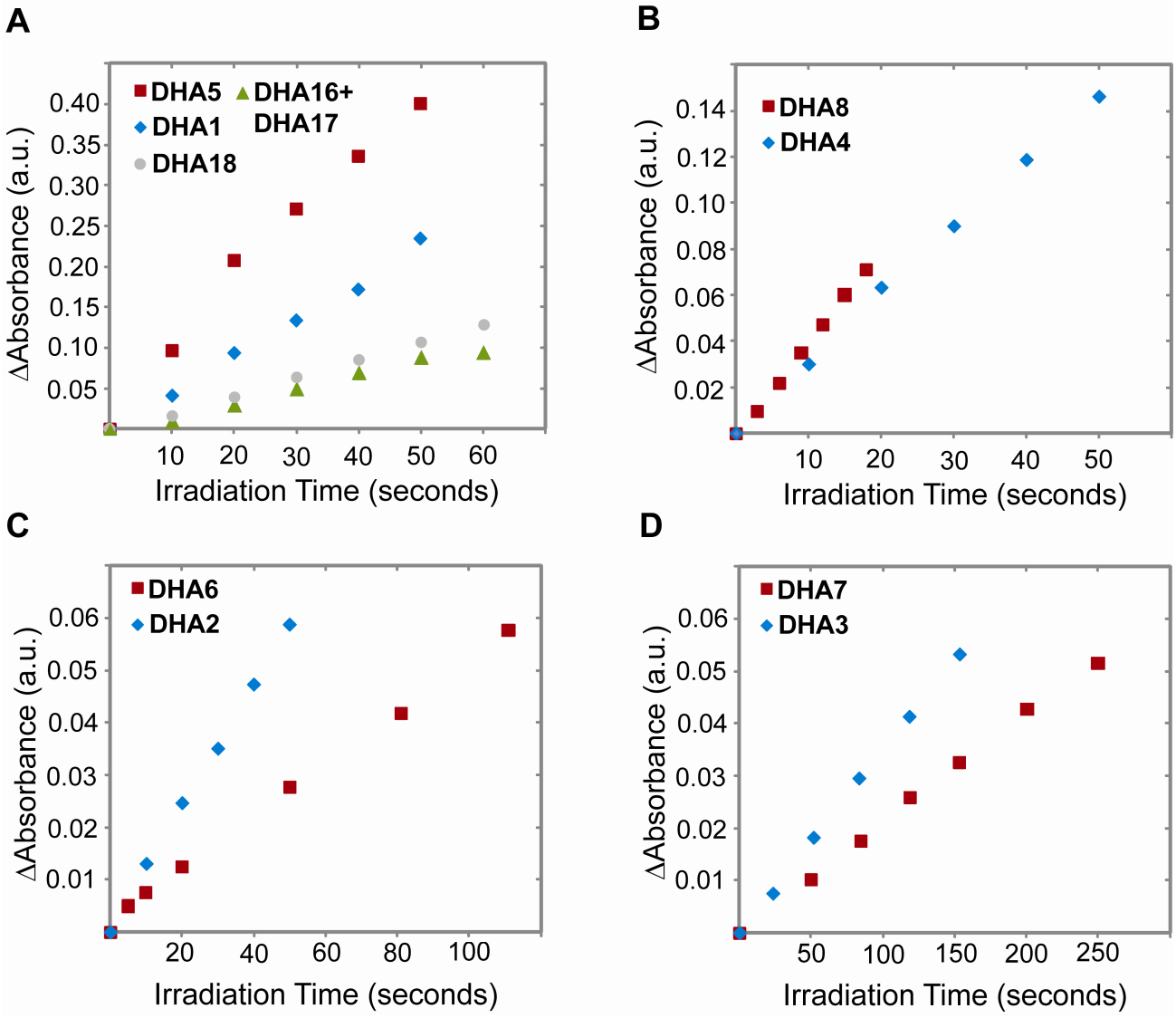

Figure 10. The effect of the *N*-substituent of DHAs on their photoreactions with RDX. Shown are the rates of evolution of the absorbance peak at 410 nm (470 nm for **DHA8**) for the photoreactions between various DHAs and RDX.

Lastly, the rate of formation of nitrated DHAs was compared to the formation of DMNA from DMA. As seen in Figure 11, the reactivity of **DHA5**, which displayed the fastest rate of nitration among **DHA1**-**18**, is comparable to that of DMA.

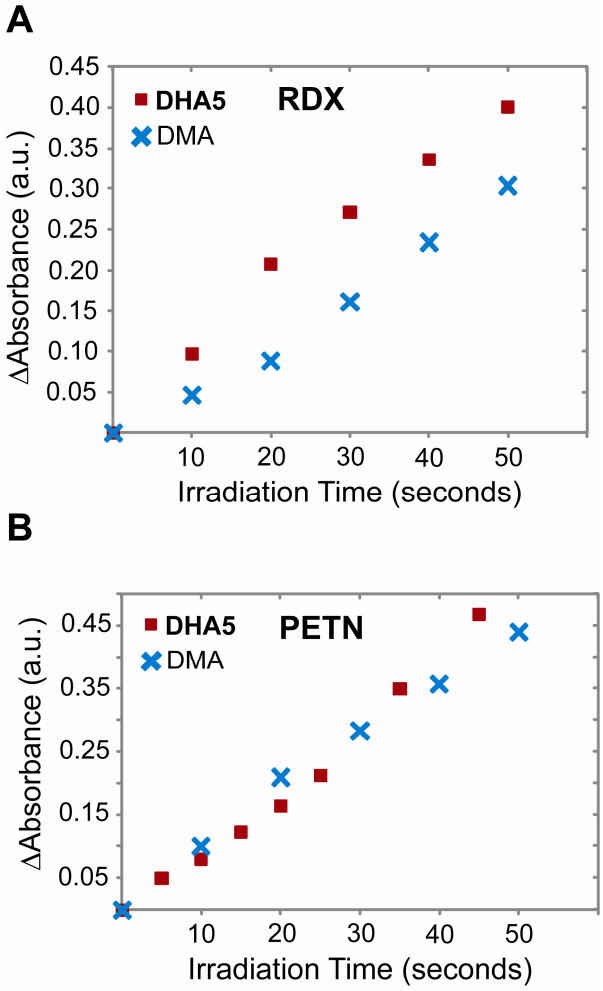

Figure 11. Comparison of the rates of nitration of **DHA5** vs DMA in the presence of (A) RDX or (B) PETN.

Solid State RDX/PETN Detection. Based on the previously-detailed rates of nitration of **DHA1-18** by the photofragmentation products of RDX and PETN, we initially chose to focus on **DHA5**, **DHA8**, **DHA11** and **DHA13** as potential indicators for RDX and PETN, as they displayed the fastest rates of reaction. Between these four DHAs, **DHA5** and **DHA8** were favored because their nitrated products displayed high fluorescence quantum yields. We chose to use **DHA5** to demonstrate detection of RDX/PETN in the solid state; however, similar results and detection limits were also obtained with **DHA8**.

In order to evaluate the utility of **DHA5** as a fluorescent indicator for RDX and PETN, the solid-state response of **DHA5** to RDX and PETN was investigated. For this study, glass slides coated with **DHA5**

were prepared by dipcoating into 8×10^{-3} M solutions of the indicator in acetonitrile and air drying. RDX and PETN solutions of varying concentration were spotted onto the surface and the slides then irradiated with a solar simulator for no longer than 120 seconds.

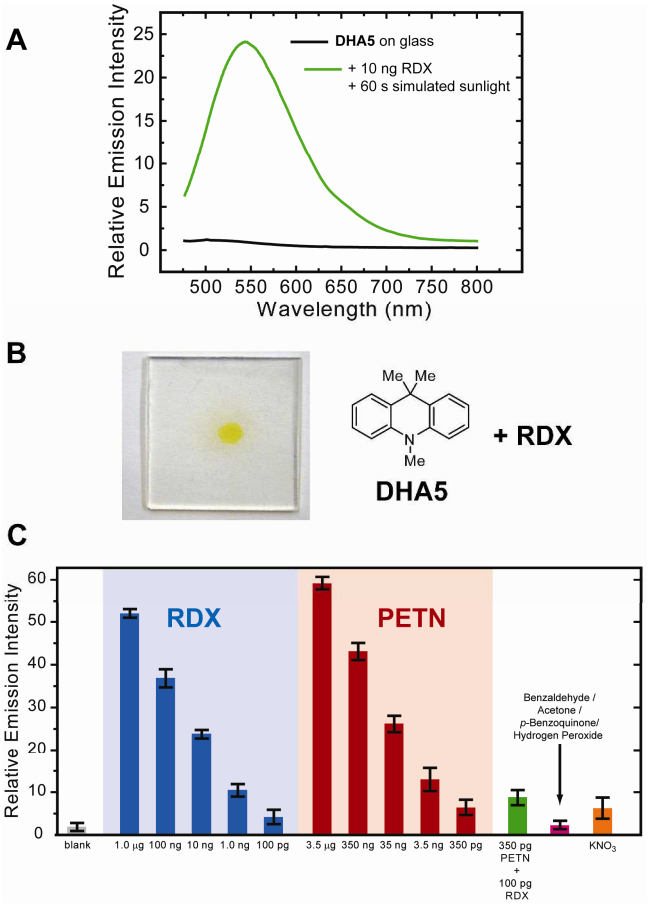

Figure 12. (A) Emission profile (λ_{ex} 420 nm) of a glass slide coated with **DHA5** (black line) and the same slide after spotting with ca. 10 ng of RDX and irradiating with a solar simulator for 60 seconds (green line). (B) Picture of a glass slide coated with **DHA5**, spotted with ca. 10 ng RDX and exposed to simulated sunlight for 120 s. (C) Limits of solid-state detection of RDX and PETN as measured by monitoring the change in emission intensity at 540 nm upon exposure (60 s) to simulated sunlight. In the case of potassium nitrate, a concentrated solution (30 mM) in acetonitrile and long exposure times (600 s) were necessary to obtain the 8-fold increase shown.

As shown in Figure 12A, an acceptable turn-on emission signal at 540 nm was generated by 10 ng of RDX after 60 seconds of irradiation with a solar simulator. In addition to a fluorescence signal, the

distinct yellow color of **27** could also be observed by eye, as shown in Figure 12B. The limits of detection of the **DHA5** chemosensor were estimated by spotting RDX or PETN solutions of varying concentrations onto the **DHA5-**coated slides and are shown in Figure 12C. In general, a greater emission signal at 540 nm was generated by PETN over RDX, possibly because PETN is more susceptible to photodegradation than RDX.

Select interferents, such as ketones and aldehydes, did not produce a significant emission signal at 540 nm. Moreover, consistent with observations made during the synthesis of **D1**, hydrogen peroxide did not react readily with **DHA5** and most likely only formed a small quantity of the radical cation of **DHA5**, which is non-emissive and therefore did not produce any emission at 540 nm.

Aqueous potassium nitrate solutions of varying concentrations were also spotted onto the **DHA5**-coated glass slides in order to gauge the response of the **DHA5** indicator to nitrate contaminants. Consistent with previous observations, sub-micromolar solutions of potassium nitrate did not generate a significant emission signal at 540 nm after one hour in either the absence of presence of simulated solar irradiation. Using a 30 mM solution of potassium nitrate, an approximately 8-fold increase in the emission intensity at 540 nm was observed after a 10 minute exposure to simulated sunlight. However, given the high nitrate concentration and relatively long irradiation time necessary to effect this emission signal, interference from nitrates during RDX/PETN detection can, in theory, be surmounted.

Within experimental error, approximately 100 pg of RDX and PETN can be detected by the **DHA5** indicator under aerobic conditions by monitoring the emission intensity at 540 nm. In the presence of nitrate interferents, this detection limit is conservatively estimated as ca. 1 ng. These detection limits, although not low enough for the detection of equilibrium vapor, are competitive with present transportation security systems that make use of swipes to collect particles.

Conclusions

We have found that the nitramine-containing explosive RDX and the nitroester-containing explosive PETN are susceptible to photofragmentation upon exposure to sunlight to produce reactive NO_x species,

such as nitrogen dioxide and nitric acid. *N*,*N*-Dimethylaniline and 9,9-disubstituted 9,10-dihydroacridines (DHAs) are capable of being selectively nitrated by the reactive, electrophilic NO_x photofragmentation products of RDX and PETN. This nitration reaction proceeds rapidly and yields only one major, singly-nitrated product. A roughly 25-fold increase in the emission signal at 550 nm is observed upon nitration of DHAs due to the generation of fluorescent donor-acceptor chromophores. By monitoring the emission intensity at ca. 550 nm, the presence of approximately 100 pg of RDX or PETN can be detected within one minute by these indicators in the solid state upon exposure to sunlight. The photonitration reaction presented herein is a unique and selective detection mechanism for nitroester and nitramine explosives that is distinct from a previously-reported photoreduction reaction to detect explosives. The rapid nitration of 9,9-diphenyl or -dimethyl substituted DHA chemosensors in the presence of RDX or PETN and the resulting strong, turn-on emission signal qualifies these DHAs as cheap, impermanent indicators for the selective, standoff identification of nitroester and nitramine explosives.

Experimental Section

Materials, Instrumentation and General Experimental Methods. Synthetic manipulations that required an inert atmosphere (where noted) were carried out under argon using standard Schlenk techniques. All solvents were of reagent grade or better unless otherwise noted. All solvents used for photophysical experiments were of spectroscopic grade. Anhydrous tetrahydrofuran, diethyl ether, toluene and dichloromethane were obtained from a dry solvent system. Spectroscopic-grade acetonitrile was degassed and stored over 4Å sieves. ^{1}H and ^{13}C NMR spectra for all compounds were acquired in $CHCl_3$ at 400 and 100 MHz, respectively. The chemical shift data are reported in units of δ (ppm) relative to tetramethylsilane (TMS) and referenced with residual $CHCl_3$. ^{19}F NMR spectra were recorded at 380 MHz. Trichlorofluoromethane was used as an external standard (0 ppm) and upfield shifts are reported as negative values. In some cases, signals associated with the CF_3 groups and proximal quaternary centers were not reported in the ^{13}C-NMR spectra due to C-F coupling and low signal-to-noise ratios. High-resolution mass spectra (HRMS) were obtained using a peak-matching protocol to determine the mass and error range of the molecular ion, employing either electron impact or electrospray as the ionization technique. GC-MS (electron impact mass spectrometer) data were recorded in the temperature range of 100-350 ^{o}C under a vacuum of at least 10^{-5} torr. GC retention times are reported in minutes. X-ray crystal structures were determined with graphite-monochromated Mo Kα radiation (λ = 0.71073 Å). All structures were solved by direct methods using SHELXS[26] and refined against F on all data by full-matrix least squares with SHELXL-97. All non-hydrogen atoms were refined anisotropically. All electrochemical measurements were made using a quasi-internal Ag wire reference electrode submerged in 0.01 M $AgNO_3$/0.1 M *n*-Bu_4NPF_6 in anhydrous MeCN. Typical CVs were recorded using a platinum button electrode as the working electrode and a platinum coil counter electrode. The ferrocene/ferrocenium (Fc/Fc^+) redox couple was used as an external reference. Ultraviolet-visible absorption spectra were corrected for background signal with either a solvent-filled cuvette (solutions) or a blank microscope slide (films). Fluorescence spectra were measured using either right-angle (solutions) or front-face (22.5°) detection (thin films). Fluorescence quantum yields were

determined by the optically dilute method[27] using quinine sulfate in 0.1M H_2SO_4 as a standard (Φ=0.53) and were corrected for solvent refractive index and absorption differences at the excitation wavelength. Fluorescence lifetimes were measured via frequency modulation using a 365 nm laser diode as the light source and the modulation of POPOP as a calibration reference. For photolysis experiments,[28] solutions were irradiated under air at 313 nm using either: (1) the Xenon lamp (450 W) from a fluorimeter, with the excitation slit set to 29.4 nm (the maximum value); (2) a 500 W Mercury Arc Lamp fitted with a 313 nm interference filter (or a 334 nm or 365 nm interference filter) and varying neutral density filters (0.5, 1.0 or 2.0 OD); or (3) a solar simulator equipped with a 450 W Xenon arc lamp, with a spectral output of 1.3 suns under AM 1.5 conditions. The first two light sources were calibrated with a potassium ferric oxalate actinometer.[29] For each measurement, reaction progress was also monitored in the dark to ensure that there was no thermal contribution to the nitration of aromatic amines by RDX and PETN. Each photolysis experiment was performed in triplicate. *N*-Phenylanthranilic acid was esterified following a literature procedure.[30] RDX and PETN were obtained from K-9 training units, which consisted of RDX/PETN adsorbed onto sand. RDX and PETN were extracted from the sand with spectral grade acetonitrile and precipitated by the addition of DI water. The solids thus isolated were recrystallized three times from chloroform / acetonitrile and stored in the dark at -4 ^{o}C.

***N,N*-Dimethyl-4-nitroaniline (DMNA).** A mixture of 0.4 mL DMA and 0.1g of either RDX or PETN were dissolved in 3.0 mL dry, degassed acetonitrile and the solution photolyzed with a xenon arc lamp at 313 nm for 60 minutes. The reaction mixture was sampled every 10 minutes to determine the GC yield of the DMNA product. Approximately 80% of DMNA (GC yield) was formed after 60 minutes of photolysis. The yellow DMNA was isolated by flash column chromatography using 50/50 hexanes/dichloromethane as an eluent. ^{1}H NMR (400 MHz, $CHCl_3$) δ 3.11 (s, 6H), 6.59 (d, J = 8.2 Hz, 2H), 8.09 (d, J = 8.2 Hz, 2H). ^{13}C NMR (100 MHz, $CHCl_3$) δ 40.2, 110.2, 126.0, 136.9, 154.3. HRMS (ESI) calc for $C_8H_{11}N_2O_2$ $[M+H]^+$ 167.0815, found 167.0819. IR (KBr plate) 695 (s), 750 (s), 820 (s), 1067 (m), 1118 (m), 1232 (m), 1347 (m), 1383 (w), 1456 (s), 1483 (s), 1582 (s), 1615 (w), 2924 (m) cm^{-1}.

General procedure for the synthesis of 9,9-disubstituted-9,10-dihydroacridines (**DHA1**-**4**). A flame-dried Schlenk flask was charged with 1.0 g methyl *N*-phenylanthranilate (**14**, 4.4 mmol) and 45 mL dry, degassed Et_2O under argon and cooled to 0 ^oC in an ice bath. 3.5 Equivalents of the appropriate Grignard reagent in Et_2O were added dropwise and the reaction allowed to stir at room temperature under argon for 3 d. After quenching with saturated ammonium chloride, the organic layer was separated, washed with brine and water and dried over $MgSO_4$, and the solvent evaporated under reduced pressure. The crude tertiary alcohol thus formed was carried on to the next step without purification. To the neat oil isolated from the previous step was added 1-2 mL of concentrated H_2SO_4 under argon and the reaction stirred at room temperature for 1 h under argon. After dilution with 30 mL DI H_2O the reaction was poured into a 10% (v/v) aqueous ammoniacal solution and extracted with ether (5 x 50 mL). The combined organic layers were washed with saturated sodium bicarbonate, brine and water and dried over $MgSO_4$, and the solvent evaporated under reduced pressure. The residue was purified by flash column chromatography to yield the desired compound.

9,9-Dimethyl-9,10-dihydroacridine (DHA1). Synthesized using 3.0 M methyl magnesium bromide in Et_2O and purified by flash column chromatography using gradient elution, starting with 10% dichloromethane in hexanes and progressing to 50% dichloromethane in hexanes. 0.41 g (45%) of a white solid was isolated. m.p. 120 ^oC. ^1H NMR (400 MHz, $CHCl_3$) δ 1.54 (s, 6H), 6.11 (s, 1H), 6.67 (dd, J = 0.8 Hz, 7.6 Hz, 2H), 6.90 (m, 2H), 7.09 (m, 2H), 7.37 (d, J = 7.6 Hz, 2H). ^{13}C NMR (100 MHz, $CHCl_3$) δ 30.7, 36.4, 113.6, 120.8, 125.7, 126.9, 129.3, 138.6. HRMS (ESI) calc for $C_{15}H_{15}N$ $[M+H]^+$ 210.1277, found 210.1284. IR(KBr plate) 745 (s), 886 (m), 1037 (m), 1318 (m), 1452 (m), 1479 (s), 1507 (m), 1580 (m), 1606 (m), 2966 (m), 3359 (m) cm^{-1}.

9,9-Diethyl-9,10-dihydroacridine (DHA2). Synthesized using 3.0 M ethyl magnesium bromide in Et_2O and purified by flash column chromatography using hexanes as the eluent. 0.36 g (35%) of a clear oil was isolated. ^1H NMR (400 MHz, $CHCl_3$) δ 0.91 (t, J = 7.6 Hz, 3H), 0.97 (t, J = 7.6 Hz, 3H), 2.24 (q, J = 7.6 Hz, 2H), 2.35 (q, J = 7.6 Hz, 2H), 5.74 (s, 1H), 6.90 (m, 3H), 7.06 (m, 5H). ^{13}C NMR (100 MHz, $CHCl_3$) δ 13.0, 13.1, 13.9, 14.8, 24.3, 31.7, 115.9, 116.8, 118.2, 118.5, 120.3, 120.5, 121.0, 121.2,

123.0, 124.9, 127.4, 127.5, 129.5, 129.7, 130.1, 130.2, 134.3, 140.1, 140.3, 141.2, 143.5, 143.7. HRMS (ESI) calc for $C_{17}H_{19}N$ $[M+H]^+$ 238.1590, found 238.1591. IR (KBr plate) 692 (m), 745 (s), 1309 (m), 1451 (m), 1507 (s), 1575 (m), 1593 (s), 2871 (m), 2930 (m), 2965 (m), 3041 (m), 3403 (m) cm^{-1}.

9,9-Diisopropyl-9,10-dihydroacridine (DHA3). Synthesized using 2.0 M isopropyl magnesium chloride in Et_2O and purified by flash column chromatography using hexanes as the eluent. 0.19 g (17%) of a clear oil was isolated. ^1H NMR (400 MHz, $CHCl_3$) δ 0.77 (d, *J* = 6.8 Hz, 3H), 1.02 (d, *J* = 6.8 Hz, 3H), 1.46 (s, 3H), 1.87 (s, 3H), 3.06 (septet, *J* = 6.8 Hz, 1H), 5.75 (s, 1H), 6.88 (m, 5H), 7.20 (m, 4H). ^{13}C NMR (100 MHz, $CHCl_3$) δ 19.7, 20.9, 22.4, 22.2, 30.6, 115.5, 118.6, 119.8, 121.2, 127.1, 129.5, 129.8, 130.0, 130.7, 136.8, 141.0, 143.5. HRMS (ESI) calc for $C_{19}H_{24}N$ $[M+H]^+$ 266.1903, found 266.1904. IR (KBr plate) 693 (s), 745 (s), 1079 (m), 1309 (s), 1450 (s), 1508 (s), 1576 (s), 1594 (s), 2961 (m), 3399 (s) cm^{-1}.

9,9-Diphenyl-9,10-dihydroacridine (DHA4). Synthesized using 3.0 M phenyl magnesium bromide in Et_2O and purified by flash column chromatography using gradient elution, starting with 10% dichloromethane in hexanes and progressing to 50% dichloromethane in hexanes. 0.83 g (57%) of a white solid was isolated. m.p. 230 ^oC. ^1H NMR (400 MHz, $CHCl_3$) δ 6.25 (s, 1H), 6.86 (m, 9H), 7.16 (m, 8H). ^{13}C NMR (100 MHz, $CHCl_3$) δ 30.1, 56.7, 113.5, 120.2, 125.6, 126.1, 126.2, 127.1, 127.4, 127.6, 127.6, 127.9, 128.5, 130.0, 130.2, 130.2, 139.7, 146.0, 149.3. HRMS (ESI) calc for $C_{25}H_{19}N$ $[M+H]^+$ 334.1590, found 334.1584. IR (KBr plate) 699 (m), 734 (m), 753 (m), 907 (m), 1315 (m), 1474 (s), 1604 (m), 3057 (w), 3393 (m) cm^{-1}.

Methyl *N*-methyl-*N*-phenylanthranilate (15). A flame-dried two-neck round bottom flask was charged with 8 g *N*-phenylanthranilic acid (37.5 mmol), 0.3 mL 15-crown-5, 300 mL dry THF and 100 mL dimethoxyethane under argon. The solution was cooled to 0 ^oC in an ice bath, 5 g of a 60 wt% dispersion of NaH in mineral oil (3 g NaH, 125 mmol) was added to the reaction mixture in small portions under argon and 15 mL dimethyl sulfate (19.99 g, 158 mmol) was added via syringe. After stirring at room temperature for 5 d under argon the reaction was poured carefully onto 800 g ice and extracted with Et_2O (5 x 50 mL). The organic layers were combined, washed thoroughly with saturated

sodium bicarbonate (3x 25 mL), brine and water, dried over $MgSO_4$ and the solvent evaporated under reduced pressure. The resulting oil was purified by flash column chromatography using gradient elution, starting with 100% hexanes and progressing to 30% dichloromethane in hexanes to yield 7.2 g (80%) of a yellow oil. ^{1}H NMR (400 MHz, $CHCl_3$) δ 3.28 (s, 3H), 3.58 (s, 3H), 6.63 (dd, J = 8.8 Hz, J = 1.2 Hz, 2H), 6.73 (td, , J = 6 Hz, J = 1.2 Hz, 1H), 7.16 (td, J = 7.2 Hz, J = 1.6 Hz, 2H), 7.27 (m, 2H), 7.53 (td, J = 8 Hz, J = 1.6 Hz, 1H), 7.79 (dd, J = 7.6 Hz, J = 1.6 Hz, 1H). ^{13}C NMR (100 MHz, $CHCl_3$) δ 40.5, 52.3, 114.4, 118.1, 125.4, 129.1, 129.2, 129.4, 131.6, 133.4, 148.3, 129.4, 167.7. HRMS (ESI) calc for $C_{15}H_{15}NO_2$ $[M+H]^+$ 242.1176, found 242.1170. IR (KBr plate) 2924 (s), 2853 (s), 1728 (m), 1594 (m), 1500 (m), 1454 (m), 1391 (w), 1253 (s), 1214 (s), 1062 (m), 1005 (m), 758 (m), 575 (m) cm^{-1}.

General procedure for the synthesis of 9,9-disubstituted-10-methyl-9,10-dihydroacridines (DHA5-9). A flame-dried Schlenk flask was charged with 1.0 g methyl *N*-methyl-*N*-phenylanthranilate (**15**, 4.1 mmol) and 45 mL dry, degassed Et_2O under argon and cooled to 0 ^oC in an ice bath. 2.5 Equivalents of the appropriate Grignard reagent in Et_2O was added dropwise and the reaction allowed to stir at room temperature under argon for 3 d. After quenching with saturated ammonium chloride, the organic layer was separated, washed with brine and water and dried over $MgSO_4$, and the solvent evaporated under reduced pressure. The crude tertiary alcohol thus formed was carried on to the next step without purification. To the neat oil isolated from the previous step was added 1-2 mL of concentrated H_2SO_4 under argon and the reaction stirred at room temperature for 1 h under argon. After dilution with 30 mL DI H_2O the reaction was poured into a 10% (v/v) aqueous ammoniacal solution and extracted with ether (5 x 50 mL). The combined organic layers were washed with saturated sodium bicarbonate, brine and water and dried over $MgSO_4$, and the solvent evaporated under reduced pressure. The residue was purified by flash column chromatography to yield the desired compound.

9,9-Dimethyl-10-methyl-9,10-dihydroacridine (DHA5). Synthesized using 3.0 M methyl magnesium bromide in Et_2O and purified by flash column chromatography using gradient elution, starting with 10% dichloromethane in hexanes and progressing to 50% dichloromethane in hexanes. 0.39 g (42%) of a light yellow solid was isolated. m.p. 93 ^oC. ^{1}H NMR (400 MHz, $CHCl_3$) δ 1.52 (s,

6H), 3.43 (s, 3H), 6.96 (m, 4H), 7.21 (m, 2H), 7.38 (d, *J* = 1.6 Hz, 2H). ^{13}C NMR (100 MHz, $CHCl_3$) δ 27.4, 33.5, 36.7, 112.3, 120.8, 123.8, 126.8, 132.8, 142.4. HRMS (ESI) calc for $C_{16}H_{17}N$ $[M+H]^+$ 224.1434, found 224.1429. IR (KBr plate) 751 (s), 1046 (m), 1268 (s), 1340 (s), 1450 (s), 1470 (s), 1590 (s), 2900 (m), 2950 (s), 2980 (s), 3050 (m) cm^{-1}.

9,9-Diethyl-10-methyl-9,10-dihydroacridine (DHA6). Synthesized using 3.0 M ethyl magnesium bromide in Et_2O and purified by flash column chromatography using hexanes as the eluent. 0.31 g (30%) of a clear oil was isolated. ^{1}H NMR (400 MHz, $CHCl_3$) δ 0.81 (t, *J* = 7.6 Hz, 3H), 0.84 (t, *J* = 7.6 Hz, 3H), 2.14 (q, *J* = 7.6 Hz, 2H), 2.27 (q, *J* = 7.6 Hz, 2H), 3.06 (s, 3H), 6.65 (m, 3H), 7.17 (m, 5H). ^{13}C NMR (100 MHz, $CHCl_3$) δ 14.2 (2), 14.3, 22.5, 22.8, 23.2, 23.4, 29.6, 30.4, 31.0, 31.2, 31.7, 37.1, 39.4, 39.6, 114.0, 114.1, 117.2, 117.3, 125.5, 125.9, 127.8, 128.1, 128.2, 128.4, 128.7, 128.9, 130.5, 132.0, 132.5, 140.0, 140.1, 141.5, 143.4, 146.1, 147.0, 149.3, 149.5. HRMS (ESI) calc for $C_{18}H_{21}N$ $[M+H]^+$ 252.1747, found 252.1742. IR (KBr plate) 692 (s), (748 (s), 1342 (m), 1444 (m), 1487 (s), 1500 (s), 1568 (m), 1592 (s), 1602 (s), 2810 (m), 2870 (m), 2963 (m), 3024 (m) cm^{-1}.

9,9-Diisopropyl-10-methyl-9,10-dihydroacridine (DHA7). Synthesized using 2.0 M isopropyl magnesium chloride in Et_2O and purified by flash column chromatography using hexanes as the eluent. 0.19 g (17%) of a clear oil was isolated. ^{1}H NMR (400 MHz, $CHCl_3$) δ 0.85 (d, *J* = 7.2 Hz, 3H), 0.89 (d, *J* = 7.6 Hz, 3H), 1.46 (s, 3H), 1.80 (s, 3H), 2.84 (septet, *J* = 7.2 Hz, 1H), 3.03 (s, 3H), 6.74 (m, 3H), 6.98 (m, 1H), 7.13 (m, 5H). ^{13}C NMR (100 MHz, $CHCl_3$) δ 21.6, 22.3, 23.8, 31.8, 39.0, 114.6, 117.4, 120.6, 121.4, 125.2, 127.4, 127.8, 128.0, 128.7, 129.4, 133.6, 140.0, 141.2, 147.2, 149.6. HRMS (ESI) calc for $C_{20}H_{25}N$ $[M+H]^+$ 280.2060, found 280.2058. IR (KBr plate) 748 (m), 1499 (m), 1601 (m), 2820 (m), 2910 (m) 3040 (m) cm^{-1}.

9,9-Diphenyl-10-methyl-9,10-dihydroacridine (DHA8). Synthesized using 3.0 M phenyl magnesium bromide in Et_2O and purified by flash column chromatography using gradient elution, starting with 10% dichloromethane in hexanes and progressing to 50% dichloromethane in hexanes. 0.79 g (55%) of a light yellow solid was isolated. m.p. 165 – 166 ^{o}C. ^{1}H NMR (400 MHz, $CHCl_3$) δ 3.29 (s, 3H), 6.84 (m, 2H), 6.91 (m, 8H), 7.18 (m, 6H), 7.26 (m, 2H). ^{13}C NMR (100 MHz, $CHCl_3$) δ 33.6,

57.3, 112.1, 120.0, 126.4, 127.4, 127.7, 130.1, 130.6, 131.4, 142.7, 146.2. HRMS (ESI) calc for $C_{26}H_{21}N$ $[M+H]^+$ 348.1747, found 348.1732. IR (KBr plate) 638 (m), 699 (m), 733 (m), 755 (m), 1270 (m), 1348 (m), 1468 (s), 1590 (m), 1589 (m), 2815 (w), 2873 (w), 3056 (m) cm^{-1}.

9,9-Di-*n*-octyl-10-methyl-9,10-dihydroacridine (DHA9). Synthesized using 2.0 M octyl magnesium bromide in Et_2O and purified by flash column chromatography using hexanes as the eluent. 0.7 g (40%) of a clear oil was isolated. ^1H NMR (400 MHz, $CHCl_3$) δ 0.85 (t, *J* = 7.6 Hz, 3H), 0.88 (t, *J* = 7.2 Hz, 3H), 1.22 (bm, 22H), 2.08 (q, *J* = 7.2 Hz, 2H), 2.25 (t, *J* = 7.6 Hz, 2H), two overlapping singlets: δ 3.08, 3.10, total 3H, 5.35 (t, *J* = 7.6 Hz, 1H), 6.67 (m, 3H), 7.17 (m, 6H). ^{13}C NMR (100 MHz, $CHCl_3$) δ 14.4, 22.9 (3), 28.3, 28.7, 29.0, 29.3, 29.5 (2), 29.6, 29.7 (2), 29.8, 30.0, 30.3, 31.1, 32.1 (2), 37.4, 39.4, 39.6, 114.0, 114.1, 117.2, 117.3, 125.5, 125.9, 128.0 (2), 128.2, 128.4, 128.6, 128.9,130.7, 132.0, 132.5, 140.0, 140.7, 141.3, 143.4, 146.1,146.9, 149.3, 149.5. HRMS (ESI) calc for $C_{30}H_{45}N$ $[M+H]^+$ 420.3625, found 420.3613. IR (KBr plate) 692 (m), 747 (m), 1095 (w), 1342 (m), 1499 (s), 1592 (s), 1602 (s), 2854 (s), 2924 (s), 2955 (s), 3024 (w) cm^{-1}.

2-Bromo-*N*-methyl-*N*-phenylaniline (18). A flame-dried two-neck round bottom flask was charged with 2-bromo-N-phenylaniline (3 g, 12.2 mmol), 0.1 mL 15-crown-5, 200 mL dry THF and 50 mL dimethoxyethane under argon. The solution was cooled to 0 ^oC in an ice bath, 0.6 g of a 60 wt% dispersion of NaH in mineral oil (0.36 g NaH, 15 mmol) was added to the reaction mixture in small portions under argon and 1.4 mL dimethyl sulfate (1.89 g, 15 mmol) was added via syringe. After refluxing for 20 h under argon the reaction was poured carefully onto 500 g ice and extracted with Et_2O (5 x 50 mL). The organic layers were combined, washed thoroughly with saturated sodium bicarbonate (3 x 25 mL), brine and water, dried over $MgSO_4$ and the solvent evaporated under reduced pressure. The resulting oil was purified by flash column chromatography using gradient elution, starting with 100% hexanes and progressing to 30% dichloromethane in hexanes to yield 2.5 g (80%) of a clear oil. ^1H NMR (400 MHz, $CHCl_3$) δ 3.22 (s, 3H), 6.56 (d, *J* = 7.6 Hz, 2H), 6.75 (t, *J* = 7.6 Hz, 1H), 7.15 (m, 3H), 7.25 (dd, *J* = 8.0 Hz, *J* = 2.0 Hz, 1H), 7.32 (td, *J* = 7.6 Hz, *J* = 1.2 Hz, 1H), 7.66 (dd, *J* = 8.0 Hz, *J* = 1.6 Hz, 1H). ^{13}C NMR (100 MHz, $CHCl_3$) δ 39.1, 113.5, 117.8, 124.4, 127.9, 128.4, 129.1, 129.2, 130.6,

134.3, 147.0, 148.7. HRMS (ESI) calc for $C_{13}H_{12}BrN$ $[M+H]^+$ 262.0226, found 262.0234. IR (KBr plate) 654 (s), 691 (s), 748 (s), 872 (s), 1139 (s), 1137 (s), 1273 (s), 1346 (s), 1438 (m), 1467 (s), 1499 (s), 1580 (s), 1601 (s), 2813 (m), 2824 (s), 3058 (m), 3089 (m) cm^{-1}.

9-Ethyl-9,10-dimethyl-9,10-dihydroacridine (DHA10). A flame-dried two-necked flask was charged with 2-bromo-*N*-methyl-*N*-phenylaniline (1.0 g, 3.8 mmol) and 100 mL dry THF under argon and cooled to -78 ^oC in a dry ice-acetone bath. 2.6 mL of a 1.6 M solution of *n*-BuLi in hexanes (4.16 mmol) was added dropwise over 5 minutes and the reaction stirred at -78 ^oC under argon for 1 h. Methyl ethyl ketone (0.302 g, 4.2 mmol) was added in one portion to the reaction mixture at -78 ^oC, the reaction allowed to warm to room temperature and stirred overnight under argon. After quenching with saturated ammonium chloride, the reaction was extracted with Et_2O, the organic layers combined, washed with brine and water and dried over anhydrous $MgSO_4$ and the solvent evaporated under reduced pressure. To the neat residue thus obtained was added 2 mL of concentrated H_2SO_4 under argon and the mixture stirred at room temperature for 1 h under argon. After dilution with 30 mL DI H_2O, the reaction was extracted with Et_2O (5 x 50 mL), the organic layers were combined, washed with brine and water and dried over anhydrous $MgSO_4$, and the solvent was evaporated under reduced pressure. The residue was purified by flash column chromatography using hexanes as the eluent to yield 0.57 g (57%) of the desired compound as a clear oil. ^1H NMR (400 MHz, $CHCl_3$) δ 1.66 (dd, J = 6.8 Hz, J = 0.8 Hz, 3H), 1.78 (t, J = 1.2 Hz, 3H), 3.10 (s, 3H), 5.49 (m, 1H), 6.66 (m, 3H), 7.18 (m, 6H). ^{13}C NMR (100 MHz, $CHCl_3$) δ 14.2, 15.2, 16.5, 24.2, 39.2, 39.6, 113.8, 114.1, 117.1, 117.4, 122.4, 124.4, 125.7, 125.9, 128.0, 128.2, 128.5, 128.8, 128.9, 130.6, 131.5, 136.4, 140.4, 144.3, 145.8, 146.9, 149.2, 149.4. HRMS (ESI) calc for $C_{17}H_{19}N$ $[M+H]^+$ 238.1590, found 238.1587. IR (KBr plate) 692 (m), 747 (m), 1345 (m), 1444 (m), 1499 (s), 1592 (s), 1602 (s), 2918 (m), 3024 (m) cm^{-1}.

9-Methyl-9-phenyl-10-methyl-9,10-dihydroacridine (DHA11). A flame-dried two-necked flask was charged with 2-bromo-*N*-methyl-*N*-phenylaniline (1.0 g, 3.8 mmol) and 100 mL dry THF under argon and cooled to -78 ^oC in a dry ice-acetone bath. 2.6 mL of a 1.6 M solution of *n*-BuLi in hexanes (4.16 mmol) was added dropwise over 5 minutes and the reaction stirred at -78 ^oC under argon for 1 h.

Acetophenone (0.49 mL, 0.51 g, 4.2 mmol) was added in one portion under argon at -78 ^{o}C, the reaction allowed to warm to room temperature and stirred overnight under argon. After quenching with saturated ammonium chloride, the reaction was extracted with Et_2O, the organic layers combined, washed with brine and water and dried over anhydrous $MgSO_4$ and the solvent evaporated under reduced pressure. To the neat residue thus obtained was added 2 mL of concentrated H_2SO_4 under argon and the mixture stirred at room temperature for 1 h under argon. After dilution with 30 mL DI H_2O, the reaction was extracted with Et_2O (5 x 50 mL), the organic layers were combined, washed with brine and water and dried over anhydrous $MgSO_4$, and the solvent was evaporated under reduced pressure. The desired product was purified by flash column chromatography using gradient elution, starting with 20% dichloromethane in hexanes and progressing to 50% dichloromethane in hexanes to yield 0.55 g (50%) of a light yellow solid. m.p. 184 ^{o}C. ^{1}H NMR (400 MHz, $CHCl_3$) δ 1.83 (s, 3H), 3.37 (s, 3H), 6.93 (m, 6H), 7.24 (m, 8H). ^{13}C NMR (100 MHz, $CHCl_3$) δ 27.4, 28.2, 31.2, 33.6, 112.1 (2), 112.3, 113.7, 113.9, 116.9, 120.0, 120.4, 120.8, 123.8, 126.2, 126.4, 126.76, 126.7, 127.1, 127.38, 127.5, 127.7, 127.8, 127.9, 128.0, 128.5, 128.7, 128.8, 128.9, 130.1, 130.5, 131.4, 132.5, 142.0, 142.7, 146.2, 148.9. HRMS (ESI) calc for $C_{21}H_{19}N$ $[M+H]^+$ 286.1590, found 286.1590. IR (KBr plate) 650 (m), 699 (m), 743 (m), 798 (m), 1290 (m), 1353 (m), 1468 (s), 1595 (m), 1631 (m), 2803 (w), 2898 (w), 3042 (m) cm^{-1}.

9-Isopropyl-9,10-dimethyl-9,10-dihydroacridine (DHA12). A flame-dried two-necked flask was charged with 2-bromo-*N*-methyl-*N*-phenylaniline (1.0 g, 3.8 mmol) and 100 mL dry THF under argon and cooled to -78 ^{o}C in a dry ice-acetone bath. 2.6 mL of a 1.6 M solution of *n*-BuLi in hexanes (4.16 mmol) was added dropwise over 5 minutes and the reaction stirred at -78 ^{o}C under argon for 1 h. Isopropyl methyl ketone (0.361 g, 4.2 mmol) was added in one portion to the reaction mixture at -78 ^{o}C, the reaction allowed to warm to room temperature and stirred overnight under argon. After quenching with saturated ammonium chloride, the reaction was extracted with Et_2O, the organic layers combined, washed with brine and water and dried over anhydrous $MgSO_4$ and the solvent evaporated under reduced pressure. To the neat residue thus obtained was added 2 mL of concentrated H_2SO_4 under argon and the mixture stirred at room temperature for 1 h under argon. After dilution with 30 mL DI H_2O, the

reaction was extracted with Et_2O (5 x 50 mL), the organic layers were combined, washed with brine and water and dried over anhydrous $MgSO_4$, and the solvent was evaporated under reduced pressure. The residue was purified by flash column chromatography using hexanes as the eluent to yield 0.62 g (60%) of the desired compound as a clear oil. ^{1}H NMR (400 MHz, $CHCl_3$) δ 1.51 (s, 3H), 1.64 (s, 3H), 1.70 (s, 3H), 3.04 (s, 3H), 6.64 (m, 3H), 7.12 (m, 6H). ^{13}C NMR (100 MHz, $CHCl_3$) δ 21.5, 22.2, 23.8, 31.8, 39.0, 114.6, 117.4, 120.6, 121.4, 125.1, 127.4, 127.8, 128.0, 128.7, 129.3, 133.6, 140.0, 141.1, 147.2, 149.5. HRMS (ESI) calc for $C_{18}H_{21}N$ $[M+H]^+$ 252.1747, found 252.1742. IR (KBr plate) 692 (m), 747 (s), 1137 (m), 1342 (m), 1443 (m), 1486 (s), 1499 (s), 1591 (s), 1601 (s), 2911 (m), 2984 (m) cm^{-1}.

9-Ethyl-9-phenyl-10-methyl-9,10-dihydroacridine (DHA13). A flame-dried two-necked flask was charged with 2-bromo-*N*-methyl-*N*-phenylaniline (1.0 g, 3.8 mmol) and 100 mL dry THF under argon and cooled to -78 ^{o}C in a dry ice-acetone bath. 2.6 mL of a 1.6 M solution of *n*-BuLi in hexanes (4.16 mmol) was added dropwise over 5 minutes and the reaction stirred at -78 ^{o}C under argon for 1 h. Propiophenone (0.56 mL, 0.56 g, 4.2 mmol) was added in one portion to the reaction mixture under argon at -78 ^{o}C, the reaction allowed to warm to room temperature and stirred overnight under argon. After quenching with saturated ammonium chloride, the reaction was extracted with Et_2O, the organic layers combined, washed with brine and water and dried over anhydrous $MgSO_4$ and the solvent evaporated under reduced pressure. To the neat residue thus obtained was added 2 mL of concentrated H_2SO_4 under argon and the mixture stirred at room temperature for 1 h under argon. After dilution with 30 mL DI H_2O, the reaction was extracted with Et_2O (5 x 50 mL), the organic layers were combined, washed with brine and water and dried over anhydrous $MgSO_4$, and the solvent was evaporated under reduced pressure. The desired product was purified by flash column chromatography using 10% dichloromethane in hexanes as the eluent to yield 0.62 g (55%) of a light yellow oil. ^{1}H NMR (400 MHz, $CHCl_3$) δ 0.74 (t, *J* = 7.2 Hz, 3H), 2.22 (q, *J* = 7.2 Hz, 2H), 3.38 (s, 3H), 6.75 (m, 4H), 6.89 (m, 2H), 7.17 (m, 3H), 7.27 (m, 4H). ^{13}C NMR (100 MHz, $CHCl_3$) δ 9.7, 33.8, 34.6, 50.5, 111.9, 113.1, 113.8, 114.0, 116.9, 119.9, 125.4, 125.6, 125.9, 126.4, 126.5, 126.6, 126.7, 127.0, 127.3, 127.5, 127.8, 127.9, 128.2, 128.3, 128.8, 128.9, 129.2, 129.4, 129.6, 130.2, 132.9, 138.7, 141.3, 142.0, 143.5, 147.3,

148.5, 149.5. HRMS (EI) calc for $C_{22}H_{21}N$ $[M]^+$ 299.1669, found 299.1673. IR (KBr plate) 633 (m), 693 (s), 747 (s), 1032 (w), 1260 (w), 1349 (m), 1448 (m), 1499 (s), 1575 (m), 1590 (s), 1601 (s), 2927 (m), 3024 (m) cm^{-1}.

10-methyl-10*H*-spiro[acridine-9,1'-cyclohexane] (DHA14). A flame-dried two-necked flask was charged with 2-bromo-*N*-methyl-*N*-phenylaniline (1.0 g, 3.8 mmol) and 100 mL dry THF under argon and cooled to -78 ^oC in a dry ice-acetone bath. 2.6 mL of a 1.6 M solution of *n*-BuLi in hexanes (4.16 mmol) was added dropwise over 5 minutes and the reaction stirred at -78 ^oC under argon for 1 h. Cyclohexanone (0.43 mL, 0.412 g, 4.2 mmol) was added in one portion to the reaction mixture at -78 ^oC, the reaction allowed to warm to room temperature and stirred overnight under argon. After quenching with saturated ammonium chloride, the reaction was extracted with Et_2O, the organic layers combined, washed with brine and water and dried over anhydrous $MgSO_4$ and the solvent evaporated under reduced pressure. To the neat residue thus obtained was added 2 mL of concentrated H_2SO_4 under argon and the mixture stirred at room temperature for 1 h under argon. After dilution with 30 mL DI H_2O, the reaction was extracted with Et_2O (5 x 50 mL), the organic layers were combined, washed with brine and water and dried over anhydrous $MgSO_4$, and the solvent was evaporated under reduced pressure. The residue was purified by flash column chromatography using hexanes as the eluent to yield 0.3 g (30%) of the desired compound as a clear oil. ^1H NMR (400 MHz, $CHCl_3$) δ 1.53 (m, 4H), 2.10 (m, 4H), 3.12 (s, 3H), 5.65 (m, 1H), 6.66 (m, 3H), 7.18 (m, 6H). ^{13}C NMR (100 MHz, $CHCl_3$) δ 22.0, 23.0, 25.6, 28.2, 39.2, 113.7, 116.9, 125.6, 126.3, 127.7, 128.2, 128.5, 130.3, 137.9, 142.8, 145.6, 149.0. HRMS (ESI) calc for $C_{19}H_{21}N$ $[M+H]^+$ 264.1747, found 264.1758. IR (KBr plate) 693 (m), 747(m), 1069 (s), 1155 (m), 1263 (m), 1345 (m), 1499 (s), 1602(s), 2853 (m), 2921 (s) cm^{-1}.

1,1,1,3,3,3-hexafluoro-2-(2-(methyl(phenyl)amino)phenyl)propan-2-ol (21). A flame-dried two-necked flask equipped with a dry ice/acetone condenser was charged with 2-bromo-*N*-methyl-*N*-phenylaniline (1.0 g, 3.8 mmol) and 100 mL dry THF under argon and cooled to -78 ^oC in a dry ice-acetone bath. 2.6 mL of a 1.6 M solution of *n*-BuLi in hexanes (4.16 mmol) was added dropwise over 5 minutes and the reaction stirred at -78 ^oC under argon for 1 h. Making sure that the dry ice/acetone

condenser remained filled, anhydrous hexafluoroacetone (HFA) gas was bubbled into the reaction flask at -78 ^{o}C under a positive pressure of argon for a total duration of 3 minutes; the pressure reading on the HFA tank was noted to be 22 psi. The reaction was allowed to warm to room temperature and the HFA allowed to reflux for an additional 3 h (making sure the dry ice/acetone condenser remained full for the duration) after which the excess HFA was removed by bubbling through a saturated KOH solution for 1 h. The reaction was quenched with saturated ammonium chloride and extracted with Et_2O (3 x 50 mL). The organic layers were combined, washed with brine and water and dried over $MgSO_4$, and the solvent was evaporated under reduced pressure. The residue was purified by flash column chromatography using 50% dichloromethane in hexanes as the eluent to yield g 1.1 g (80%) of the desired compound as a white crystalline solid after drying in vacuo for 3d. ^{1}H NMR (400 MHz, $CHCl_3$) δ 3.08 (s, 3H), 6.87 (dd, *J* = 8.0 Hz, *J* = 1.6 Hz, 2H), 6.98 (m, 2H), 7.21 (m, 2H), 7.36 (m, 2H), 7.75 (d, *J* = 8.0 Hz, 1H), 11.51 (s, 1H). ^{13}C NMR (100 MHz, $CHCl_3$) δ 40.3, 80.3 (quintet), 115.0, 115.5, 118.8, 119.2 (2), 119.4, 120.6 121.5, 121.6, 122.0, 122.1, 122.9, 124.9 (3), 127.2, 127.7, 127.8, 127.9, 128.3, 128.9 (2), 129.0, 129.2, 129.3, 129.4, 129.6, 132.3, 149.2, 151.6. ^{19}F NMR (380 MHz, $CHCl_3$) δ -76.4, -75.1. HRMS (ESI) calc for $C_{16}H_{13}F_6NO$ $[M+H]^+$ 350.0974, found 350.0961. IR (KBr plate) 479 (m), 693 (s), 709 (s), 754 (s), 848 (m), 936 (m), 954 (s), 968 (s), 1121 (s), 1147 (m), 1192 (s), 1260 (s), 1496 (s), 1577 (m), 1603 (m), 2719 (m), 2973 (m), 3066 (m), 3854 (broad) cm^{-1}.

10-methyl-9,9-bis(trifluoromethyl)-9,10-dihydroacridine (DHA15). 1,1,1,3,3,3-hexafluoro-2-(2-(methyl(phenyl)amino)phenyl)propan-2-ol (0.2 g, 0.57 mmol) was dissolved in 15 mL $POCl_3$ and the solution refluxed under argon for 3 d. Excess $POCl_3$ was distilled off using a short path distillation head, the residue was dissolved in $CHCl_3$, poured into a 10% (v/v) aqueous ammoniacal solution and the biphasic system stirred at room temperature for one hour. The organic layer was separated and the aqueous layer extracted with Et_2O (3 x 50 mL). The organic layers were combined, washed with brine and water and dried over $MgSO_4$, and the solvent evaporated under reduced pressure. The residue was purified by flash column chromatography using 10% dichloromethane in hexanes as the eluent to yield 0.15 g (80%) of the desired compound as a light-blue oil. ^{1}H NMR (400 MHz, $CHCl_3$) δ 3.46 (s, 3H),

7.00 (m, 4H), 7.42 (m, 2H), 7.89 (m, 2H). ^{13}C NMR (100 MHz, $CHCl_3$) δ 29.8, 35.1, 111.8, 114.7, 120.3, 130.3 (quintet), 130.7, 141.8. ^{19}F NMR (380 MHz, $CHCl_3$) δ -65.9. HRMS (EI) calc for $C_{16}H_{11}F_6N$ $[M]^+$ 332.0868, found 332.0874. IR (KBr plate) 479 (m), 693 (s), 709 (s), 758 (s), 848 (m), 954 (s), 1116 (s), 1163 (m), 1192 (s), 1260 (s), 1489 (s), 1573 (m), 1594 (m), 2840 (m), 2972 (m), 3054 (m) cm^{-1}.

Methyl *N*-(*p*-tolyl)-*N*-phenylanthranilate (22). A flame-dried Schlenk flask was charged with **14** (5 g, 22 mmol), 4-bromotoluene (3 mL, 4.17 g, 24 mmol), copper powder (1.56 g, 24 mmol), copper (I) iodide (100 mg), potassium carbonate (3.3 g, 24 mmol), and 5 mL hexyl ether under argon. The resulting mixture was heated to 190 ^{o}C in a sand bath for 24 h. Upon cooling to room temperature, the reaction mixture was diluted with dichloromethane, passed through a celite plug and the solvents evaporated under reduced pressure. The residual oil thus obtained was purified by flash column chromatography (30% dichloromethane in hexanes) to yield 5.2 g (75%) of an off-white solid. m.p. 110-111 ^{o}C. ^{1}H NMR (400 MHz, $CHCl_3$) δ 2.28 (s, 3H), 3.42 (s, 3H), 6.91 (m, 7H), 7.15 (m, 4H), 7.39 (t, J = 7.6 Hz, 1H), 7.66 (d, J = 7.6 Hz, 1H). ^{13}C NMR (100 MHz, $CHCl_3$) δ 20.7, 51.7, 121.6, 122.0, 123.5, 123.8, 128.5, 128.7, 128.8, 129.6, 131.1, 132.1, 132.5, 145.1, 146.7, 148.0, 167.9. HRMS (EI) calc for $C_{21}H_{19}NO_2$ $[M+H]^+$ 318.1489, found 318.1481. IR (KBr plate) 693 (m), 713 (m), 753 (m), 813 (m), 1085 (m), 1125 (m), 1244 (s), 1271 (s), 1289 (s), 1320 (s), 1448 (s), 1492 (s), 1508 (s), 1594 (s), 1722 (s), 2947 (m), 3026 (m) cm^{-1}.

9,9-Dimethyl-10-(*p*-tolyl)-9,10-dihydroacridine (DHA16) + 2,9,9-Trimethyl-10-phenyl-9,10-dihydroacridine (DHA17). A flame-dried Schlenk flask was charged with 1.0 g methyl *N*-(*p*-tolyl)-*N*-phenylanthranilate (**22**, 3.1 mmol) and 45 mL dry, degassed Et_2O under argon and cooled to 0 ^{o}C in an ice bath. 2.5 Equivalents of 3.0 M methyl magnesium bromide in Et_2O (2.7 mL) was added dropwise and the reaction allowed to stir at room temperature under argon for 3 d. After quenching with saturated ammonium chloride, the organic layer was separated, washed with brine and water and dried over $MgSO_4$, and the solvent evaporated under reduced pressure. The crude tertiary alcohol thus formed was carried on to the next step without purification. To the neat oil isolated from the previous step was added

1-2 mL of concentrated H_2SO_4 under argon and the reaction stirred at room temperature for 1 h under argon. After dilution with 30 mL DI H_2O the reaction was poured into a 10% (v/v) aqueous ammoniacal solution and extracted with ether (5 x 50 mL). The combined organic layers were washed with saturated sodium bicarbonate, brine and water and dried over $MgSO_4$, and the solvent evaporated under reduced pressure. The residue was purified by flash column using gradient elution, starting with 10% dichloromethane in hexanes and progressing to 50% dichloromethane in hexanes. 0.52 g (55%) of a mixture of **DHA16** and **DHA17** as white solid was isolated. **DHA16** and **DHA17** could not be separated from each other. m.p. 100-102 ^oC. ^1H NMR (400 MHz, $CHCl_3$) δ 1.66 (s, 9H), 2.27 (s, 3H), 2.46 (s, 3H), 6.13 (d, *J* = 8.4 Hz, 1H), 6.22 (dd, *J* = 1.2, 8.0 Hz, 1H), 6.26 (dd, *J* = 1.2 Hz, 8.0 Hz, 1H), 6.74 (dd, *J* = 1.2, 8.0 Hz, 1H), 6.92 (m, 5H), 7.18 (d, *J* = 8.4 Hz, 2 H), 7.30 (d, *J* = 8.4 Hz, 2H), 7.43 (m, 5H), 7.59 (m, 2H). ^{13}C NMR (100 MHz, $CHCl_3$) δ 21.0, 21.6, 31.5, 31.6, 35.0, 36.2, 114.1, 114.3, 114.3, 120.4, 120.6, 125.4, 125.5, 126.1, 126.5, 126.6, 127.2, 128.4, 129.8, 130.1, 130.1, 130.2, 131.1, 131.2, 131.6, 131.8, 138.2, 138.7, 139.0, 141.3, 141.7. HRMS (ESI) calc for $C_{22}H_{21}N$ $[M+H]^+$ 300.1747, found 300.1756. IR (KBr plate) 745 (s), 886 (m), 1037 (m), 1318 (m), 1452 (m), 1479 (s), 1507 (m), 1580 (m), 1606 (m), 2966 (m) cm^{-1}.

Methyl *N*-(2-mesityl)-*N*-phenylanthranilate (24). A flame-dried Schlenk flask was charged with **14** (5 g, 22 mmol), 2-bromomesitylene (3.67 mL, 4.77 g, 24 mmol), copper powder (1.56 g, 24 mmol), copper (I) iodide (100 mg), potassium carbonate (3.3 g, 24 mmol), and 5 mL hexyl ether under argon. The resulting mixture was heated to 190 ^oC in a sand bath for 24 h. Upon cooling to room temperature, the reaction mixture was diluted with dichloromethane, passed through a celite plug and the solvents evaporated under reduced pressure. The residual oil thus obtained was purified by flash column chromatography (30% dichloromethane in hexanes) to yield 4.18 g (55%) of an off-white solid. m.p. 90 ^oC. ^1H NMR (400 MHz, $CHCl_3$) δ 2.03 (s, 6H), 2.30 (s, 3H), 3.26 (s, 3H), 6.65 (dd, *J* = 0.8 Hz, 8.4 Hz, 1H), 6.81 (m, 3H), 6.93 (m, 3H), 7.11 (m, 2H), 7.21 (m, 1H), 7.60 (dd, *J* = 1.6, 7.6 Hz, 1H). ^{13}C NMR (100 MHz, $CHCl_3$) δ 19.0, 21.2, 51.5, 114.2, 117.3, 119.4, 121.1, 121.3, 122.5, 122.7, 123.2, 129.0, 129.3, 129.3, 129.6, 130.3, 130.5, 131.4, 131.9, 132.7, 134.3, 136.4, 136.9, 137.8, 138.1, 140.9, 145.0,

148.4, 168.9. HRMS (EI) calc for $C_{23}H_{23}NO_2$ $[M+H]^+$ 346.1802, found 346.1804. IR (KBr plate) 741 (m), 756 (m), 1238 (m), 1319 (m), 1448 (s), 1483 (s), 1593 (s), 1719 (s), 2857 (m), 2918 (m), 2948 (m), 3026 (m) cm^{-1}.

9,9-Dimethyl-10-(2-mesityl)-9,10-dihydroacridine (DHA18). A flame-dried Schlenk flask was charged with 1.0 g methyl *N*-(2-mesityl)-*N*-phenylanthranilate (**24**, 2.9 mmol) and 45 mL dry, degassed Et_2O under argon and cooled to 0 ^oC in an ice bath. 2.5 Equivalents of 3.0 M methyl magnesium bromide in Et_2O (2.4 mL) was added dropwise and the reaction allowed to stir at room temperature under argon for 3 d. After quenching with saturated ammonium chloride, the organic layer was separated, washed with brine and water and dried over $MgSO_4$, and the solvent evaporated under reduced pressure. The crude tertiary alcohol thus formed was carried on to the next step without purification. To the neat oil isolated from the previous step was added 1-2 mL of concentrated H_2SO_4 under argon and the reaction stirred at room temperature for 1 h under argon. After dilution with 30 mL DI H_2O the reaction was poured into a 10% (v/v) aqueous ammoniacal solution and extracted with ether (5 x 50 mL). The combined organic layers were washed with saturated sodium bicarbonate, brine and water and dried over $MgSO_4$, and the solvent evaporated under reduced pressure. The residue was purified by flash column using gradient elution, starting with 10% dichloromethane in hexanes and progressing to 50% dichloromethane in hexanes. 0.57 g (60%) of a white solid was thus isolated. m.p. 85 ^oC. ^1H NMR (400 MHz, $CHCl_3$) δ 1.69 (s, 6H), 1.96 (s, 6H), 2.37 (s, 3H), 6.07 (dd, J = 1.6, 8.4 Hz, 2H), 6.90 (m, 4H), 7.06 (s, 2H), 7.44 (dd, J = 1.6, 7.6 Hz, 2H). ^{13}C NMR (100 MHz, $CHCl_3$) δ 18.0, 20.2, 21.4, 33.5, 36.1, 112.7, 119.8, 120.4, 120.7, 126.3, 127.2, 128.6, 128.6, 129.3, 129.7, 130.4, 135.2, 138.1, 138.5, 138.7. HRMS (ESI) calc for $C_{22}H_{21}N$ $[M+H]^+$ 300.1747, found 300.1756. IR (KBr plate) 745 (s), 886 (m), 1315 (m), 1484 (s), 1507 (m), 1580 (m), 1606 (m), 2966 (m) cm^{-1}.

10,10'-dimethyl-9,9,9',9'-tetraphenyl-9,9',10,10'-tetrahydro-2,2'-biacridine (D1). A flame-dried Schlenk flask was charged with **DHA8** (1.0 g, 2.8 mmol) and 10 mL dry dichloromethane under argon. Triethyloxonium hexachloroantimonate (1.26 g, 2.8 mmol) was added to this solution in one portion under argon. The reaction was stirred at room temperature for 12 h. A 10% aqueous solution of sodium

thiosulfate was then added, the organic layer separated, washed with brine and water and dried over $MgSO_4$, and the solvent evaporated under reduced pressure. The residue was purified by flash column using 50% dichloromethane in hexanes as eluent. 0.40 g (40%) of a faint-yellow solid was thus isolated. m.p. 340 ^oC (decomp.). ^1H NMR (400 MHz, $CHCl_3$) δ 3.27 (s, 6H), 6.88 (m, 18H), 7.17 (m, 16H). ^{13}C NMR (100 MHz, $CHCl_3$) δ 33.6, 57.4, 112.0, 112.4, 120.0, 125.3, 125.9, 126.3, 126.5, 127.4, 127.5, 127.7, 127.9, 128.3, 128.7, 130.2, 130.3, 130.5, 131.3, 131.8, 132.7, 141.5, 142.7, 146.0. HRMS (ESI) calc for $C_{52}H_{41}N_2$ $[M+H]^+$ 693.3264, found 693.3267. IR (KBr plate) 638 (m), 697 (m), 733 (m), 755 (m), 1270 (m), 1357 (m), 1463 (s), 1590 (m), 1589 (m), 2815 (w), 2873 (w), 3056 (m) cm^{-1}.

9,9-Dimethyl-2-nitro-9,10-dihydroacridine (26). A mixture of 0.5 g **DHA1** (2.3 mmol) and 0.8 g of either RDX or PETN were dissolved in 3.0 mL dry, degassed acetonitrile and the solution photolyzed with a solar simulator (1.3 suns AM 1.5) for 60 minutes. The reaction mixture was sampled every 10 minutes to determine the GC yield of the nitrated product. Approximately 80% of **26** (GC yield) was formed after 60 minutes of photolysis. Compound **26** was isolated by flash column chromatography using 50/50 hexanes/dichloromethane as an eluent. ^1H NMR (400 MHz, $CHCl_3$) δ 1.62 (s, 6H), 6.64 (s, 1H), 6.69 (d, *J* = 8.8 Hz, 1H), 6.75 (d, *J* = 8.8 Hz, 1H), 7.03 (m, 1H), 7.15 (m, 1H), 7.40 (d, *J* = 7.6 Hz, 1H), 8.02 (dd, *J* = 2.4, 8.8 Hz, 1H), 8.30 (s, 1H). ^{13}C NMR (100 MHz, $CHCl_3$) δ 30.7, 36.4, 113.6, 121.8, 126.7, 127.9, 130.2, 148.6. HRMS (ESI) calc for $C_{15}H_{14}N_2O_2$ $[M+H]^+$ 255.1128, found 255.1123. IR (KBr plate) 753 (s), 1053 (m), 1232 (m), 1347 (m), 1383 (w), 1456 (s), 1483 (s), 1582 (s), 1615 (w), 2924 (m) cm^{-1}.

2-Nitro-9,9-diphenyl-9,10-dihydroacridine (28). Method A. A mixture of 0.5 g **DHA4** (1.5 mmol) and 0.8 g of either RDX or PETN were dissolved in 3.0 mL dry, degassed acetonitrile and the solution photolyzed with a solar simulator (1.3 suns AM 1.5) for 60 minutes. The reaction mixture was sampled every 10 minutes to determine the GC yield of the nitrated product. Approximately 80% of **28** (GC yield) was formed after 60 minutes of photolysis. Compound **28** was isolated by flash column chromatography using 50/50 hexanes/dichloromethane as an eluent. ^1H NMR (400 MHz, $CHCl_3$) δ 7.12 (broad m, 16H), 8.02 (dd, *J* = 8.8, 2.2 Hz, 1H), 8.30 (d, *J* = 2.2 Hz, 1H). ^{13}C NMR (100 MHz, $CHCl_3$) δ

56.7, 113.5, 120.2, 125.6, 126.1, 126.2, 127.1, 127.4, 127.5, 127.6, 127.9, 128.5, 131.0, 133.2, 137.3, 142.7, 146.0, 149.3. HRMS (ESI) calc for $C_{25}H_{19}N_2O_2$ $[M+H]^+$ 379.1441, found 379.1447. IR (KBr plate) 699 (m), 762 (m), 907 (m), 1300 (m), 1330 (m), 1483 (s), 1529 (m), 1585 (s), 2922 (m), 3410 (m) cm^{-1}.

2-Nitro-9,9-diphenyl-9,10-dihydroacridine (28). Method B. Compound **28** was also synthesized by nitrating **DHA4**: A 25 mL round bottom flask was charged with 0.5 g **DHA4** (1.5 mmol) and 20 mL dry dichloromethane under argon and the solution was cooled to -78 ^oC in an acetone/dry ice bath. Approximately 0.2 g of 25% HNO_3 on silica gel was then added to the solution and the reaction stirred at -78^oC for 1 h. Upon warming to room temperature, the reaction was filtered and the solvent evaporated under reduced pressure. The residue was purified by flash column chromatography using 50/50 hexanes/dichloromethane as eluent. 40% of the mononitrated product (**28**) and 30% of the dinitrated product was thus isolated.

9,9-Dimethyl-2-nitro-10-(2-mesityl)-9,10-dihydroacridine (30). A mixture of 0.5 g **DHA18** (1.5 mmol) and 0.8 g of either RDX or PETN were dissolved in 3.0 mL dry, degassed acetonitrile and the solution photolyzed with a solar simulator (1.3 suns AM 1.5) for 60 minutes. The reaction mixture was sampled every 10 minutes to determine the GC yield of the nitrated product. Approximately 82% of **30** (GC yield) was formed after 60 minutes of photolysis. Compound **30** was isolated by flash column chromatography using 50/50 hexanes/dichloromethane as an eluent. ^1H NMR (400 MHz, $CHCl_3$) δ 1.74 (s, 6H), 1.96 (s, 6H), 2.41 (s, 3H), 6.11 (d, J = 9.2 Hz, 1H), 6.17 (dd, J = 2.8, 8.0 Hz, 1H), 7.01 (m, 2H), 7.11 (s, 2H), 7.48 (m, 1H), 7.84 (dd, J = 2.4, 9.2 Hz, 1H), 8.36 (d, J = 2.8 Hz, 1H). ^{13}C NMR (100 MHz, $CHCl_3$) δ 17.8, 21.4, 33.6, 36.3, 68.8, 112.4, 113.8, 122.8,123.2, 123.9, 126.4, 127.7, 129.7, 130.0, 130.7, 134.1, 137.0, 137.5, 139.1, 141.0, 144.1. HRMS (ESI) calc for $C_{24}H_{25}N_2O_2$ $[M+H]^+$ 373.1911, found 373.1913. IR (KBr plate) 750 (m) 848 (m), 1289 (s), 1306 (s), 1320 (s), 1475 (s), 1496 (s), 1592 (m), 1651 (s), 2918 (m), 2969 (m) cm^{-1}.

9,9-Diethyl-2-nitro-9,10-dihydroacridine (31) and 9-Ethyl-9-vinyl-9,10-dihydroacridine (33). A mixture of 0.5 g **DHA2** (2.1 mmol) and 0.8 g of either RDX or PETN were dissolved in 3.0 mL dry,

degassed acetonitrile and the solution photolyzed with a solar simulator (1.3 suns AM 1.5) for 60 minutes. Compounds **31** and **33** were isolated by flash column chromatography using 50/50 hexanes/dichloromethane as an eluent. Compound **33** co-eluted with unreacted **DHA2** and, therefore, could not be completely separated from **DHA2**. **Compound 31**: ^{1}H NMR (400 MHz, $CHCl_3$) δ 0.59 (t, *J* = 7.2 Hz, 6H), 1.96 (quartet, *J* = 7.2 Hz, 4H), 6.47 (s, 1H), 6.60 (d, *J* = 8.8 Hz, 1H), 6.67 (d, *J* = 1.2 Hz, 1H), 7.00 (m, 1H), 7.12 (m, 1H), 7.24 (m, 1H), 7.97 (d, *J* = 2.8 Hz, 1H), 8.00 (s, 1H). ^{13}C NMR (100 MHz, $CHCl_3$) δ 9.7, 38.8, 46.3, 112.9, 114.1, 122.8, 123.9, 124.1, 124.5, 125.2, 127.0, 127.4, 137.6, 145.2. HRMS (ESI) calc for $C_{17}H_{19}N_2O_2$ $[M+H]^+$ 283.1441, found 283.1443. IR (KBr plate) 746 (m), 823 (m), 1242 (s), 1282 (s), 1294 (s), 1329 (m), 1462 (m), 1487 (s), 1530 (s), 1578 9s), 1609 (m), 2932 (m), 2968 (m), 3352 (s) cm^{-1}. **Compound 33**: ^{1}H NMR (400 MHz, $CHCl_3$) δ 0.91 (t, *J* = 7.6 Hz, 3H), 0.97 (t, *J* = 7.6 Hz, 3H), 1.48 (d, *J* = 6.8 Hz, 2H), 1.79 (d, *J* = 6.8 Hz, 3H), 2.24 (q, *J* = 7.6 Hz, 2H), 2.35 (q, *J* = 7.6 Hz, 2H), 5.48 (m, 1H), 5.72 (m, 1H), 5.74 (s, 1H), 6.90 (m, 4H), 7.06 (m, 5H). ^{13}C NMR (100 MHz, $CHCl_3$) δ 13.0, 13.1, 13.9, 14.8, 24.3, 31.7, 115.9, 116.8, 118.2, 118.5, 120.3, 120.5, 121.0, 121.2, 123.0, 124.9, 127.4, 127.5, 129.5, 129.7, 130.1, 130.2, 134.3, 140.1, 140.3, 141.2, 143.5, 143.7. HRMS (ESI) calc for $C_{17}H_{17}N$ $[M+H]^+$ 236.1434, found 236.1438. IR (KBr plate) 692 (m), 745(m), 1309(m), 1451 (m), 1506(s), 1575 (m), 1594 (s), 2925(m), 2963(m), 3405 (m) cm^{-1}.

Acknowledgement. T.L.A. would like to thank the Chesonis Family Foundation and the Corning Foundation for graduate fellowships. The authors thank Dr. Lindsey E. McQuade from the Lippard Laboratory for providing samples of NO and Corning Inc. for donating samples of Vycor glass slides. Financial support for this work was also provided by the Army Research Office and the National Science Foundation (ECCS – 0731100).

Supporting Information Available. Additional tables and figures, experimental procedures, spectral characterization data, and crystallographic information file. This material is available free of charge via the Internet at http://pubs.acs.org.

TOC graphic.

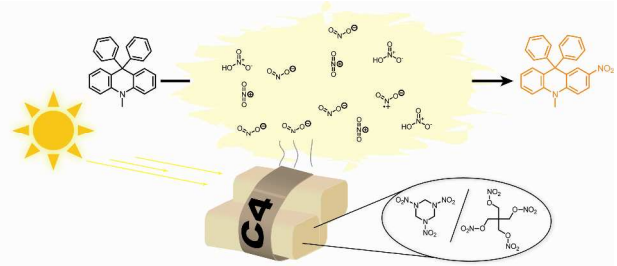

References and Notes

(1) Jungreis, E. in *Spot Test Analysis: Clinical, Environmental, Forensic, and Geochemical Applications*, 2nd ed., J Wiley, New York, **1997**.

(2) For representative examples see: (a) Che, Y.; Yang, X.; Liu, G.; Yu, C.; Ji, H.; Zuo, J.; Zhao, J.; Zang, L. *J. Am. Chem. Soc*. **2010**, *132*, 5743-5750. (b) Lan, A.; Li, K.; Wu, H.; Olson, D. H.; Emge, T. J.; Ki, W.; Hong, M.; Li, J. *Angew. Chem. Int. Ed*. **2009**, *48*, 2334-2338. (c) Tao, S.; Yin, J.; Li, G. *J. Mater. Chem*. **2008**, *18*, 4872-4878.

(3) (a) Toal, S. J.; Trogler, W. C. *J. Mater. Chem*. **2006**, *16*, 2871-2883. (b) Yang, J.-S.; Swager, T. M. *J. Am. Chem. Soc*. **1998**, *120*, 5321-5322.

(4) Engel, Y.; Elnathan, R.; Pevzner, A.; Davidi, G.; Flaxer, E.; Patolsky, F. *Angew. Chem. Int. Ed*. **2010**, *49*, 6830-6835.

(5) (a) Bruschini, C. *Subsurf. Sens. Technol. Appl*. **2001**, *2*, 299-336. (b) Takats, Z.; Cotte-Rodriguez, I.; Talaty, N.; Chen, H.; Cooks, R. G. *Chem. Commun*. **2005**, 1950-1952.

(6) Eilbert, R. F. in *Aspects of Explosives Detection*, Eds: M. Marshall, J. C. Oxley, Elsevier, London, **2009**, pp. 89-130.

(7) Andrew, T. L.; Swager, T. M. *J. Am. Chem. Soc*. **2007**, *129*, 7254-7255.

(8) Cope, W. C.; Barab, J. *J. Am. Chem. Soc*. **1917**, *39*, 504-514.

(9) Balakrishnan, V. K.; Halasz, A.; Hawari, J. *Environ. Sci. Technol*. **2003**, *37*, 1838-1843.

(10) Greiss, P. *Ber. Dtsch. Chem. Ges*. **1879**, *12*, 427-434.

(11) The original reagent reported by Greiss was composed of sulfanilic acid and α-naphthylamine; however, a more stable version of this formulation (the Zeller-Greiss reagent) containing sulfanilamide

and *N*-(α-naphthyl)-ethylenediamine hydrochloride has since been adopted: Zeller, H. D. *Analyst*, **1955**, *80*, 632-640.

(12) (a) Hawari, J.; Halasz, A.; Groom, C.; Deschamps, S.; Paquet, L.; Beaulieu, C.; Corriveau, A. *Environ. Sci. Technol*. **2002**, *36*, 5117-5123. (b) Just, C. L.; Schnoor, J. L. *Environ. Sci. Technol*. **2004**, *38*, 290-295. (c) Burton, D. T.; Turley, S. D. *Bull. Environ. Contam. Toxicol*. **1995**, *55*, 89-95. (d) Glover, D. J.; Hoffsommer, J. C. Technical Report for Naval Surface Weapons Center: Silver Spring, MD, February **1979**.

(13) (a) Sanchez, J. C.; Trogler, W. C. *J. Mater. Chem*. **2008**, *18*, 3143-3156. (b) Roos, B. D.; Brill, T. B. *Combust. Flame*. **2002**, *128*, 181-190.

(14) (a) Peyton, G. R.; LaFaivre, M. H.; Maloney, S. W. CERL Technical Report for US Army Corps of Engineers: Champaign, IL, November 1999. (b) Gowenlock, B. G.; Pfab, J.; Young, V. M. *J. Chem. Soc., Perkin Trans. 2*, **1997**, 915-919. (c) Pace, M. D. *J. Phys. Chem*. **1994**, *98*, 6251-6257.

(15) Bark, L. S.; Catterall, R. *Mikrochim. Acta*. **1960**, *4*, 553-558.

(16) Demethylation of DMA has been observed in other cases: (a) Macdonald, T. L.; Gutheim, W. G.; Martin, R. B.; Guengerich, F. P. *Biochemistry*, **1989**, *28*, 2071-2077. (b) Doyle, M. P.; Can Lente, M. A.; Mowat, R.; Fobare, W. F. *J. Org. Chem*. **1980**, *45*, 2570-2575.

(17) DMNA generally displays a low fluorescence quantum yield (< 5%) and is susceptible to photolytic cleavage upon excitation: (a) Costela, A.; Garcia-Moreno, I.; Garcia, O.; Sastre, R. *Chem. Phys. Lett*. **2001**, *347*, 115-120 (laser irradiation at 337 nm); (b) Görner, H.; Döpp, D. *Photochem. Photobiol. Sci.* **2002**, *1*, 270-277.

(18) Donor-acceptor anilines containing a nitro group as the "acceptor" component have been previously shown to possess large molar extinction coefficients and moderate fluorescence quantum yields. For example, see: Gruen, H.; Görner, H. *J. Phys. Chem.* **1989**, *93*, 7144-7152.

(19) Compound **17** was synthesized following a previously published procedure: Campeau, L.-C.; Parisien, M.; Jean, A.; Fagnou, K. *J. Am. Chem. Soc.*, **2006**, *128*, 581-590, but is also commercially available.

(20) Oka, H.; Kouno, H.; Tanaka, H. *J. Mater. Chem.* **2007**, *17*, 1209-1215.

(21) The poor reactivity of the hexafluoroisopropanol group toward Friedel-Crafts reactions has been observed before: Amara, J. P.; Swager, T. M. *Macromolecules*, **2006**, *39*, 5753-5759 and references therein.

(22) Seo, E. T.; Nelson, R. F.; Fritsch, J. M.; Marcoux, L. S.; Leedy, D. W.; Adams, R. N. *J. Am. Chem. Soc*. **1966**, *88*, 3498-3503.

(23) Rathore, R.; Kumar, A. S.; Lindeman, S. V.; Kochi, J. K. *J. Org. Chem.* **1998**, *63*, 5847-5856.

(24) Nitric acid on silica gel (SiO_2:HNO_3) was previously used to controllably mono-nitrate electron rich calixarenes: Xu, B.; Swager, T. M. *J. Am. Chem. Soc.* **1993**, *115*, 1160-1162.

(25) Strongly solvent-dependent fluorescence quantum yields have been previously observed for donor-acceptor chromophores. For example, see ref. 18.

(26) (a) Sheldrick, G. M. *Acta Cryst. A* **1990**, *46*, 467. (b) Sheldrick, G. M. SHELXL 91, Universtität Göttingen, Göttingen, Germany, 1997

(27) Demas, J. N.; Crosby, G. A. *J. Phys. Chem*. **1971**, *75*, 991.

(28) For a representative reference on the procedure followed see: Hill, R.D.; Puddephatt, R. J. *J. Am. Chem. Soc.* **1985**, *107*, 1218.

(29) Hatchard, C.G.; Parker, C. A. *Proc. R. Soc. London A* **1956**, *235*, 518.

(30) Craig, D. *J. Am. Chem. Soc.* **1935**, *57*, 195.

Supporting Information for:

Detection of Explosives via Photolytic Cleavage of Nitroesters and Nitramines

*Trisha L. Andrew, Timothy M. Swager**
Department of Chemistry, Massachusetts Institute of Technology,
77 Massachusetts Avenue, Cambridge, Massachusetts 02139
tswager@mit.edu

Table of Contents

Table S1. Optical Properties of DHAs in acetonitrile.

cmpd	λ_{max}/nm (log ε)	λ_{em}/nm	Φ[a]	τ/ns
DHA1	284 (4.1)	352	0.18	2.7
DHA2	288 (4.1)	390	0.04	2.2
DHA3	288 (4.1)	376	0.09	2.7
DHA4	285 (4.0), 320 (3.8)	355	0.13	1.6
DHA5	285 (4.1)	355	0.14	2.8
DHA6	246 (4.1), 290 (4.0)	382	0.12	2.3
DHA7	257 (4.1), 298 (3.9)	345	0.10	2.7
DHA8	294 (3.9)	359	0.14	1.7
DHA9[b]	247 (4.1), 290 (3.9)	345	0.15	2.8
DHA10	246 (4.3), 290 (4.1)	352	0.12	2.5
DHA11	289 (4.3)	355	0.14	1.7
DHA12	247 (4.0), 292 (3.9)	382	0.06	1.7
DHA13	245 (4.8), 296 (4.4)	355	0.09	2.2
DHA14	247 (4.0), 297 (3.8)	345	0.15	2.4
DHA15	280 (4.3), 311 (4.0)	354	0.18	2.5
DHA16 + **DHA17**	290 (4.2)	371	0.05	2.7
DHA18	290 (4.2)	371	0.03	2.5

[a] Measured against quinine sulfate in 0.1N H_2SO_4 (Φ 0.54) [b] in THF

Table S2. Electrochemical Properties of Select DHAs.

cmpd	E_{pa}/V vs SCE	E_{onset}/V vs SCE
DHA1	1.19	0.77
DHA2	1.05	0.77
DHA4	1.07	0.87
DHA5	1.27	0.86
DHA6	1.30	0.86
DHA7	1.51	0.92
DHA8	1.20	0.95
DHA9	1.35	0.85
DHA11	1.08	0.87
DHA15	1.65	1.18
DHA16 + **DHA17**	1.04	0.83
DHA18	1.08	0.83
DMA[a]	1.36	0.77
TPA[b]	1.48	0.95

[a] *N*,*N*-Dimethylaniline. [b] Triphenylamine.

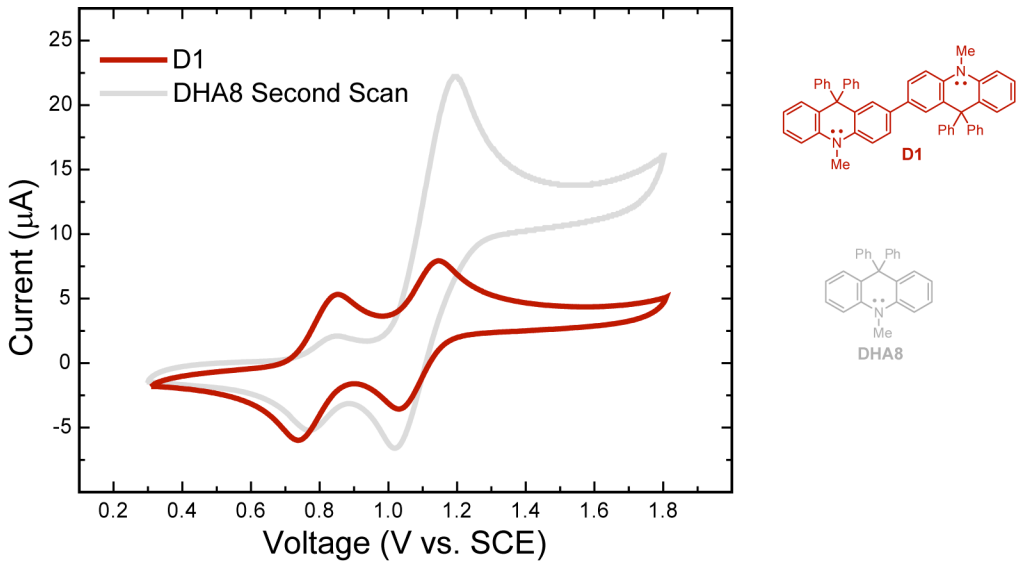

Figure S1. Cyclic voltammogram (CV) of **D1** (red line) and the second scan of the CV of **DHA8** (grey line). The CV of **D1** displays the same peaks observed to appear after an initial oxidative sweep of **DHA8**, thus confirming that **DHA8** dimerizes in the electrochemical cell.

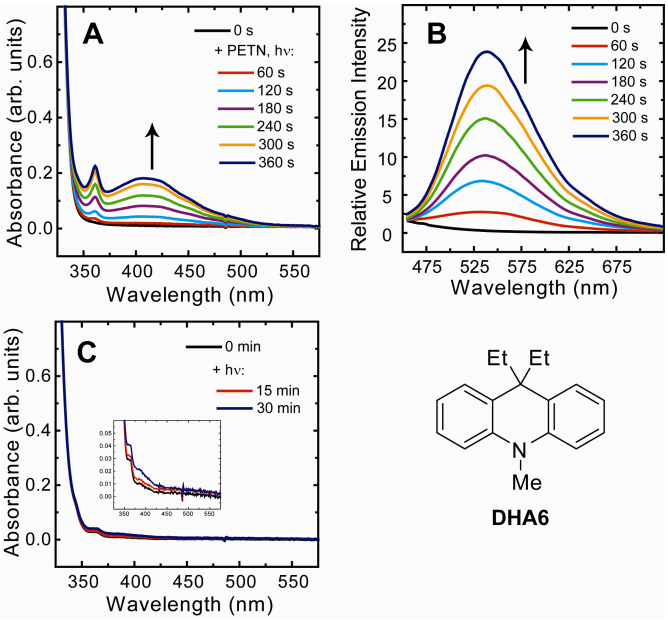

Figure S2. Absorption (A) and emission (B, λ_{ex} = 415 nm) profiles of the photoreaction of **DHA6** with PETN in acetonitrile upon exposure to simulated sunlight. [**DHA6**] = 1.3×10^{-4} M. [PETN] = 5.4×10^{-5} M. The absorption profile for the extended irradiation of a blank, aerated solution of **DHA6** is also shown (C).

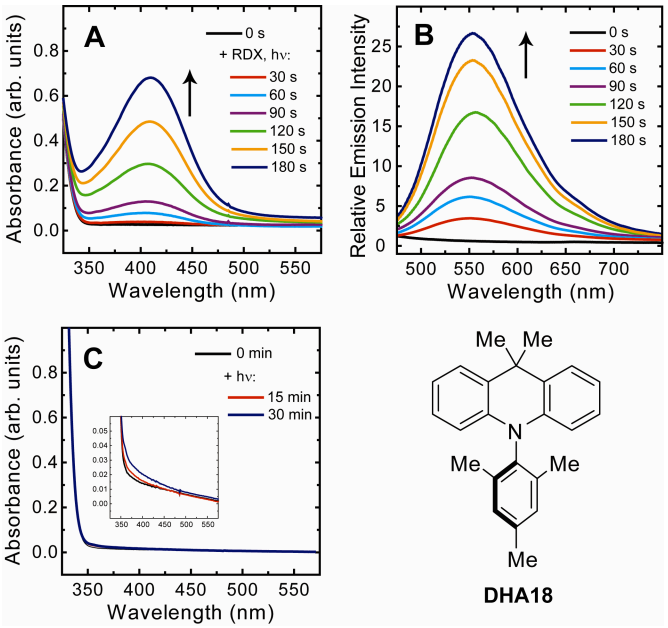

Figure S3. Absorption (A) and emission (B, λ_{ex} = 415 nm) profiles of the photoreaction of **DHA18** with RDX in acetonitrile upon exposure to simulated sunlight. [**DHA18**] = 1.3×10^{-4} M. [RDX] = 5.4×10^{-5} M. The absorption profile for the extended irradiation of a blank, aerated solution of **DHA18** is also shown (C).

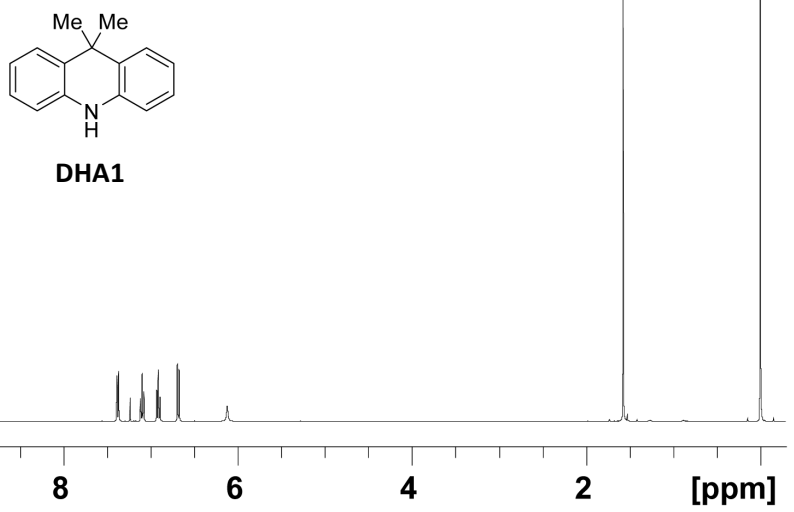

DHA1

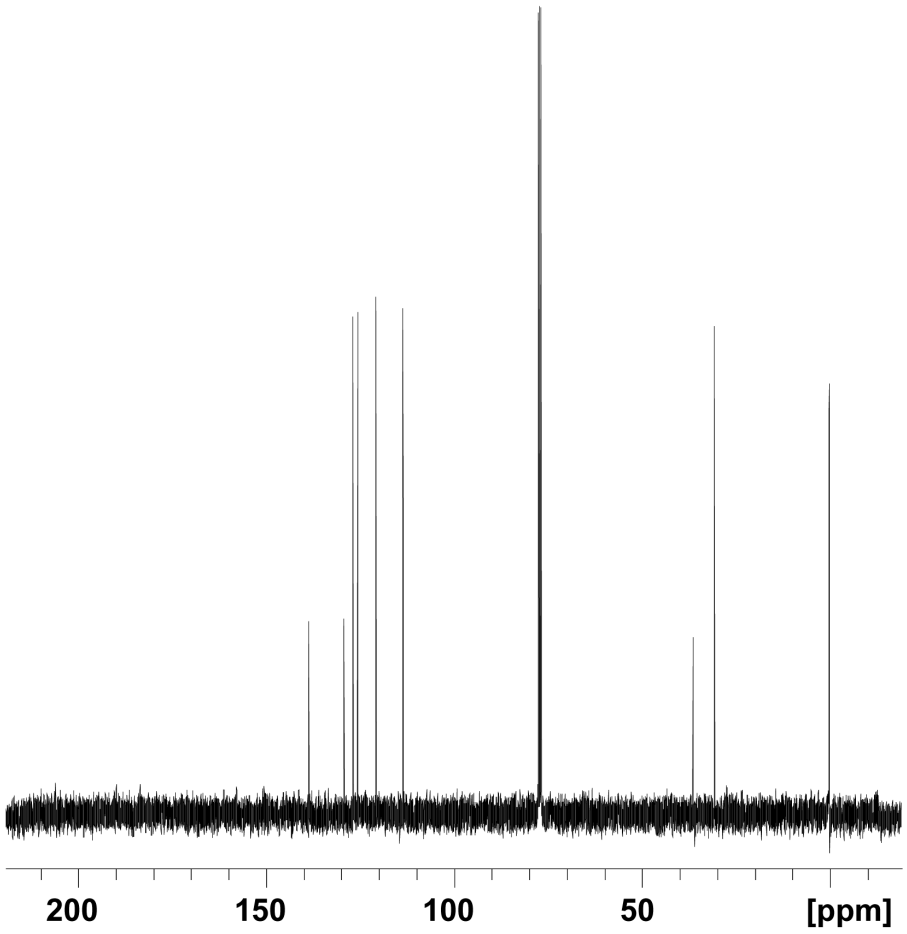

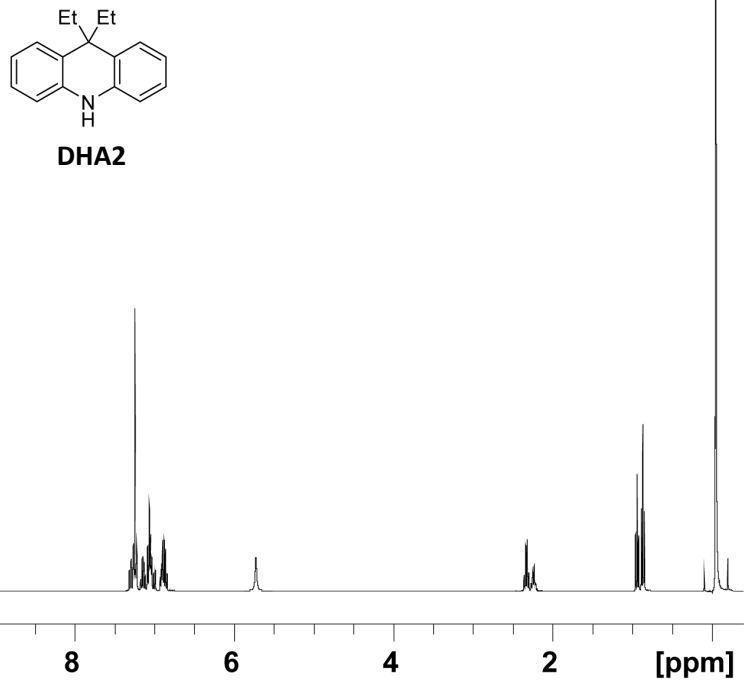
Et
Et
N
H
DHA2
8
6
4
2
[ppm]

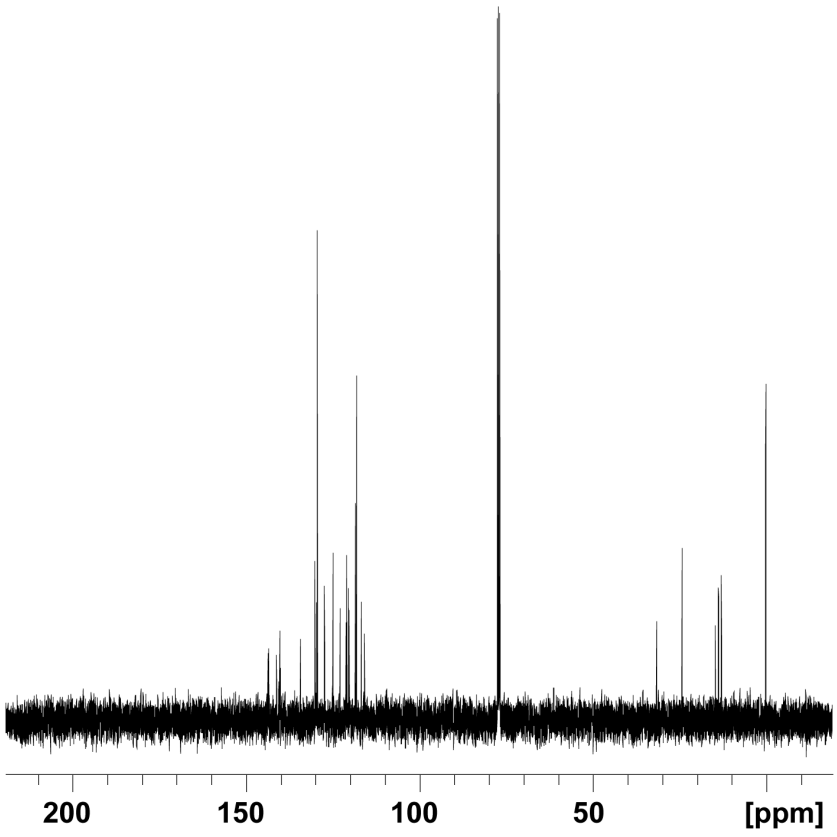
200
150
100
50
[ppm]

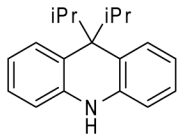

DHA3

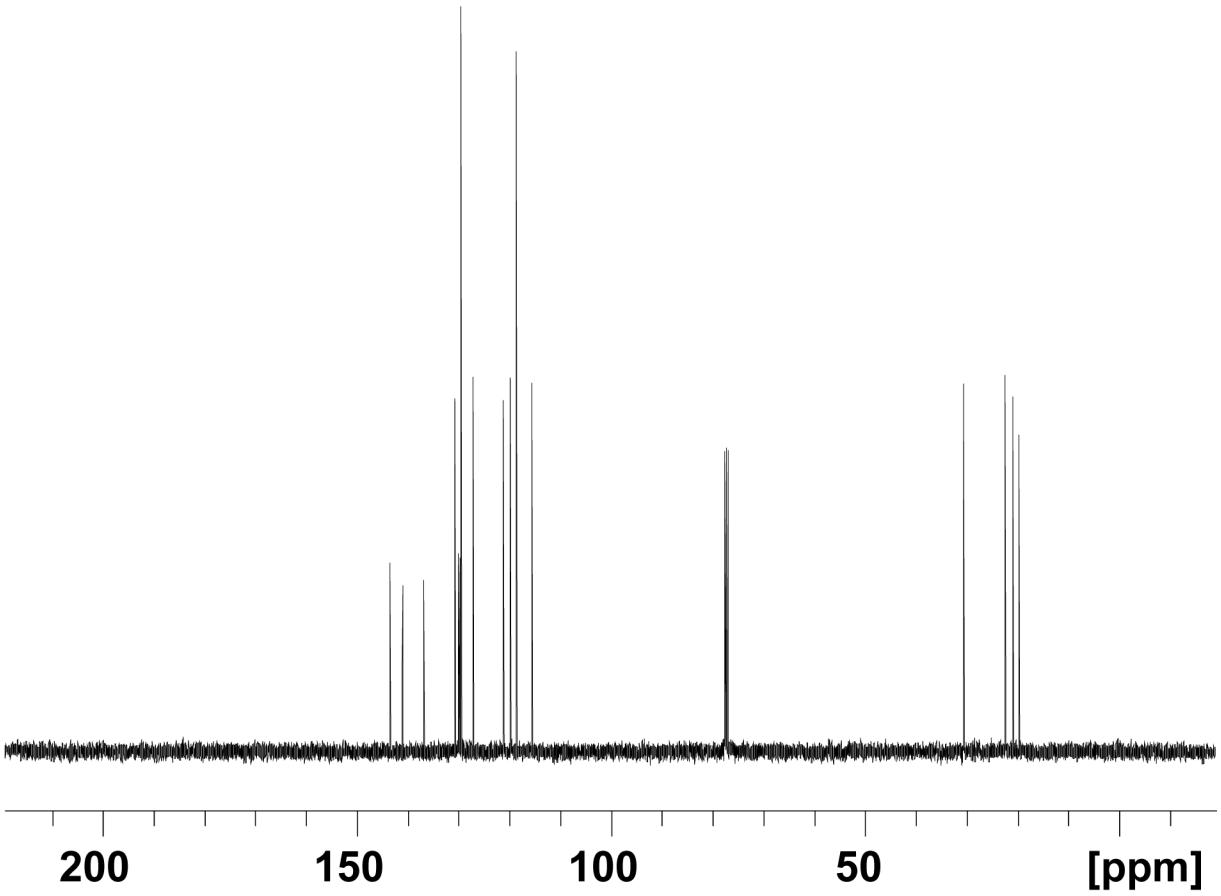

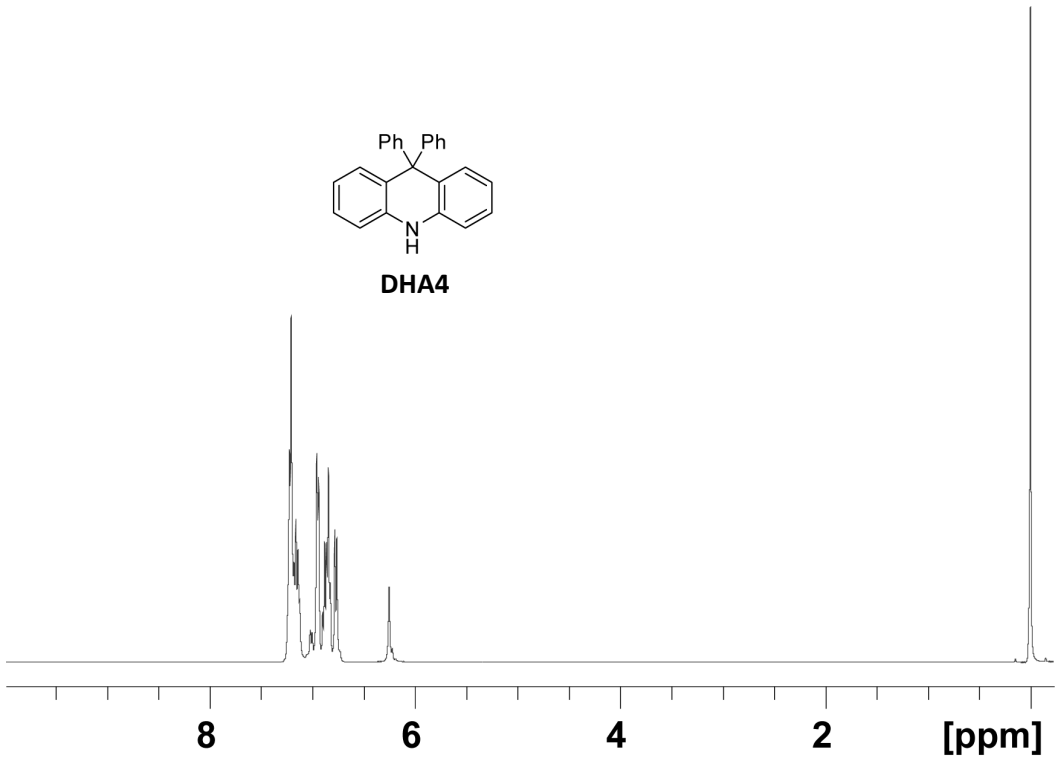

DHA4

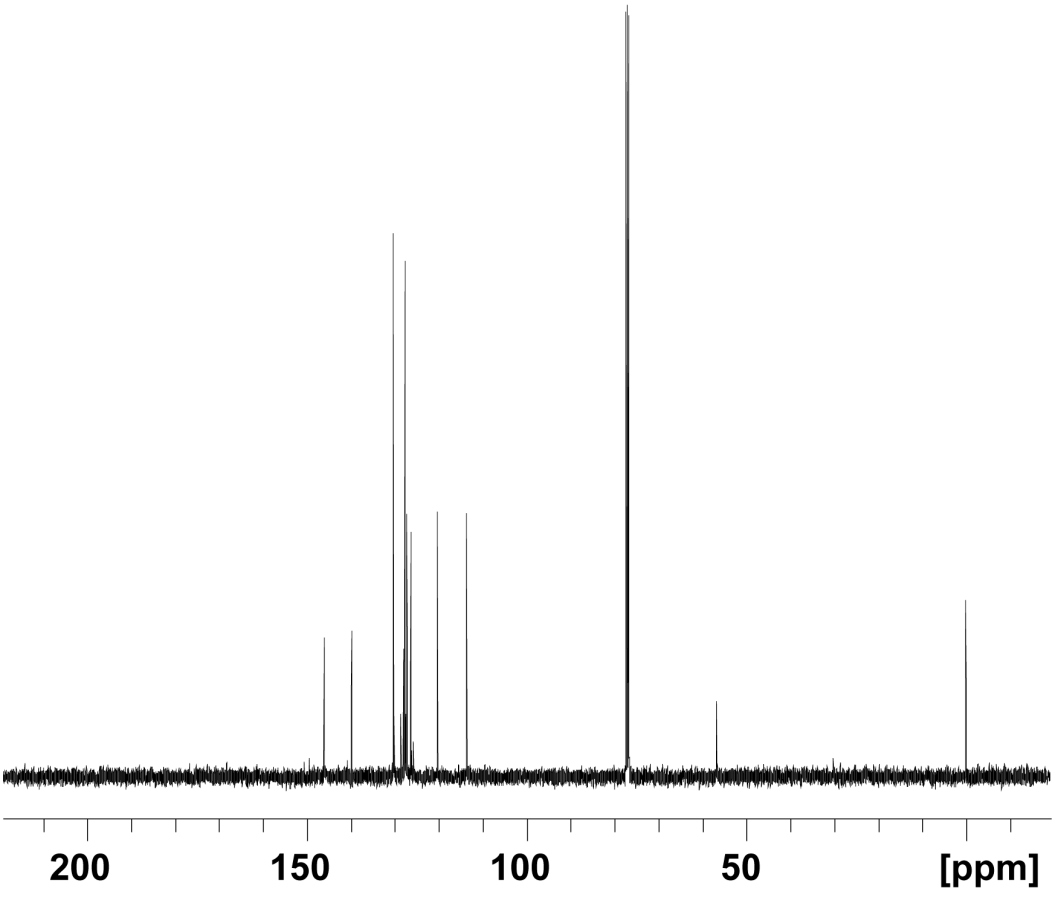

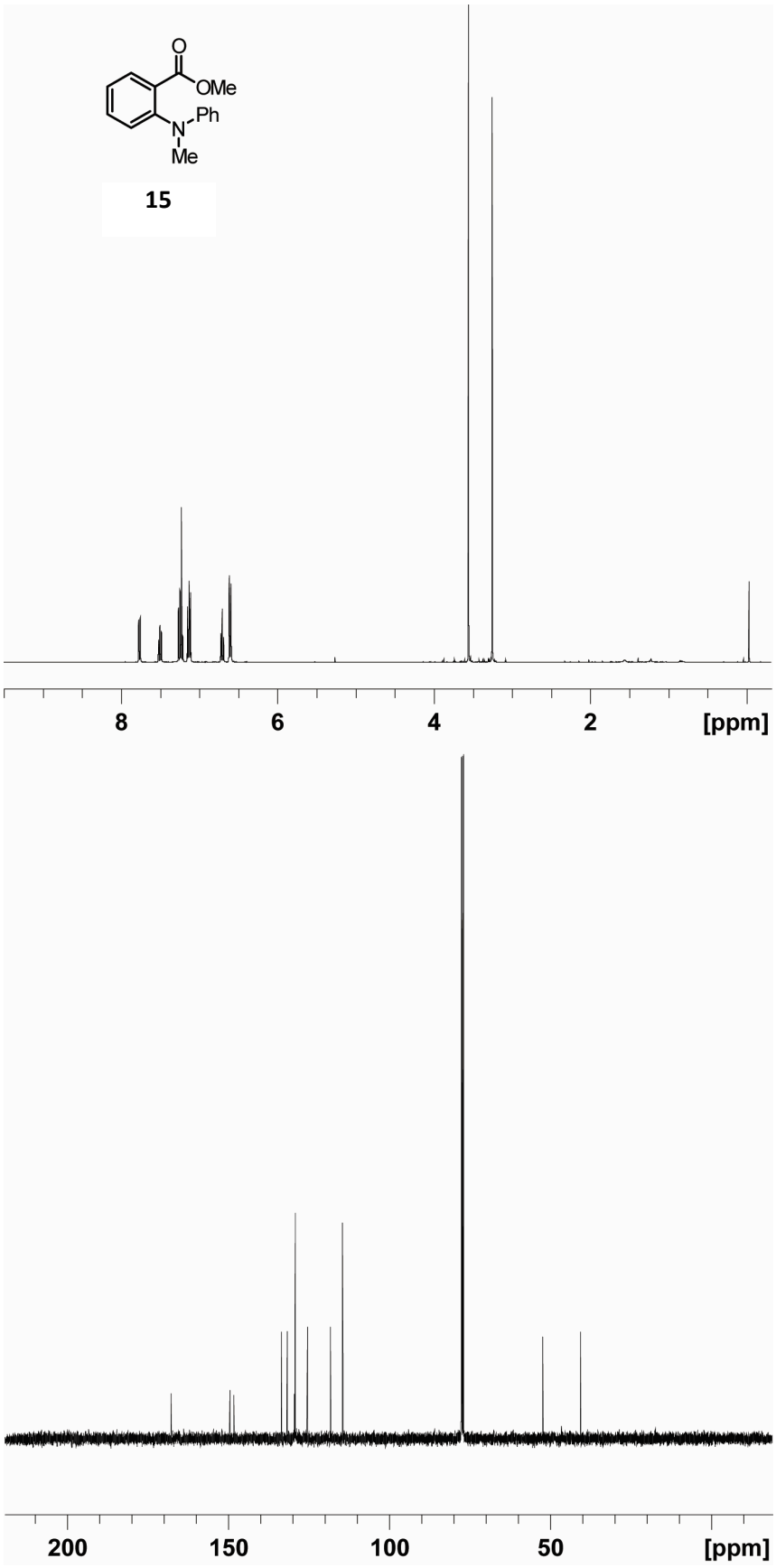
O
OMe
Ph
N
Me
15
8
6
4
2
[ppm]
200
150
100
50
[ppm]

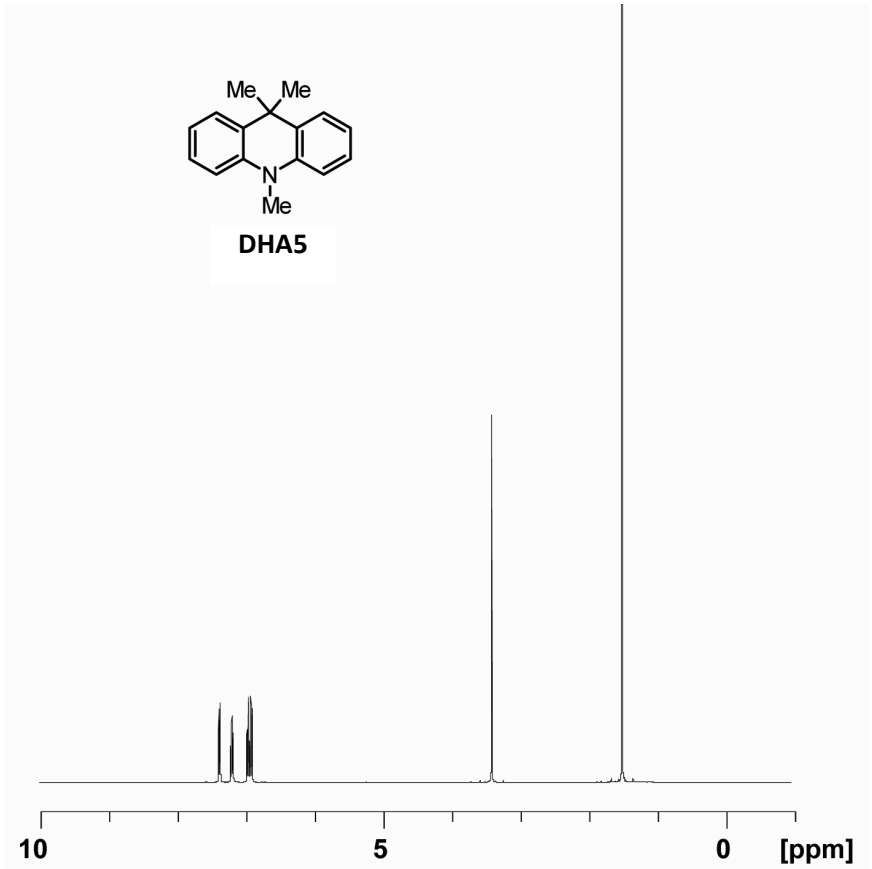
Me
Me
N
Me
DHA5
10
5
0
[ppm]

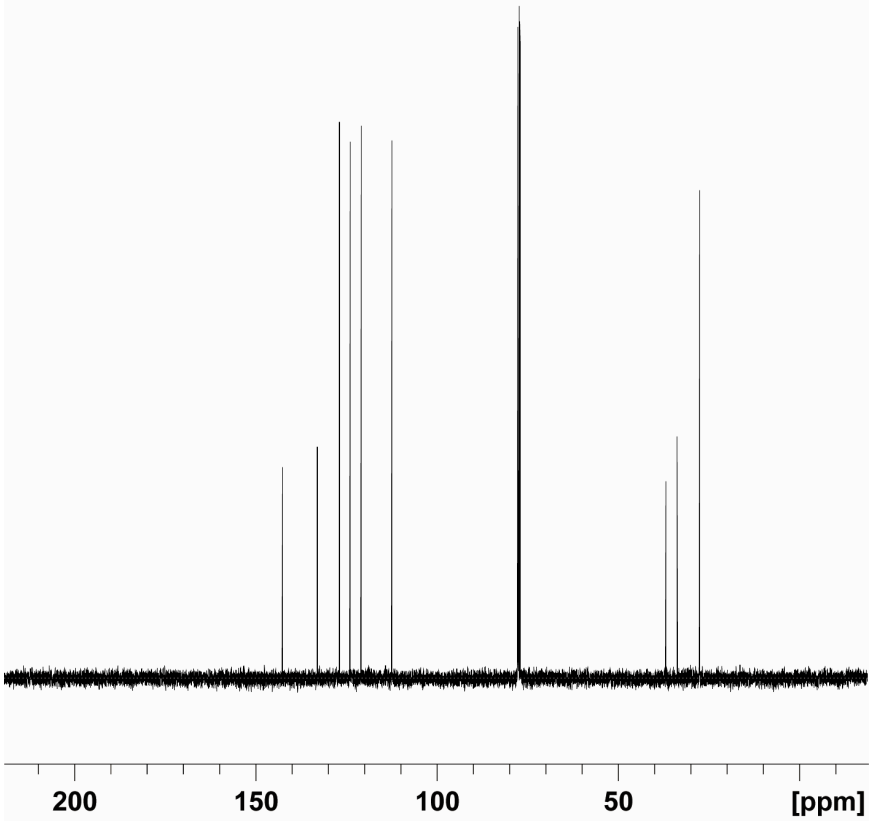
200
150
100
50
[ppm]

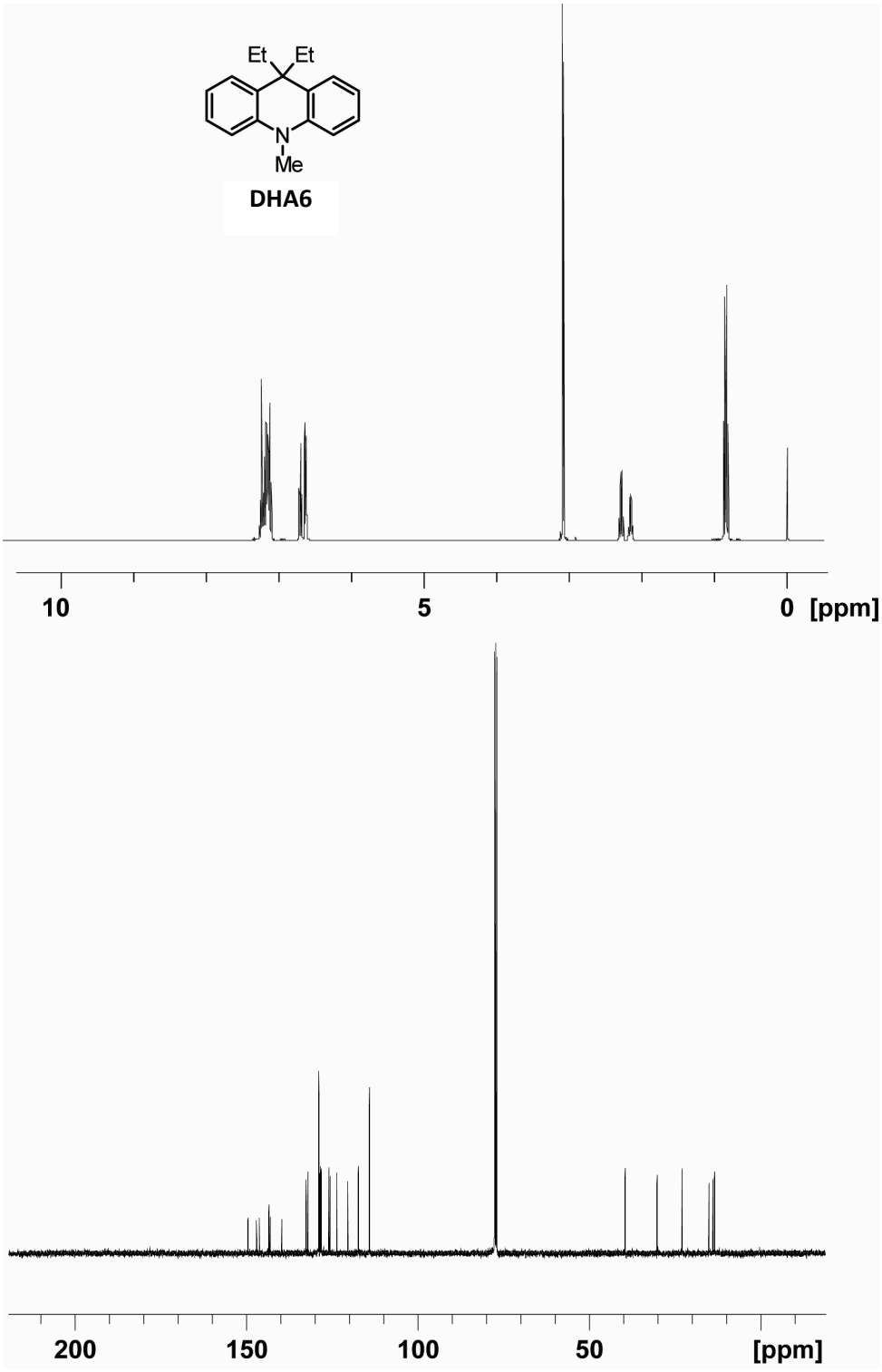
Et
Et
N
Me
DHA6
10
5
0
[ppm]
200
150
100
50
[ppm]

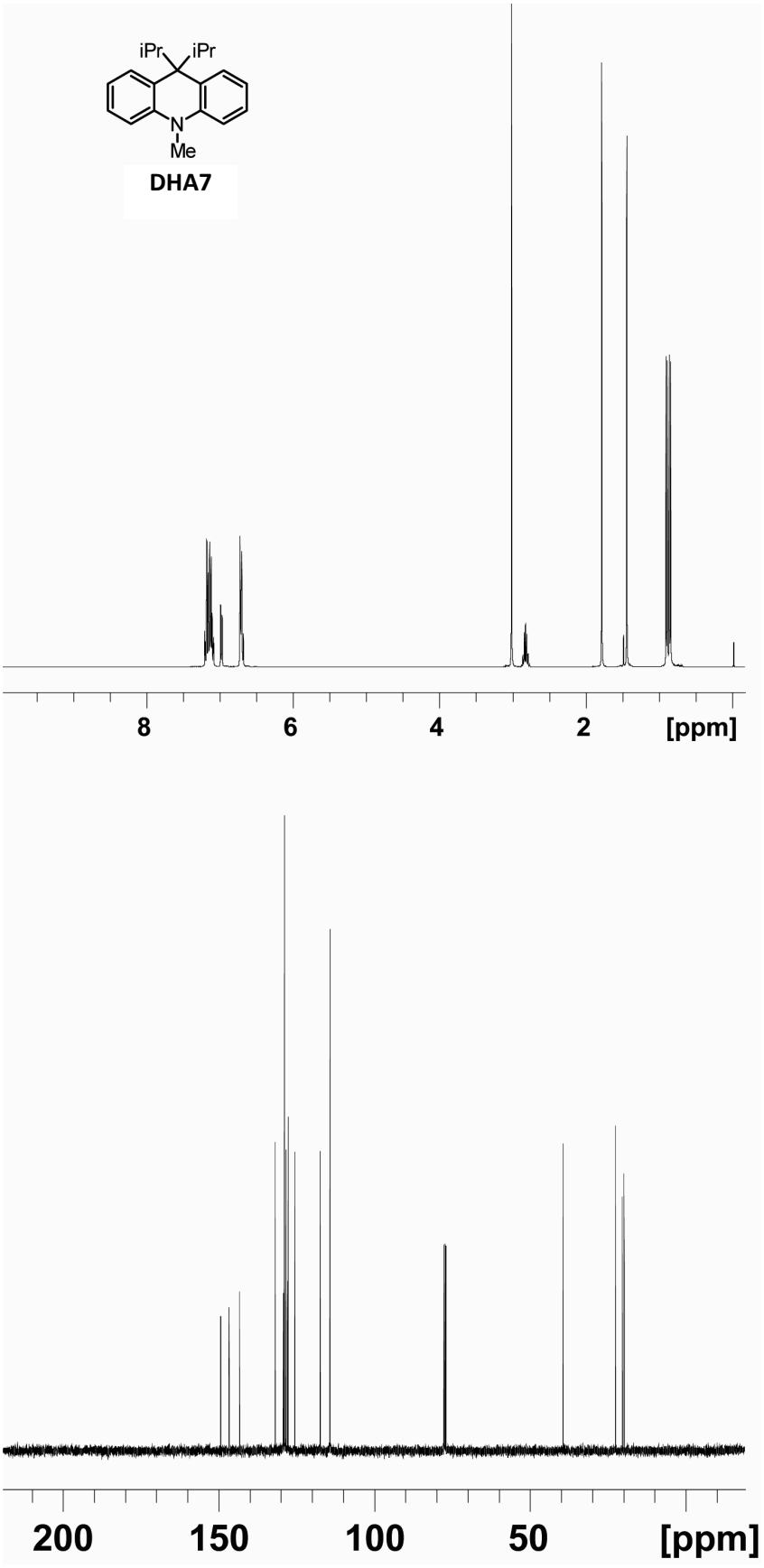
iPr
iPr
N
Me
DHA7
8
6
4
2
[ppm]
200
150
100
50
[ppm]

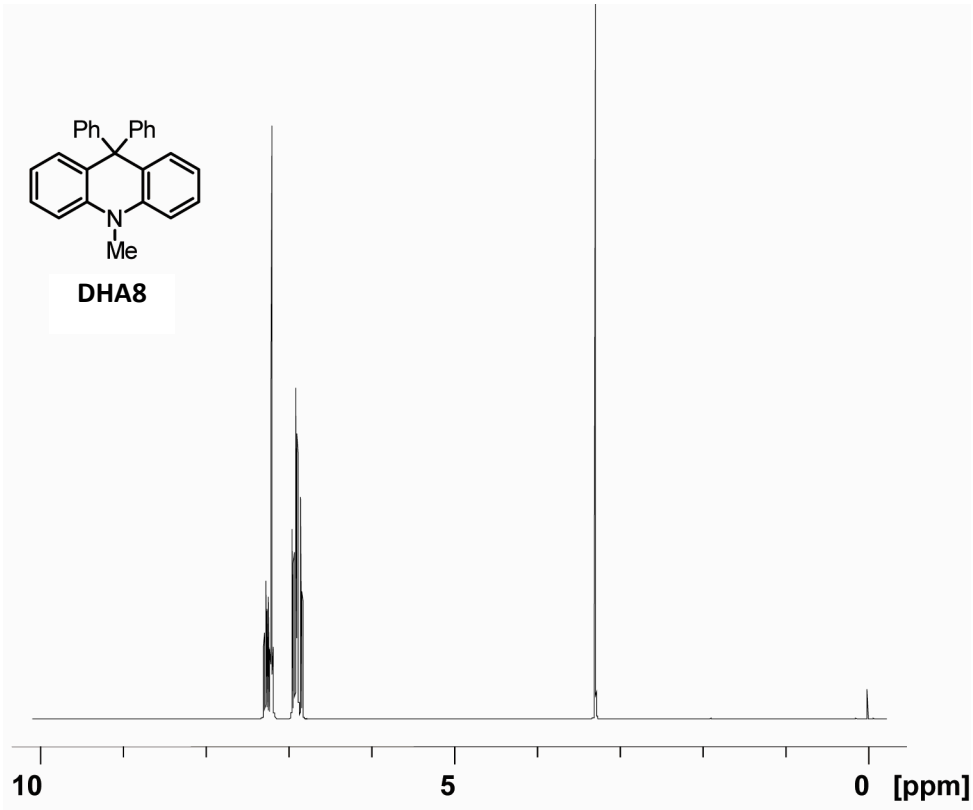
Ph
Ph
N
Me
DHA8
10
5
0
[ppm]

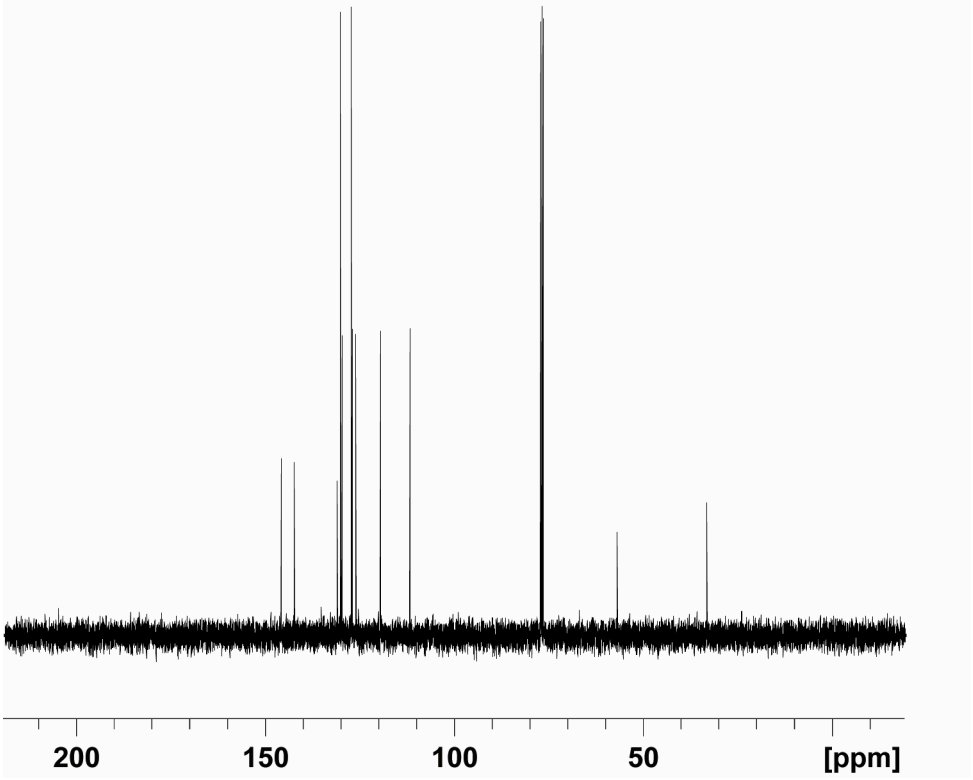
200
150
100
50
[ppm]

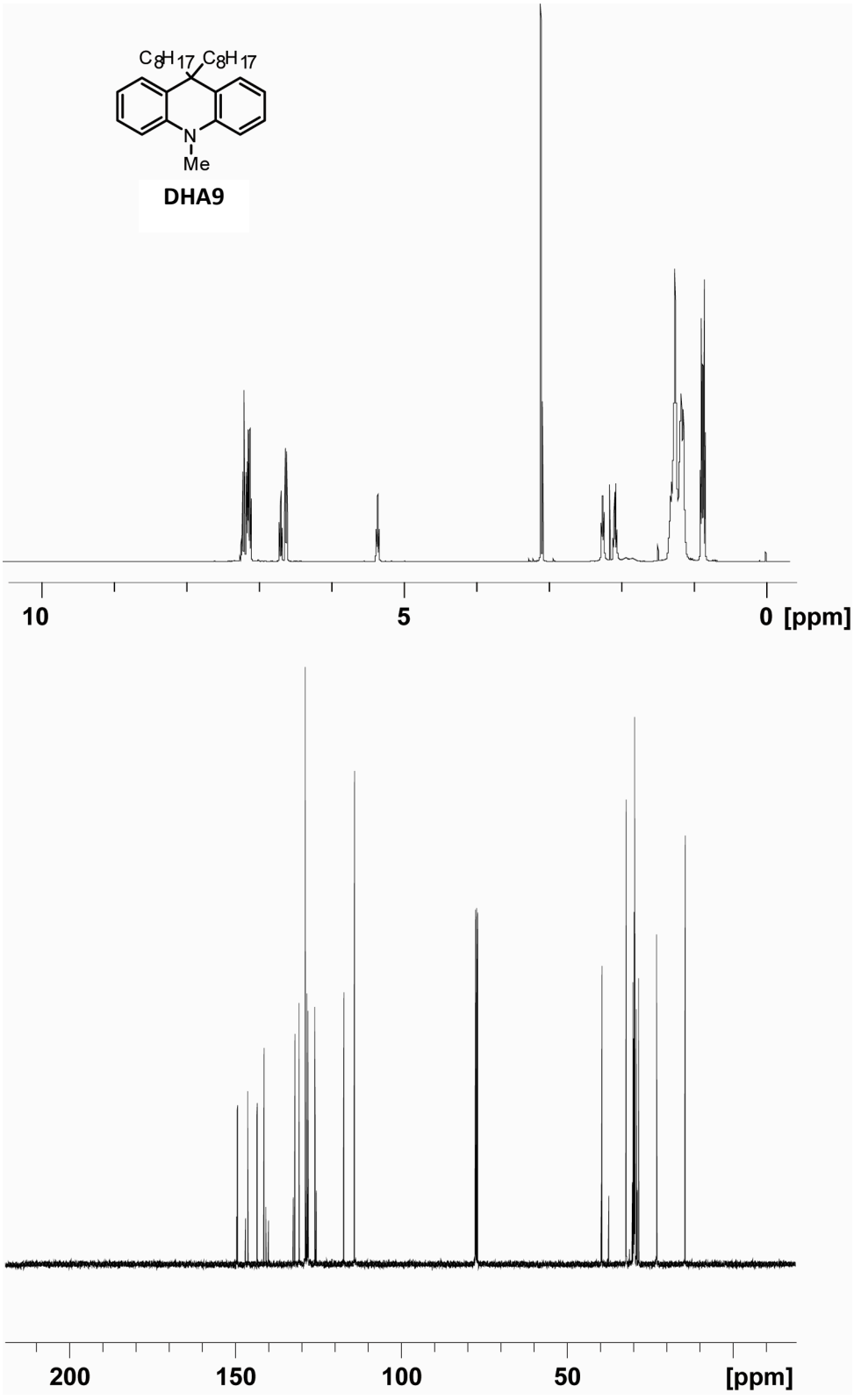
C8H17
C8H17
N
Me
DHA9
10
5
0 [ppm]
200
150
100
50
[ppm]

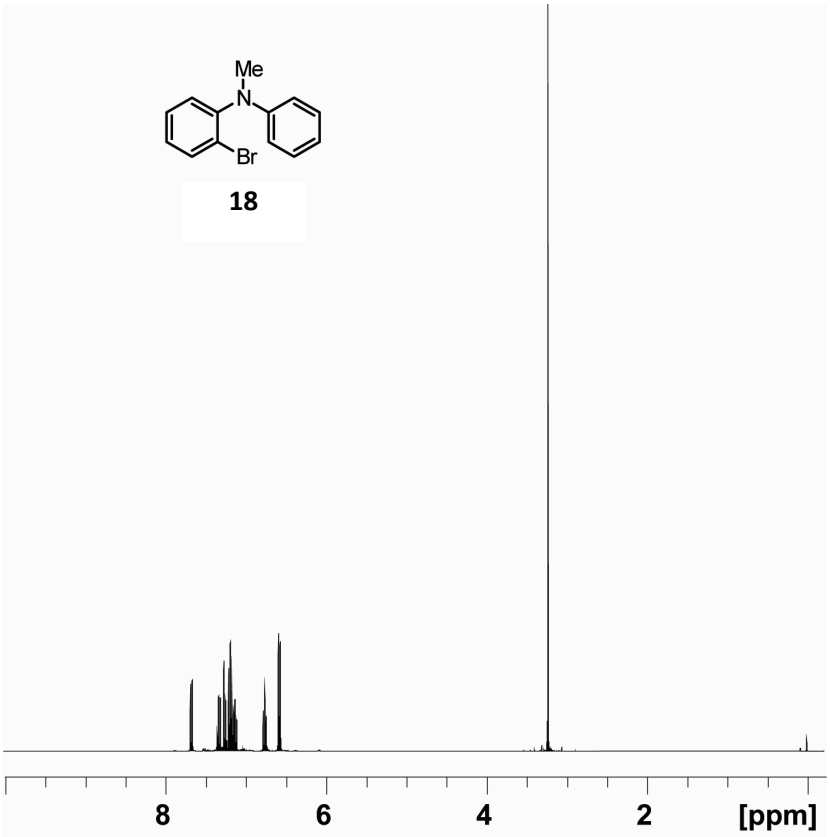
Me
N
Br
18
8
6
4
2
[ppm]

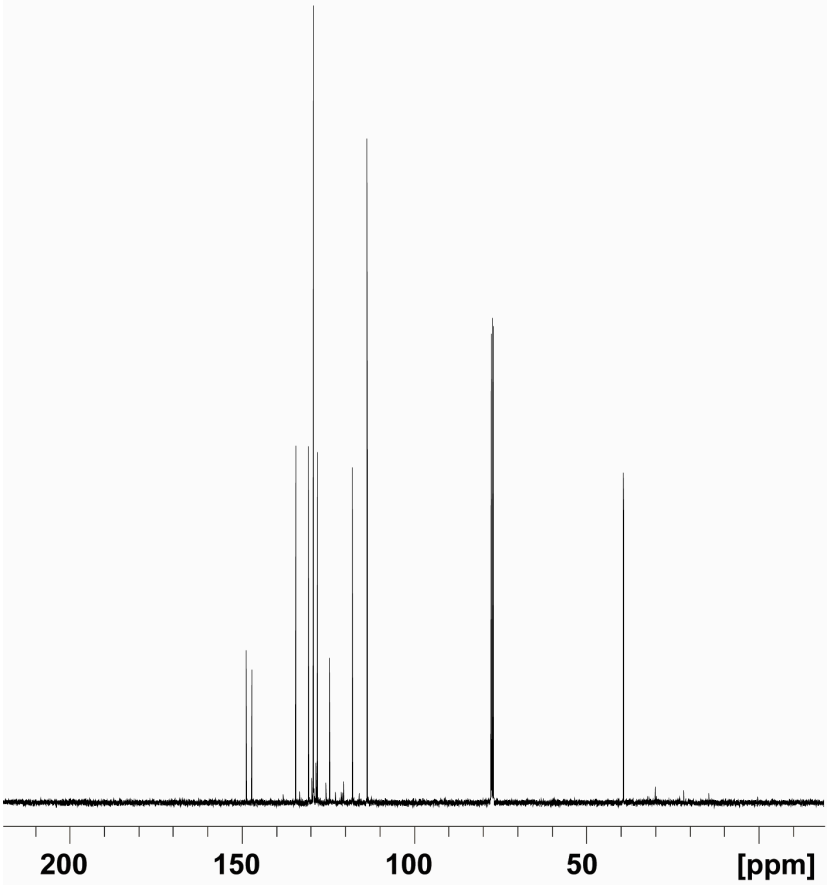
200
150
100
50
[ppm]

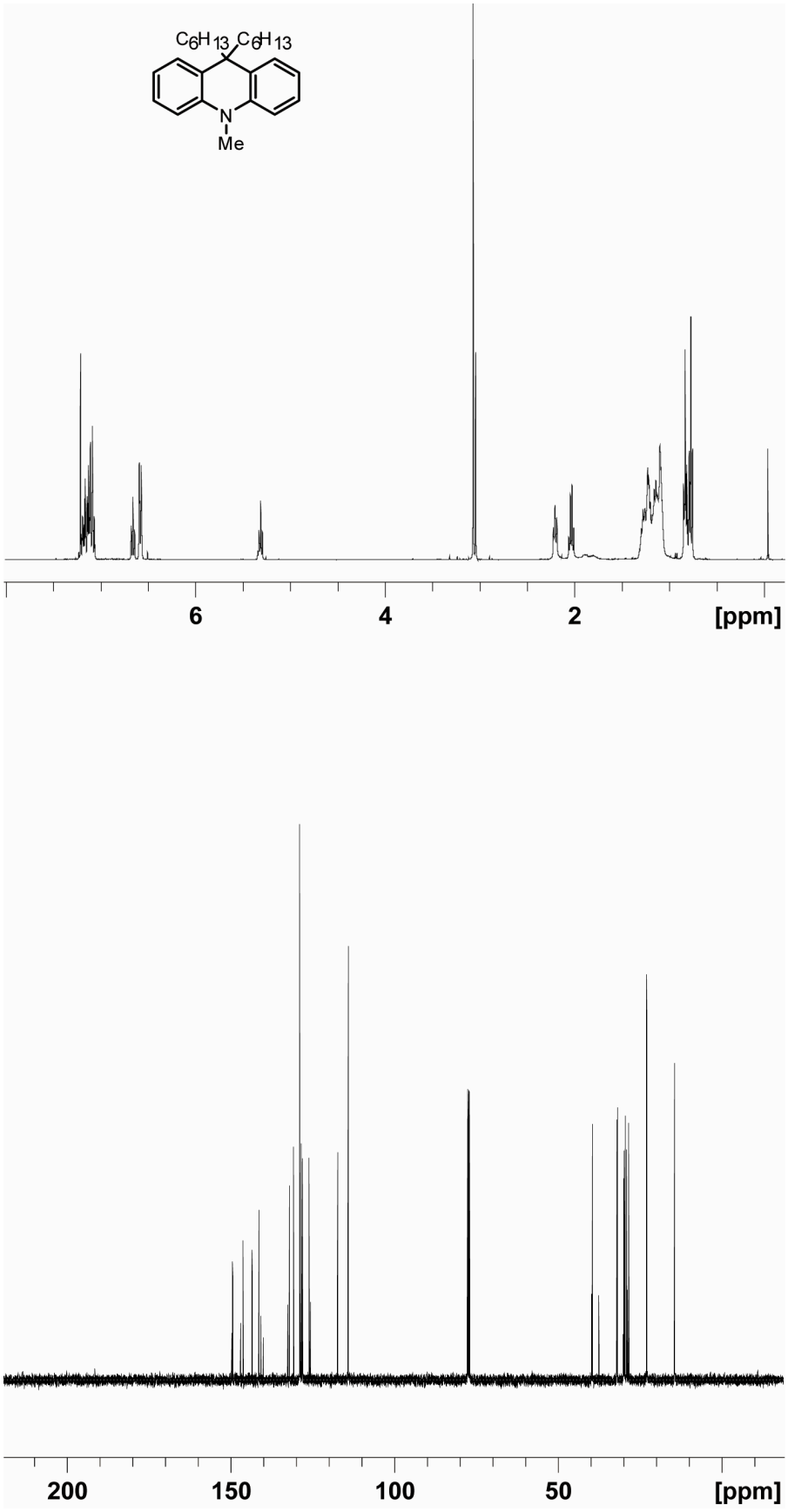
C6H13
C6H13
N
Me
6
4
2
[ppm]
200
150
100
50
[ppm]

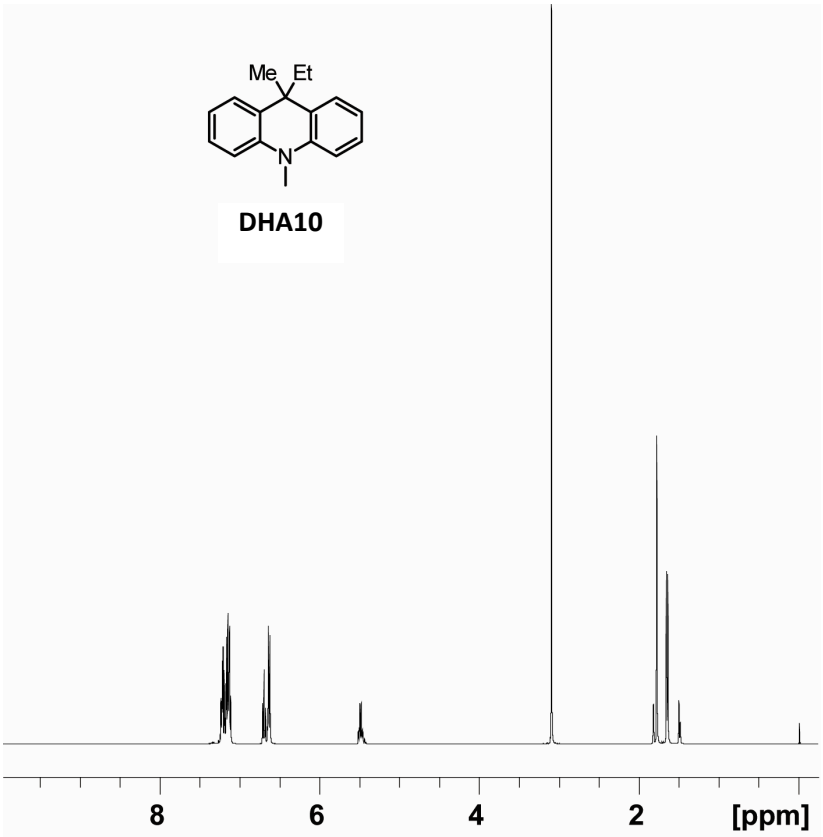
Me
Et
N
DHA10
8
6
4
2
[ppm]

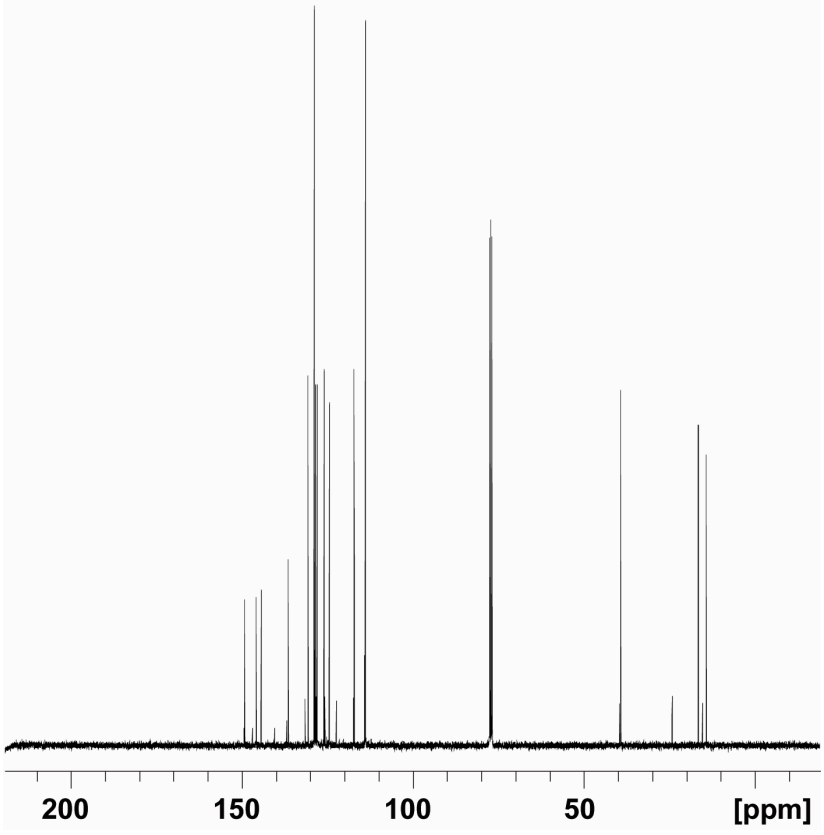
200
150
100
50
[ppm]

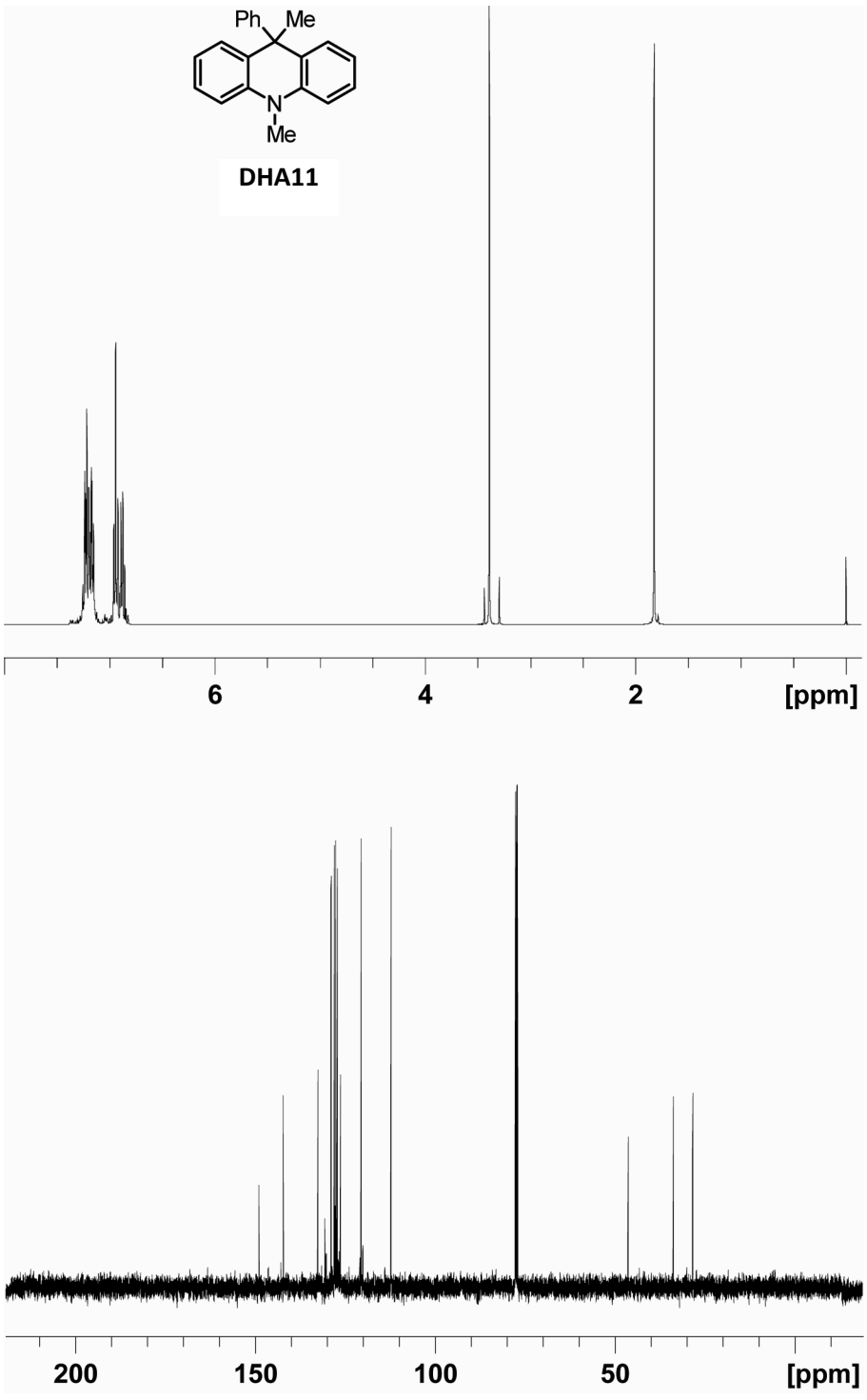
Ph
Me
N
Me
DHA11
6
4
2
[ppm]
200
150
100
50
[ppm]

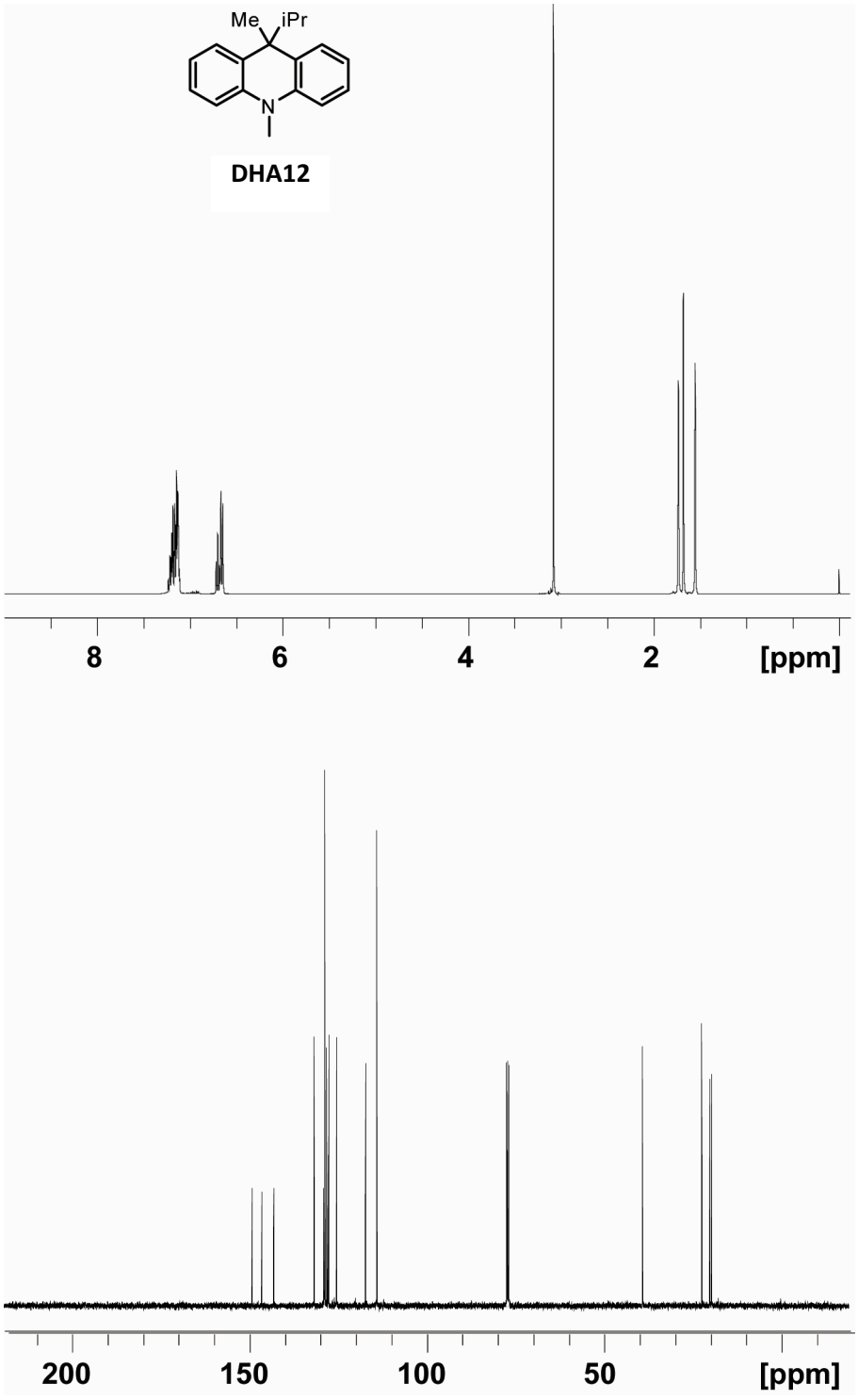
Me
iPr
N
DHA12
8
6
4
2
[ppm]
200
150
100
50
[ppm]

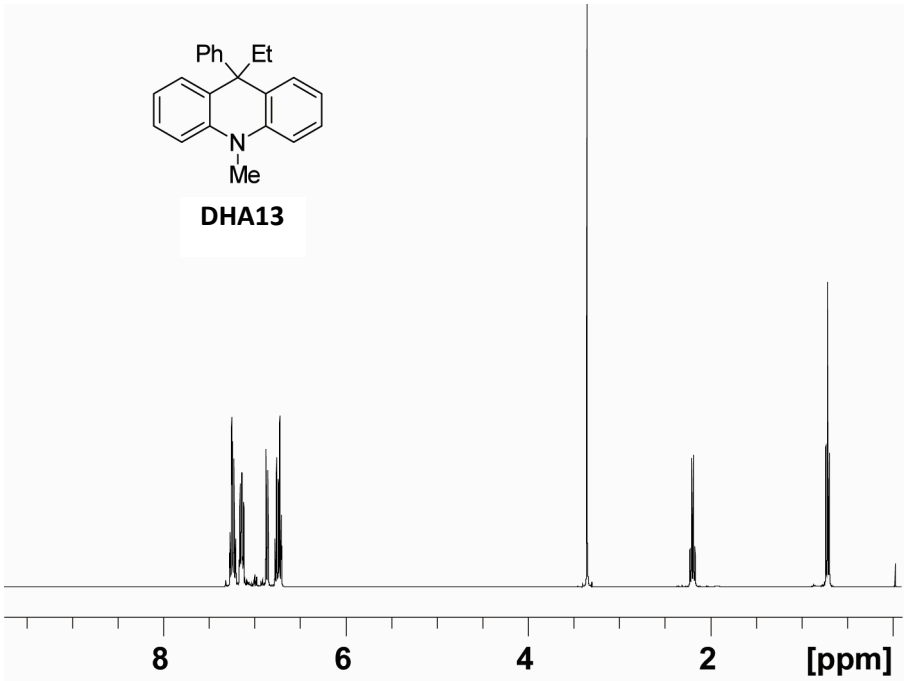
Ph
Et
N
Me
DHA13
8
6
4
2
[ppm]

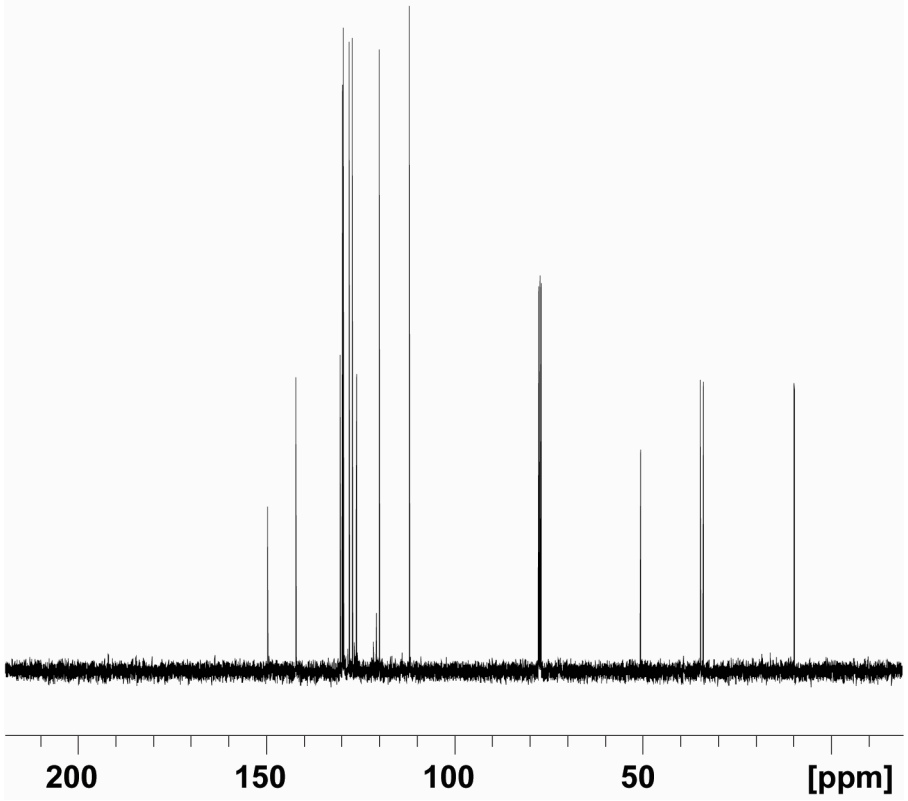
200
150
100
50
[ppm]

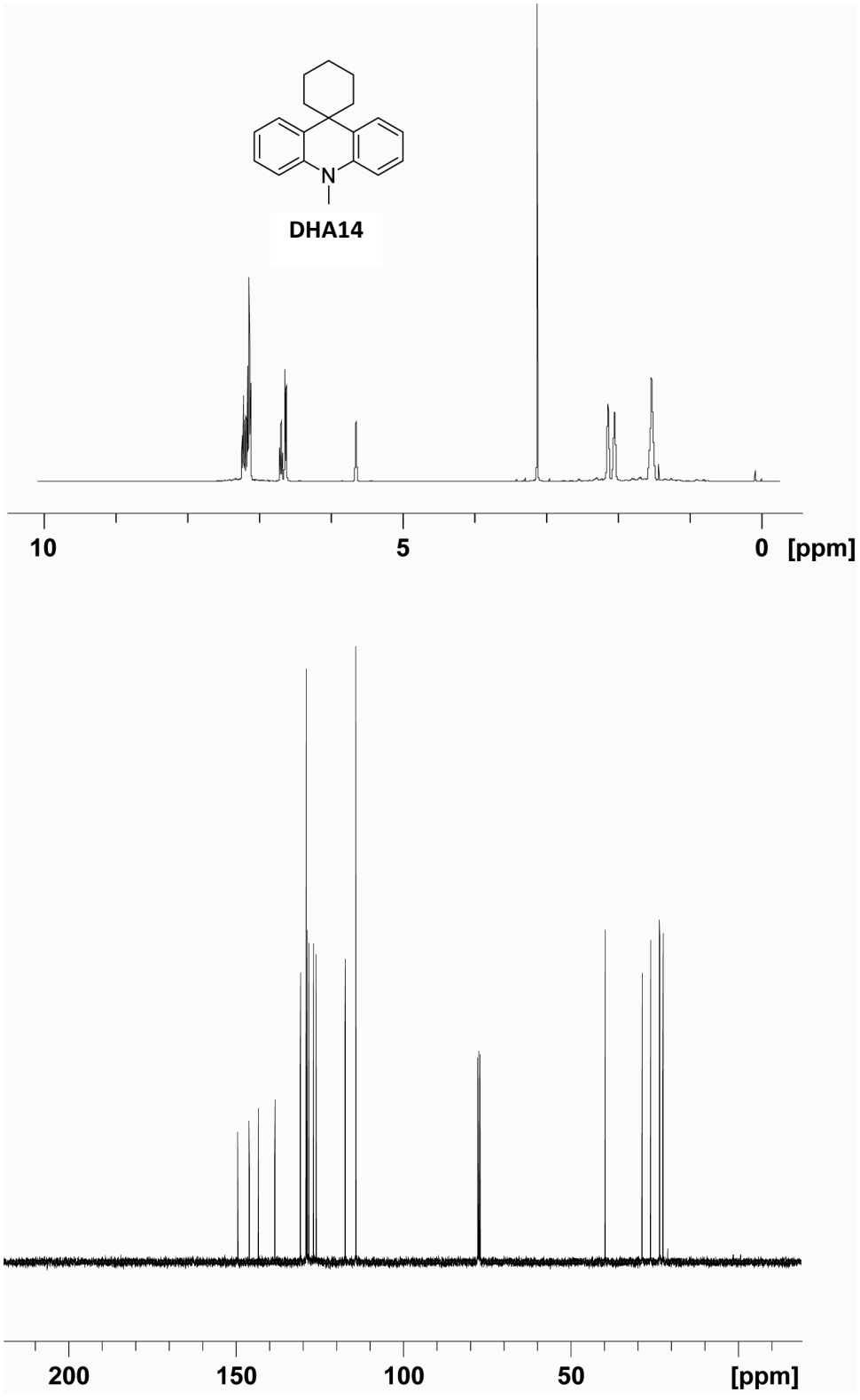
N
DHA14
10
5
0
[ppm]
200
150
100
50
[ppm]

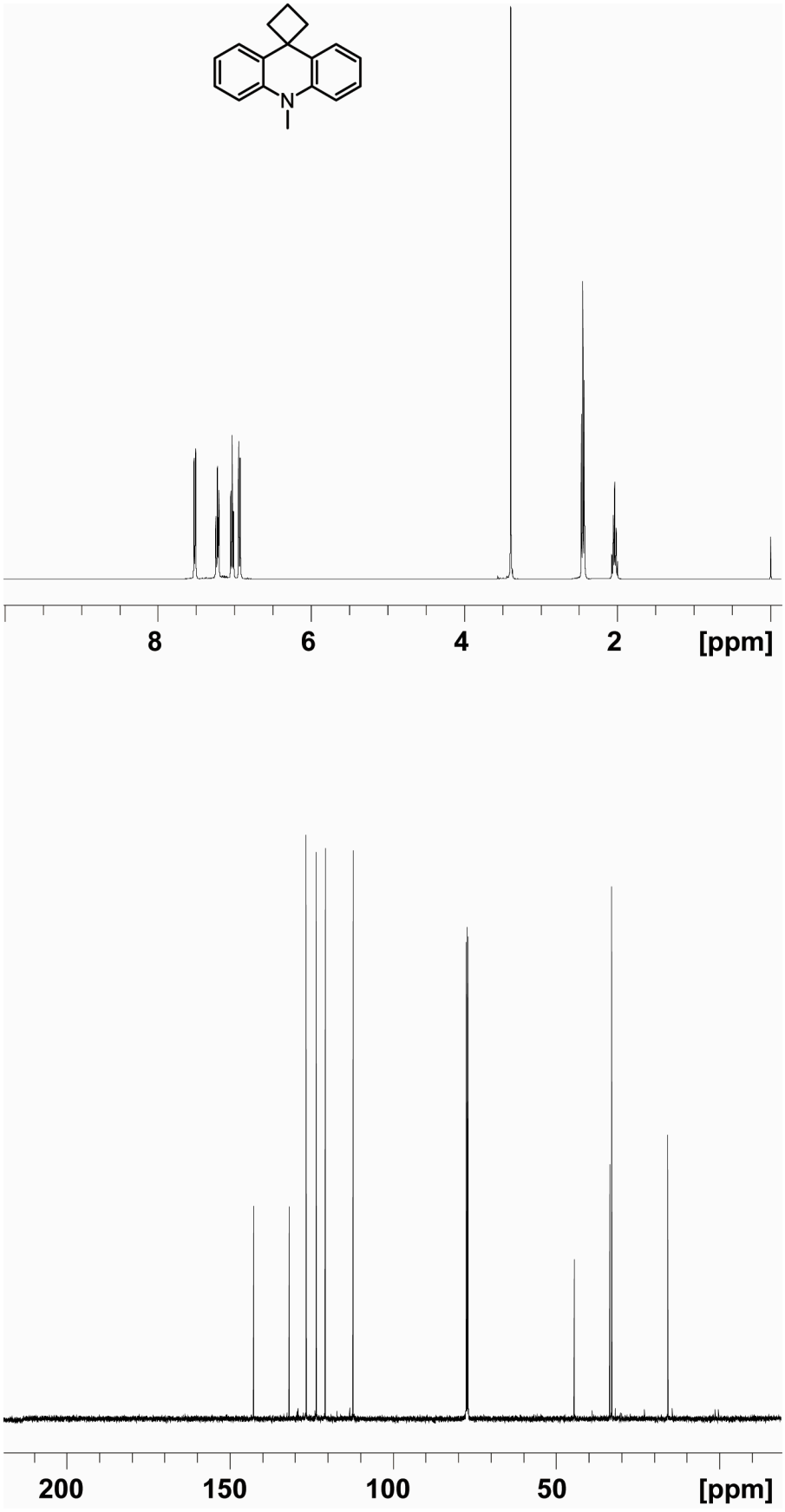
N
8
6
4
2
[ppm]
200
150
100
50
[ppm]

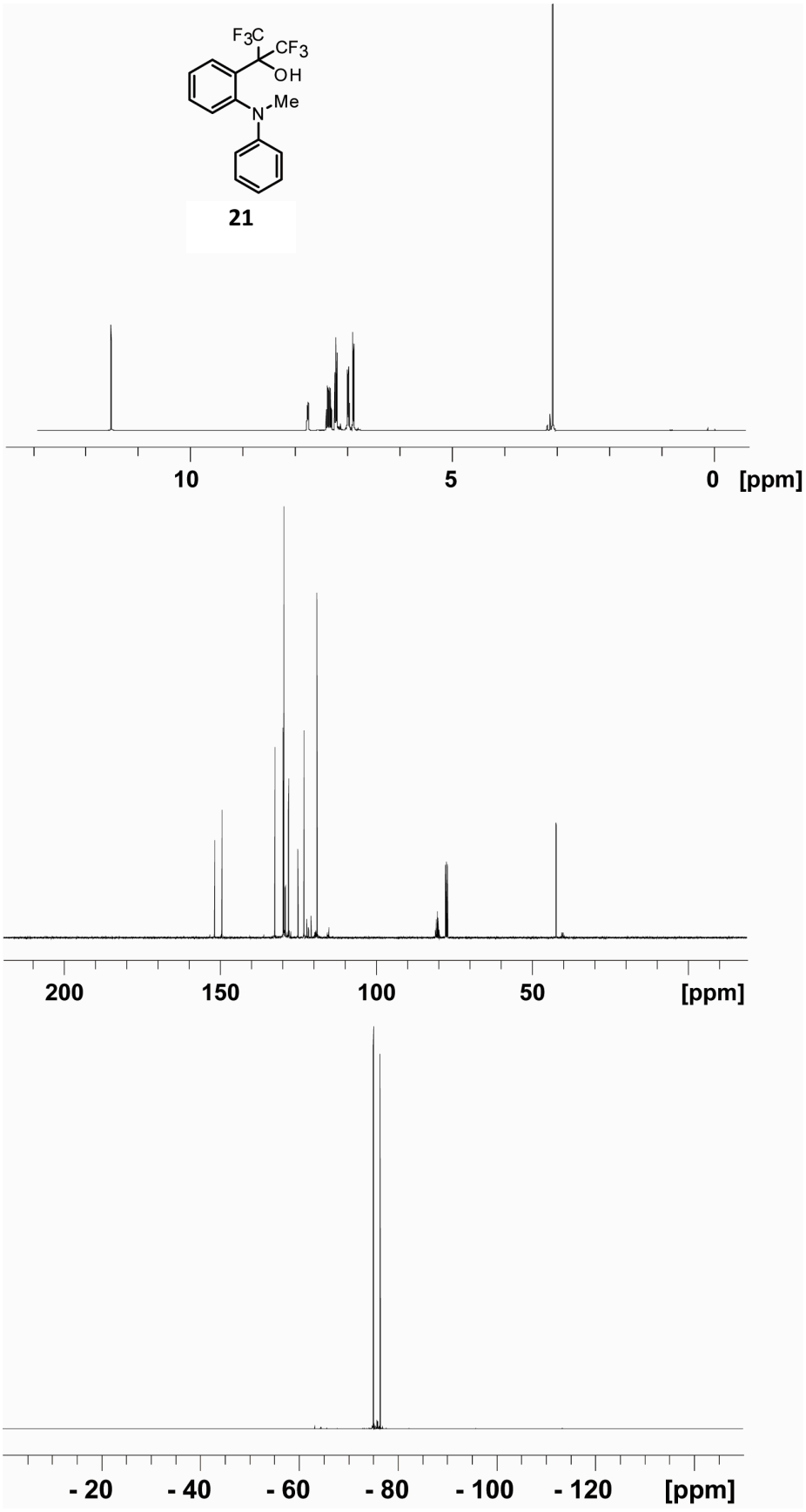
F3C
CF3
OH
N
Me
21
10
5
0
[ppm]
200
150
100
50
[ppm]
- 20
- 40
- 60
- 80
- 100
- 120
[ppm]

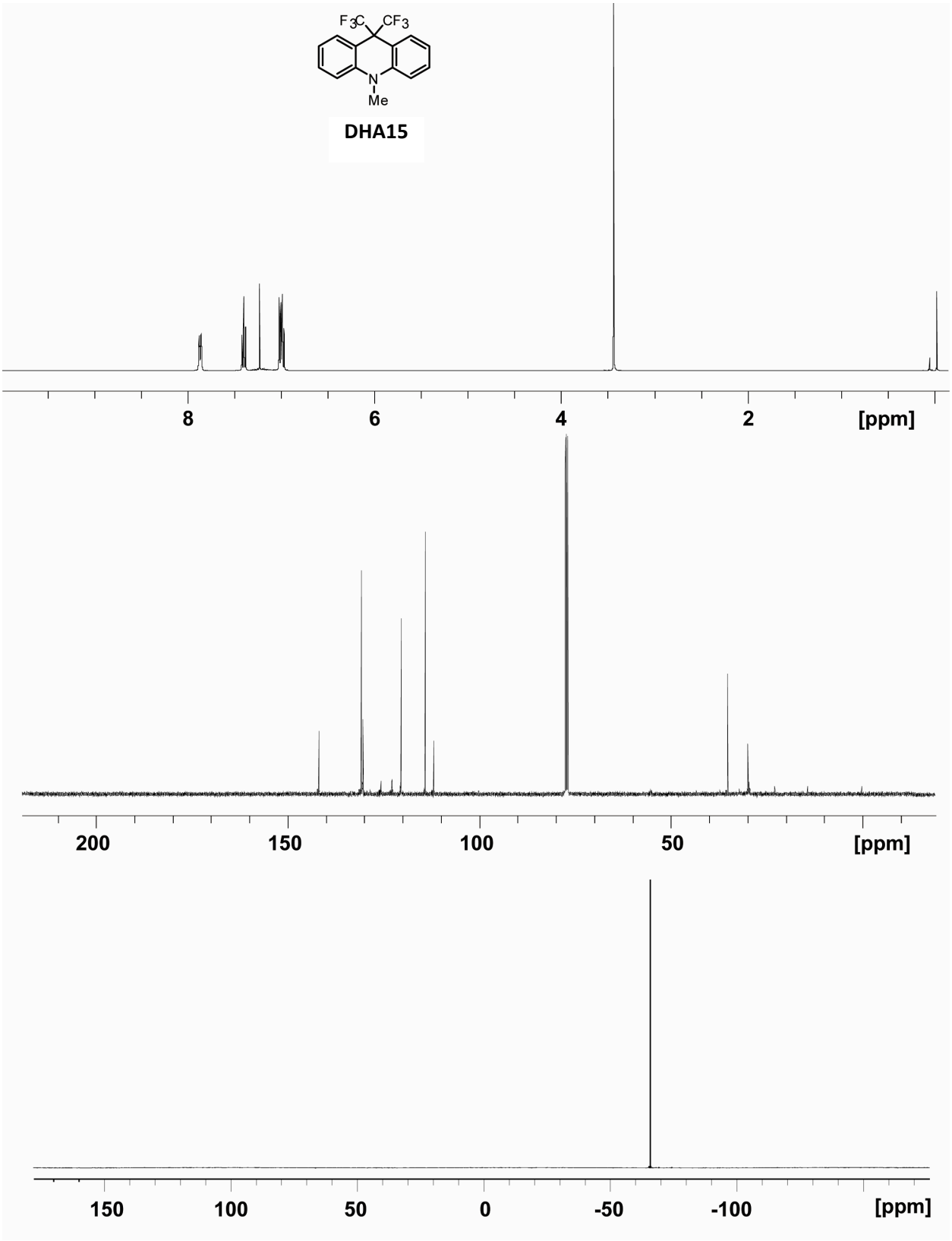
F3C
CF3
N
Me
DHA15
8
6
4
2
[ppm]
200
150
100
50
[ppm]
150
100
50
0
-50
-100
[ppm]

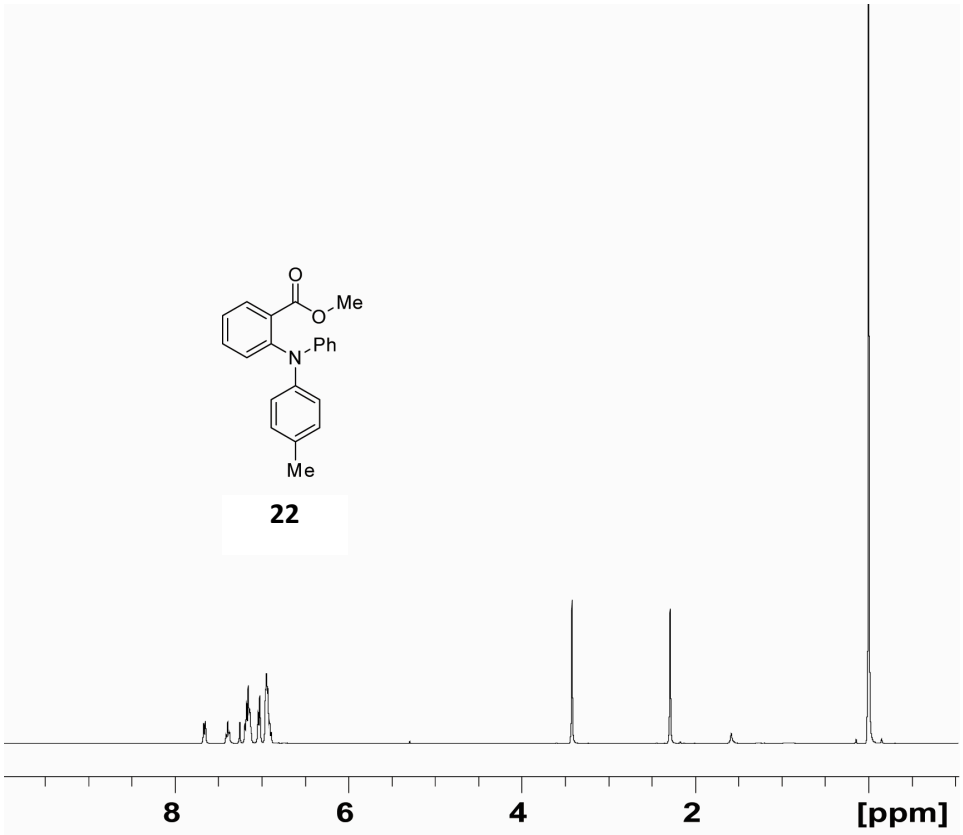

22

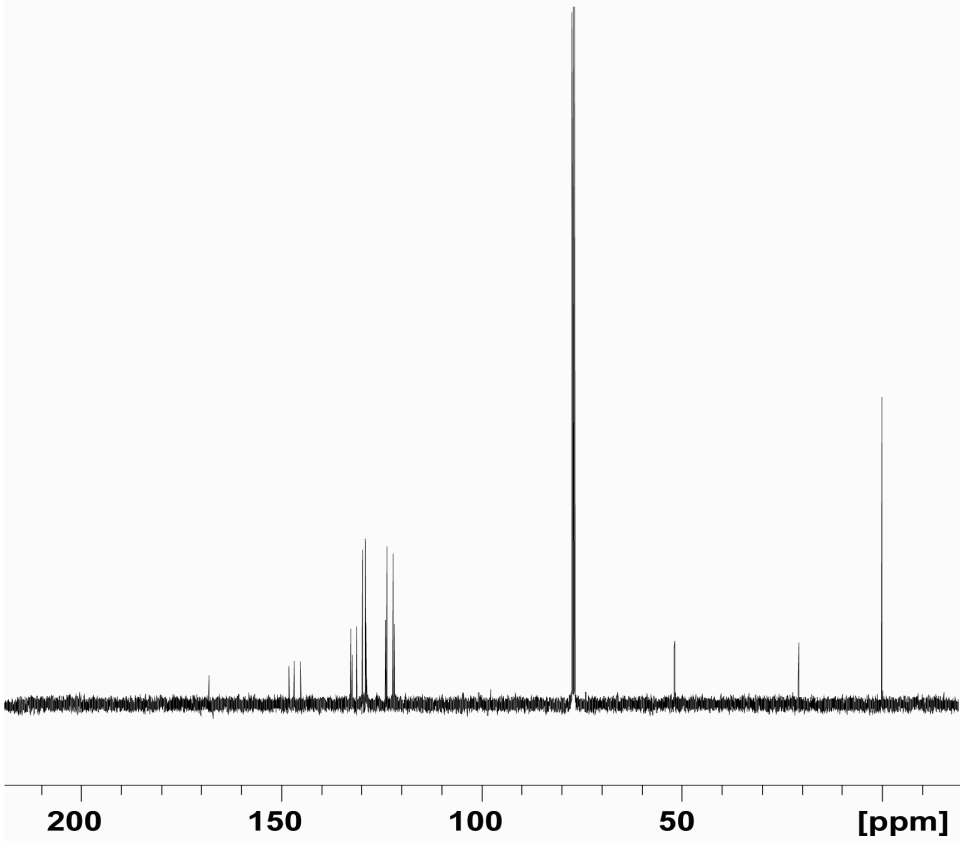

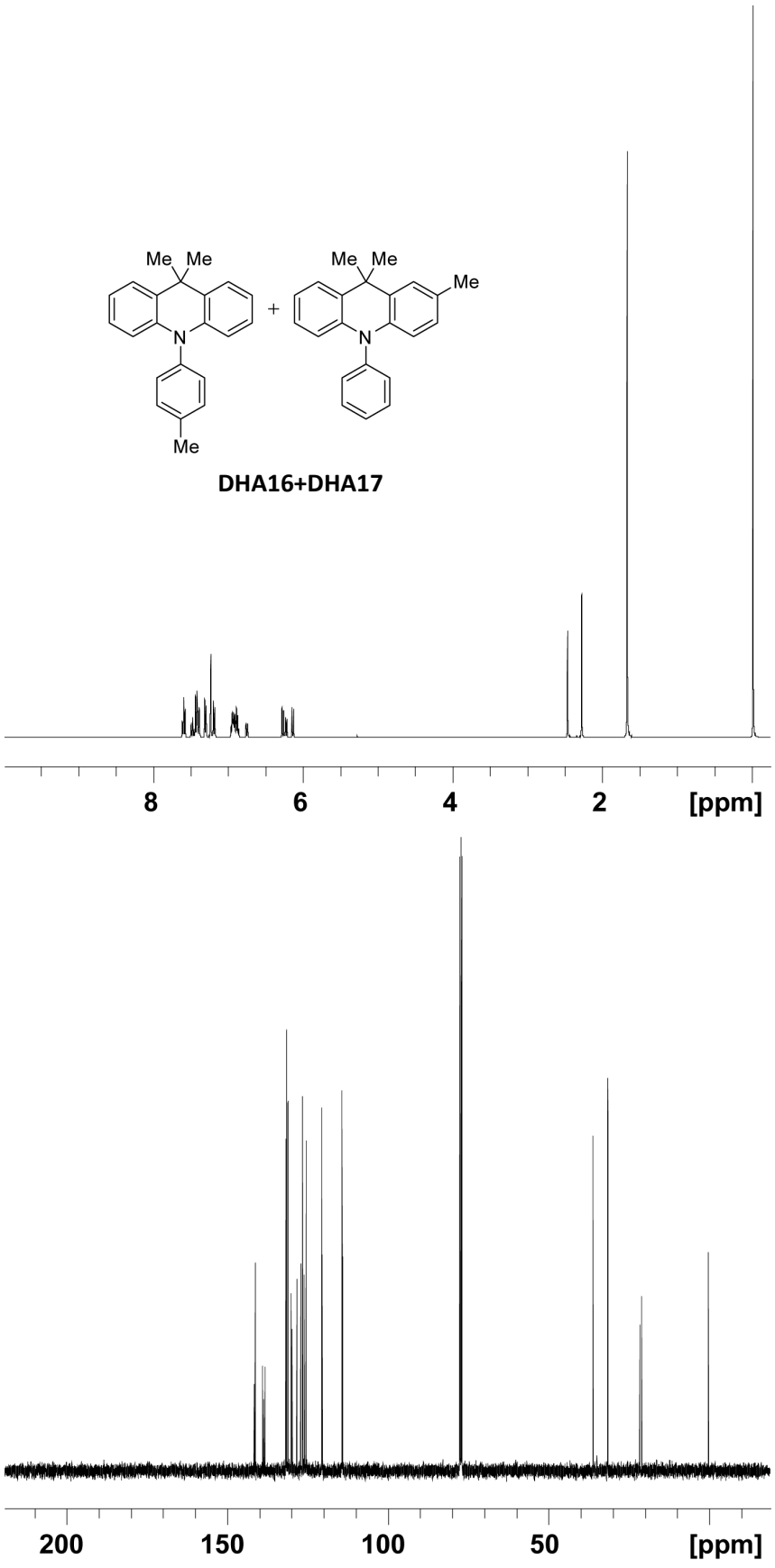
Me Me
N
Me
+
Me Me
N
Me
DHA16+DHA17
8
6
4
2
[ppm]
200
150
100
50
[ppm]

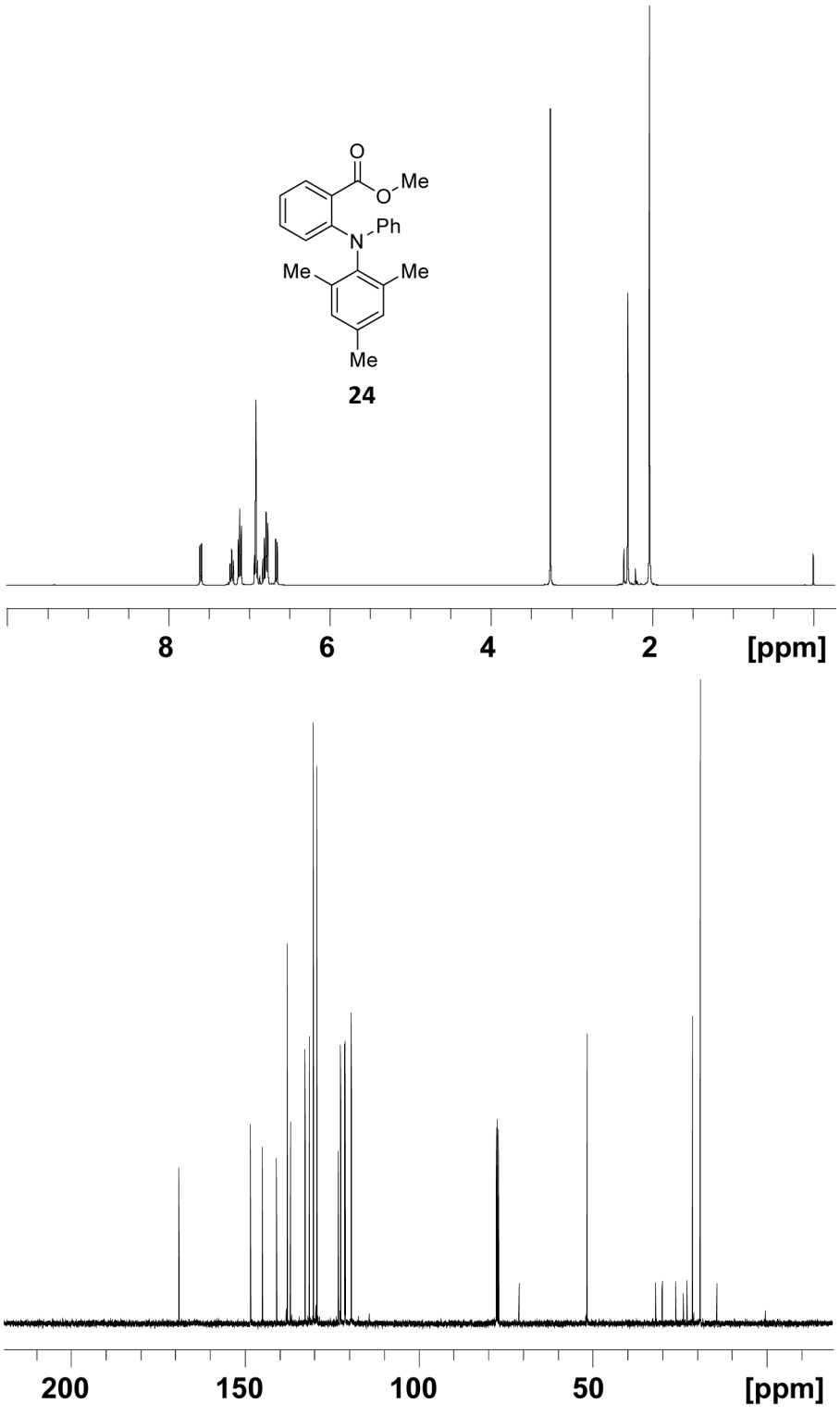

24

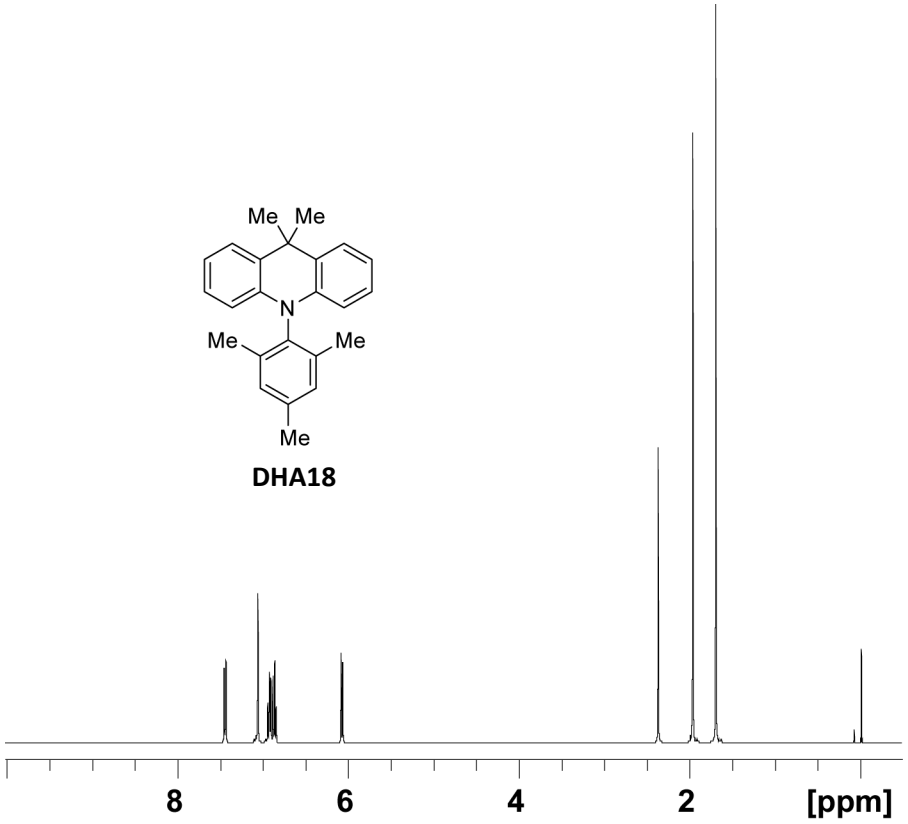

DHA18

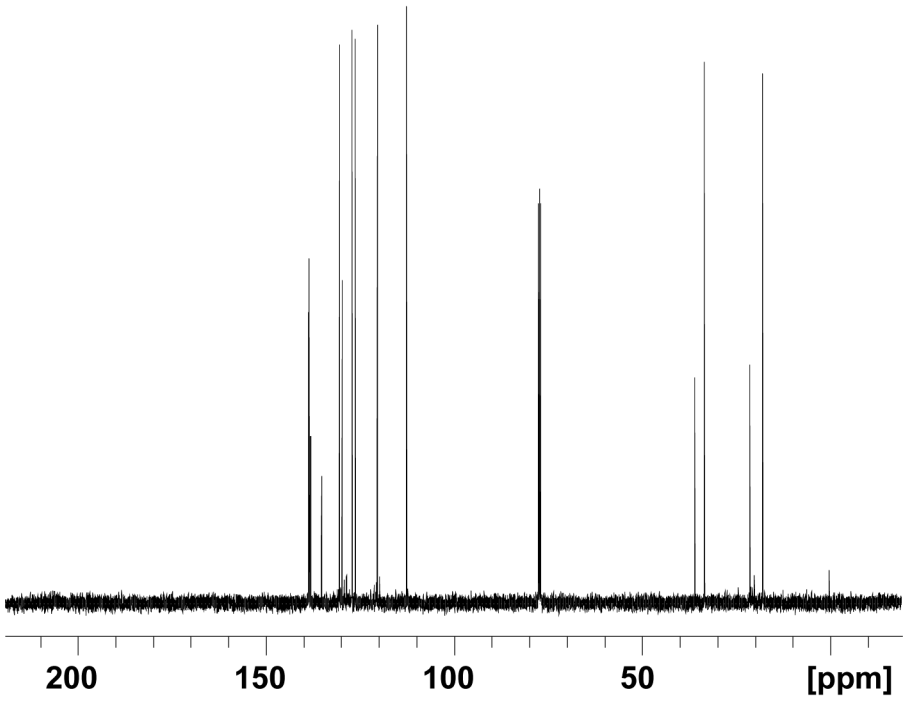

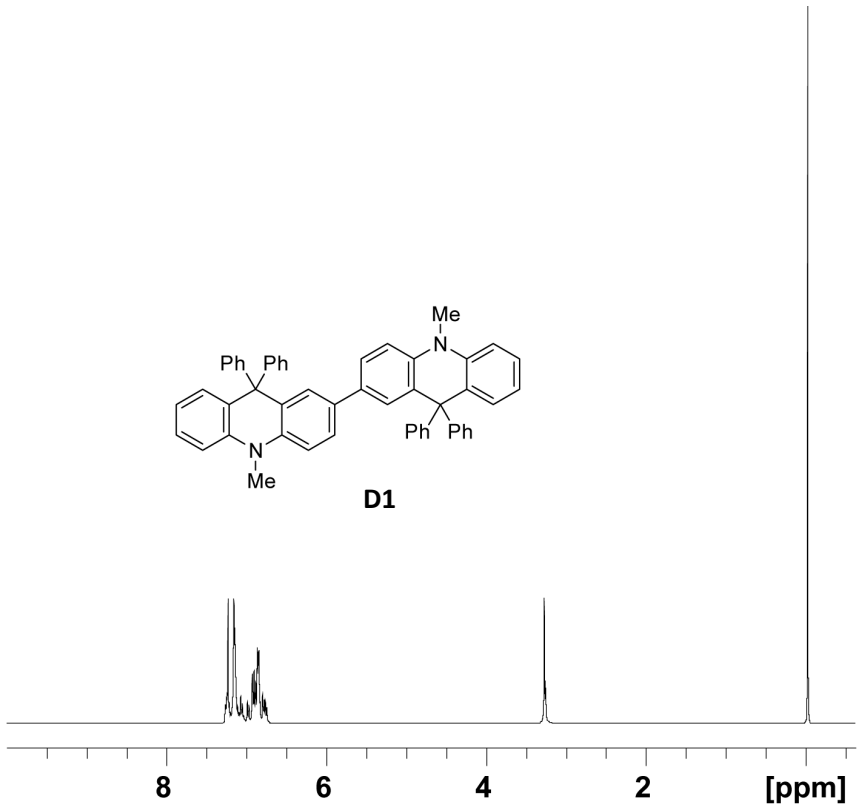

D1

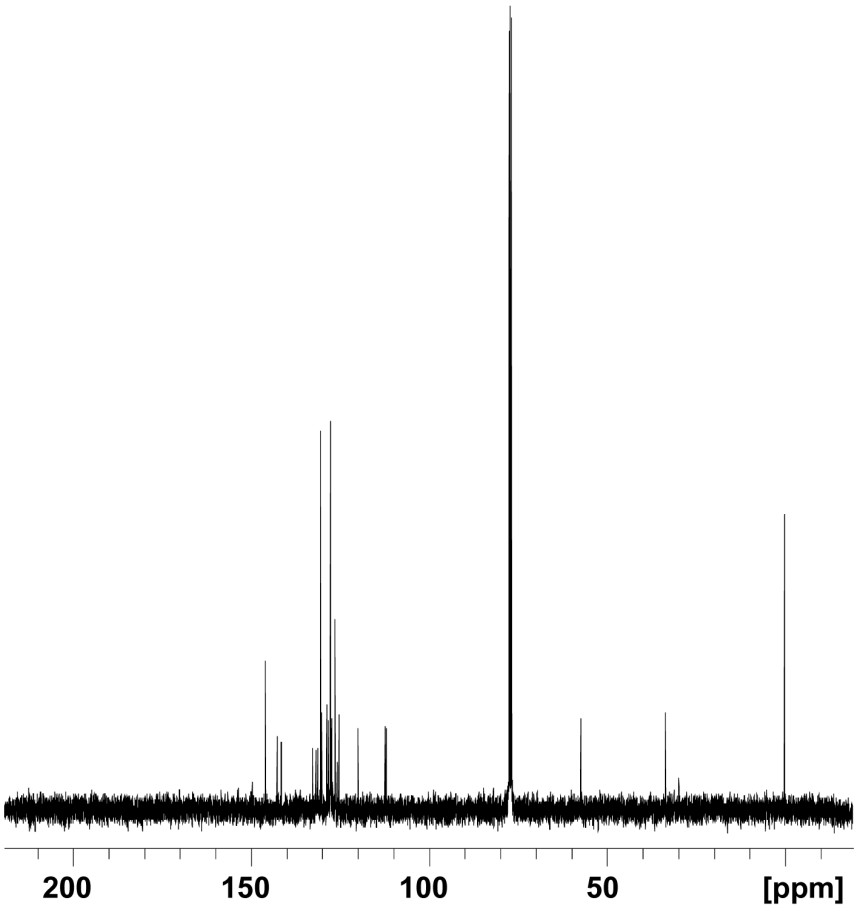

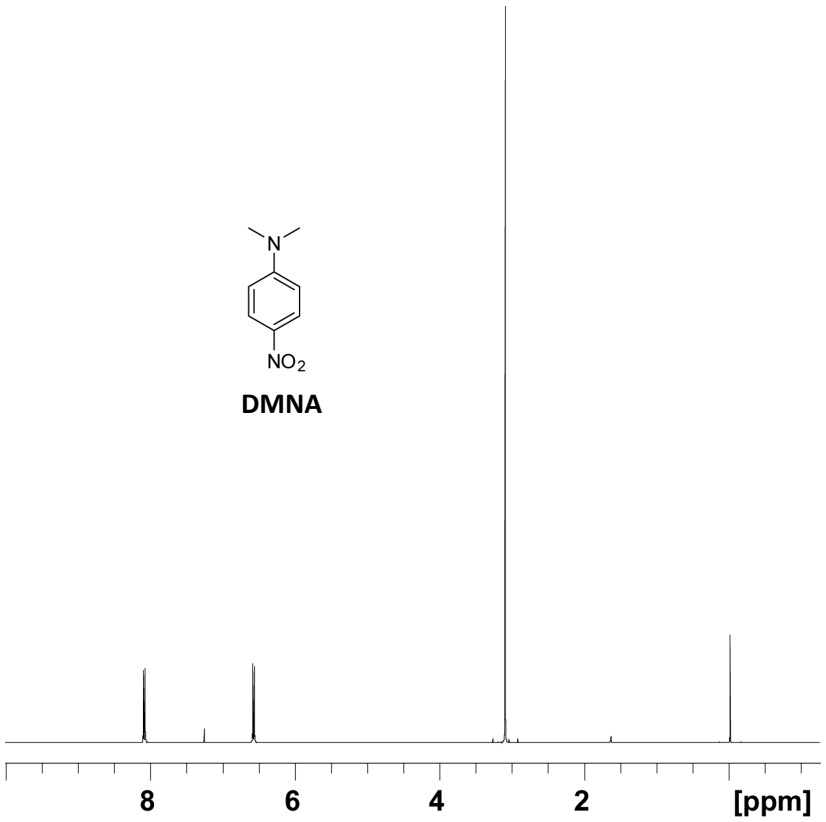

DMNA

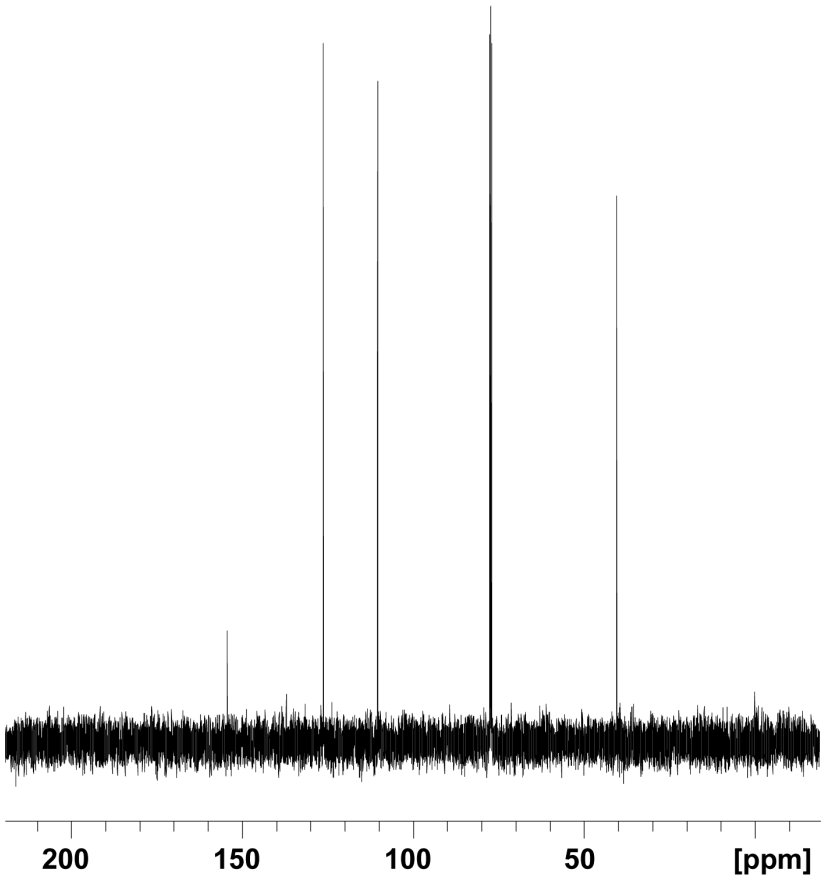

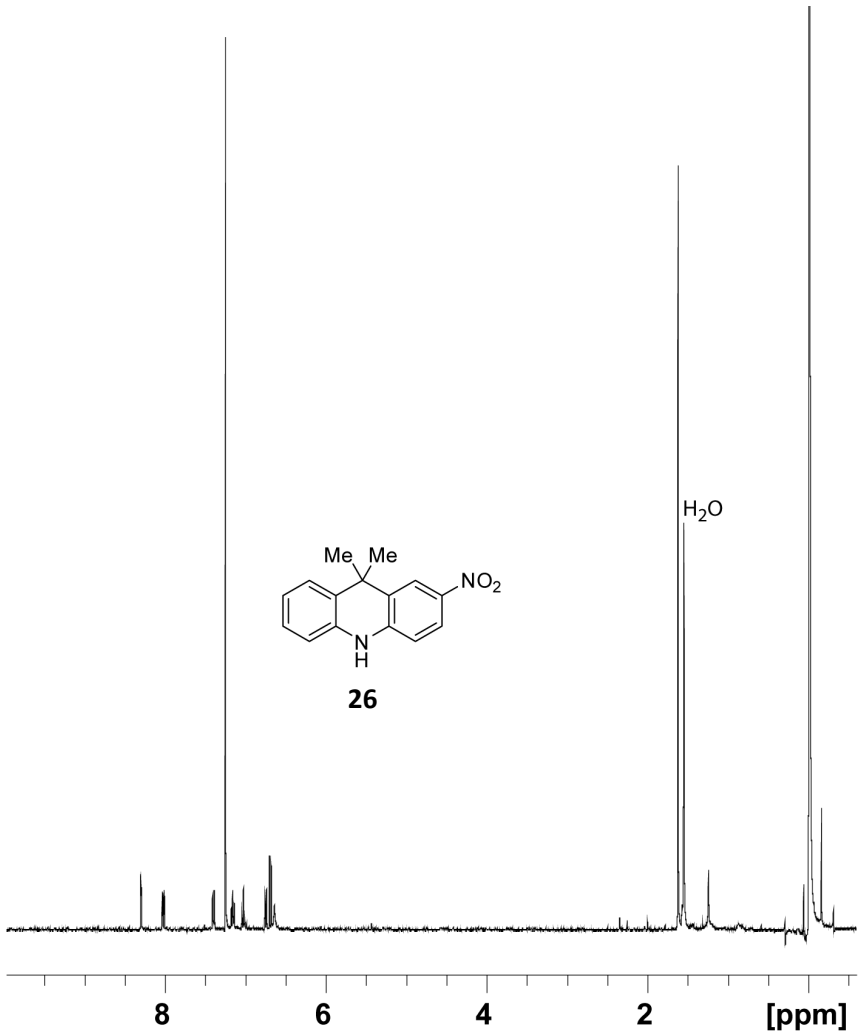

26

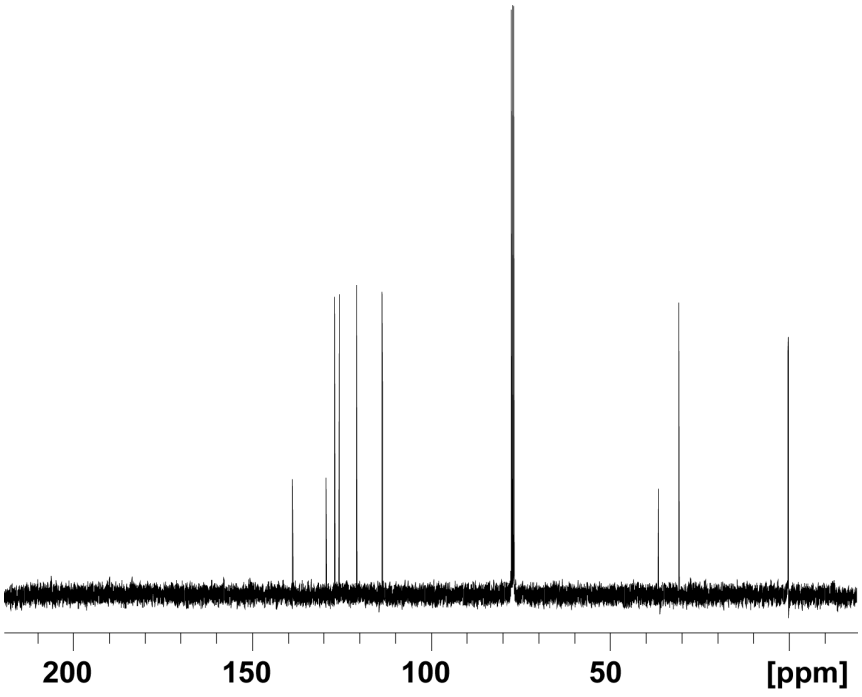

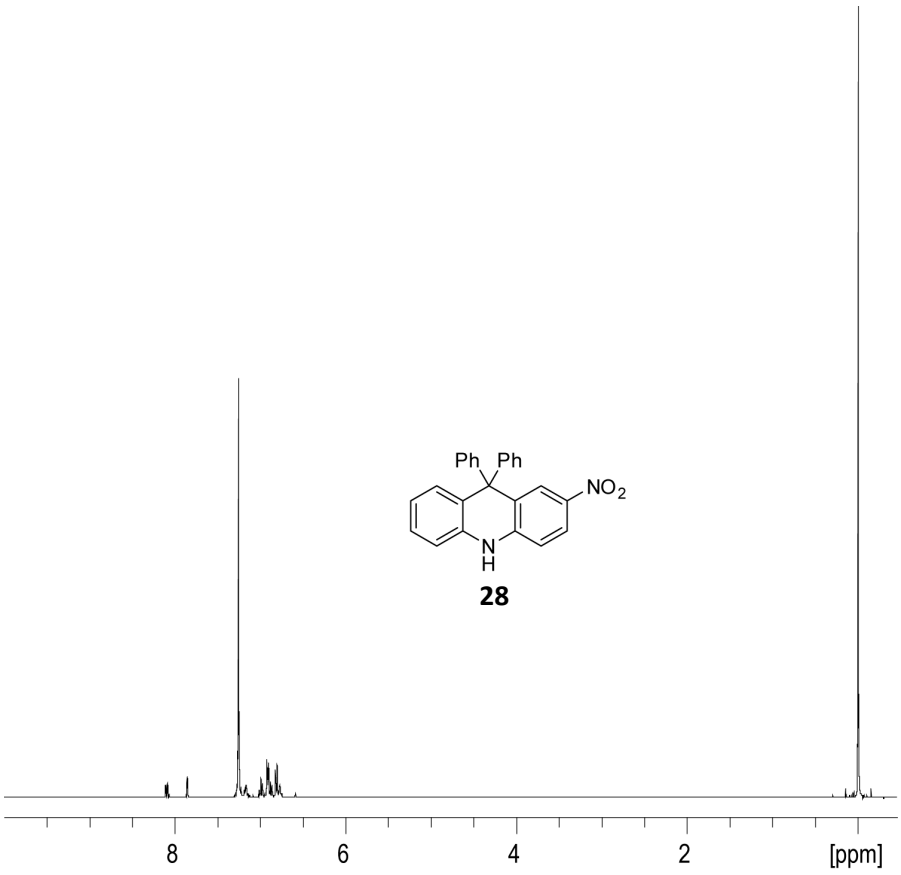

28

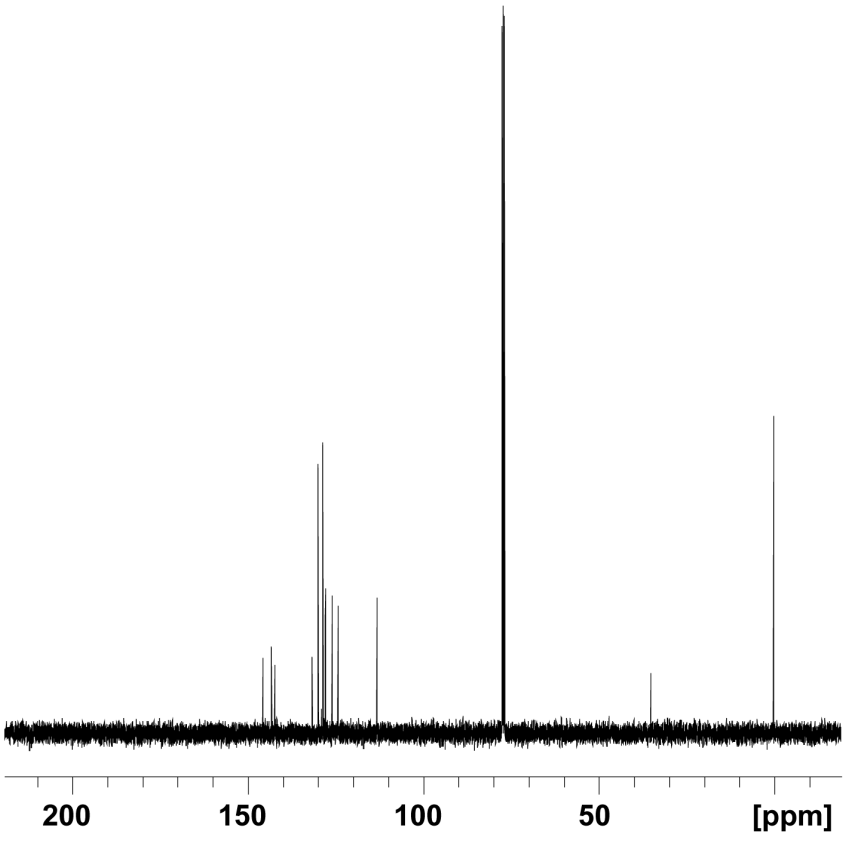

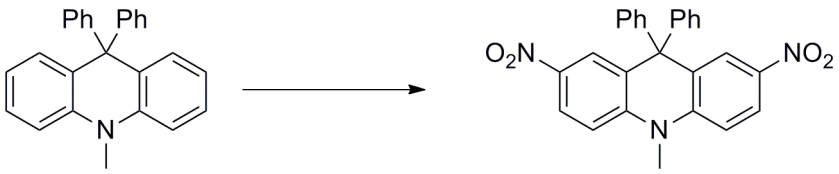

2,7-Dinitro-10-methyl-9,9-diphenyl-9,10-dihydroacridine (**35**). A 25 mL round bottom flask was charged with 0.5 g **DHA8** (1.4 mmol) and 20 mL dry dichloromethane under argon and the solution was cooled to -78 ^{o}C in an acetone/dry ice bath. Approximately 0.2 g of 25% HNO_3 on silica gel was then added to the solution and the reaction stirred at -78^{o}C for 1 h. Upon warming to room temperature, the reaction was filtered and the solvent evaporated under reduced pressure. The residue was purified by flash column chromatography using 50/50 hexanes/dichloromethane as eluent. 80% of 2,7-dinitro-9,9-diphenyl-10-methyl-9,10-dihydroacridine was thus isolated.

^{1}H NMR (400 MHz, $CHCl_3$) δ 3.5 (s, 3H), 6.81 (dd, *J* = 2.4, 8.0 Hz, 4H), 7.11 (d, *J* = 9.2 Hz, 2H), 7.28 (m, 6 H), 7.78 (d, *J* = 2.8 Hz, 2H), 8.24 (dd, *J* = 2.8, 9.2 Hz, 2H).

^{13}C NMR (100 MHz, $CHCl_3$) δ 35.1, 57.1, 113.2, 124.3, 126.1, 127.9, 128.6, 129.0, 130.0, 131.7, 142.3, 143.2, 145.8.

HRMS (ESI) calc for $C_{26}H_{20}N_3O_4$ $[M+H]^+$ 438.1448, found 438.1451.

IR (KBr plate) 699 (m), 762 (m), 907 (m), 1300 (m), 1330 (m), 1483 (s), 1529 (m), 1585 (s), 2922 (m), 3410 (m) cm^{-1}.

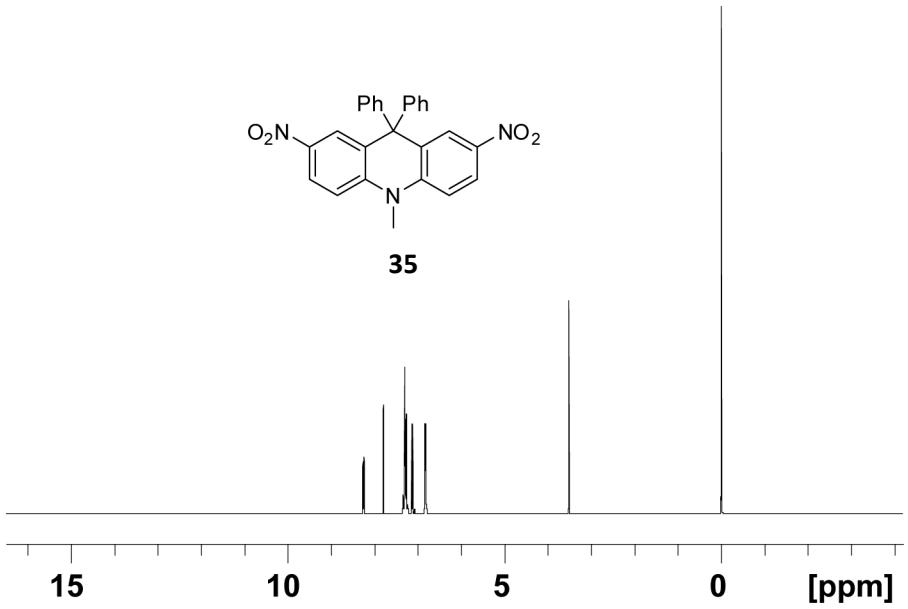

35

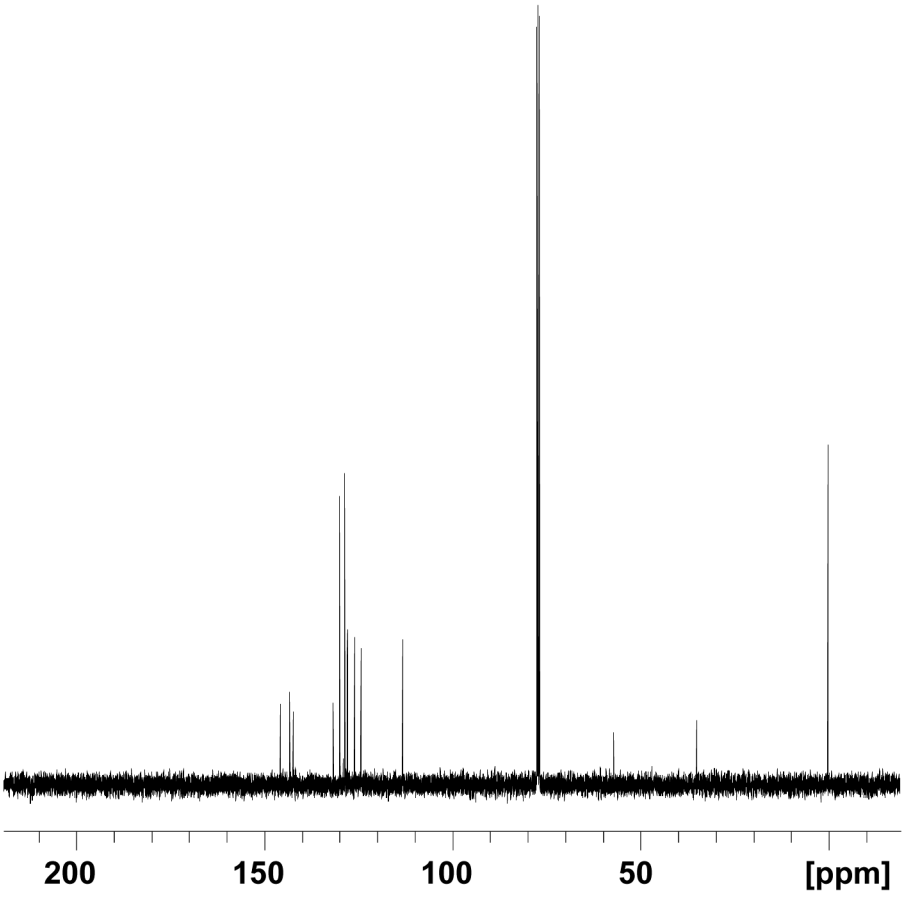

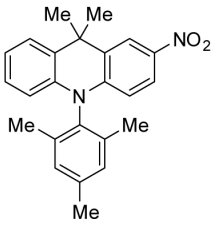

30

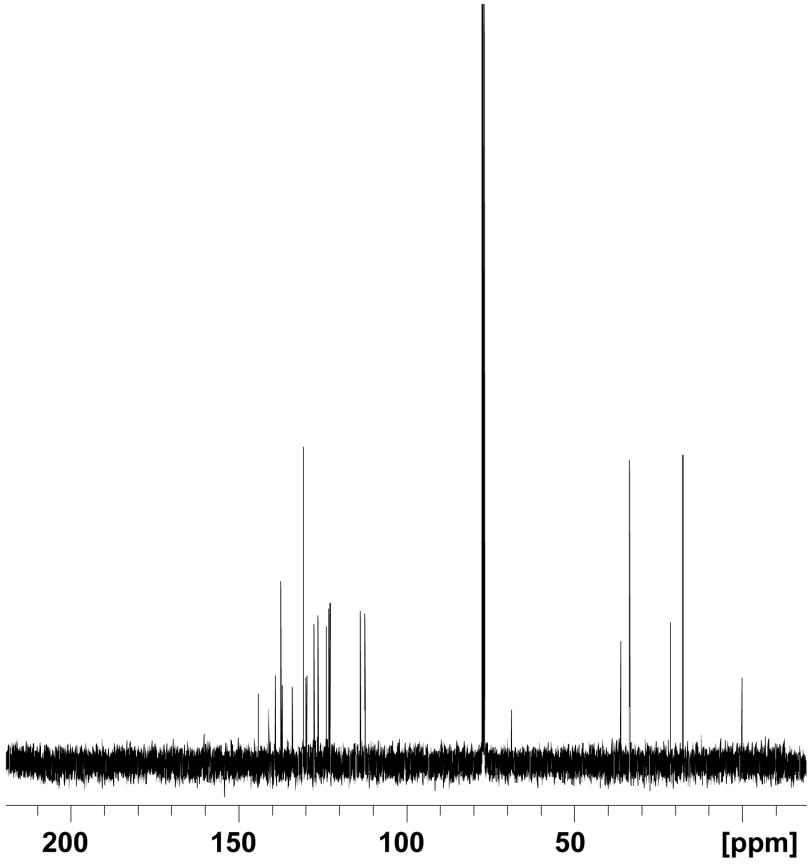

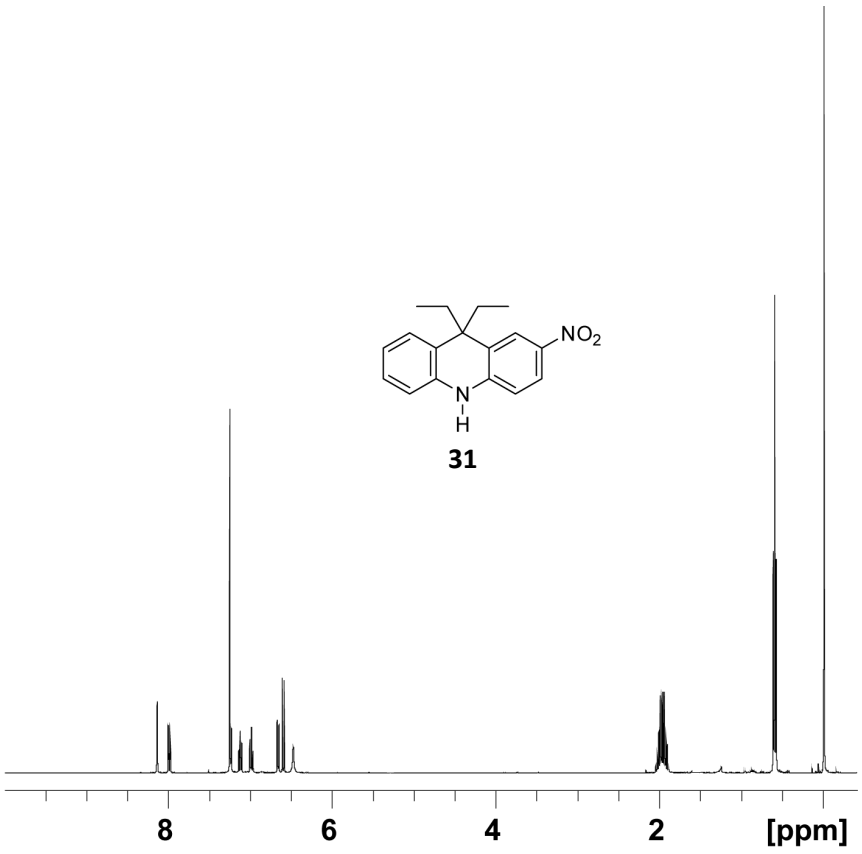

31

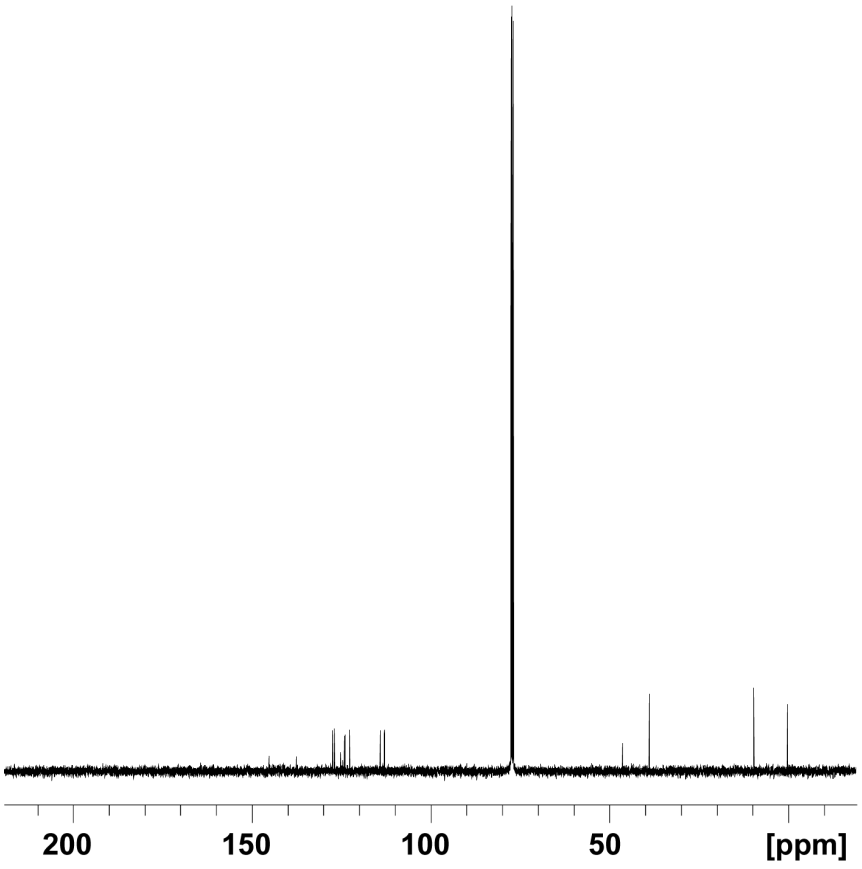

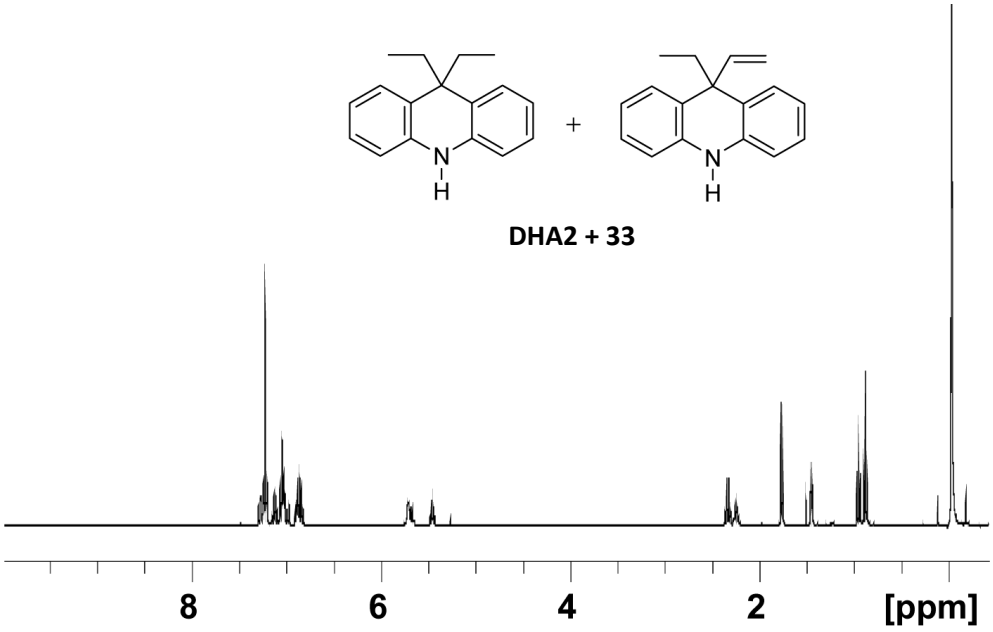

DHA2 + 33